Title
Design of a medical image data warehouse for epilepsy diagnosis and research

Author
Hoo, Kent Soo, Jr.

Publication Date
2002

Peer reviewed|Thesis/dissertation

DESIGN OF A MEDICAL IMAGE DATA WAREHOUSE FOR EPILEPSY DIAGNOSIS AND RESEARCH

by

Kent Soo Hoo, Jr.

DISSERTATION

Submitted in partial satisfaction of the requirements for the degree of

DOCTOR OF PHILOSOPHY

in

Bioengineering

in the

GRADUATE DIVISIONS

of the

UNIVERSITY OF CALIFORNIA SAN FRANCISCO

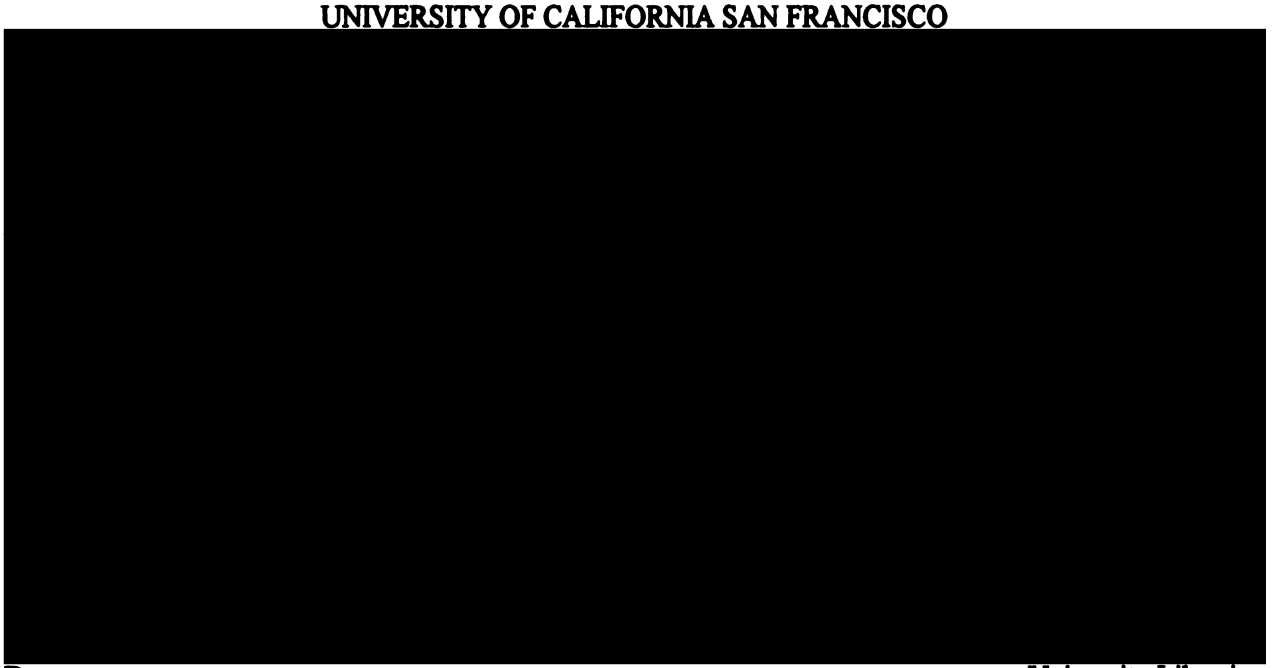

Date University Librarian

Degree Conferred: .....

DEDICATION

I wish to dedicate this thesis to my beloved mother, father, brother, sister, and wife. Their limitless patience and steadfast support are responsible for the completion of my doctoral work. Mom, I needed you to be the force behind me, urging me forward when I got bogged down. Dad, I appreciate the quiet way that you also encouraged me to complete my dissertation work. Kevin, you are the best brother, friend, and confidante anyone could possibly hope for; I hope that I can be worthy of your love. Kristi, thank you for your love and support. Stella, thank you for taking care of me so I could concentrate on the thesis; I couldn't have done it without you.

PREFACE

I wish to acknowledge my thesis advisor, Stephen T.C. Wong, who has supported and guided me throughout my graduate studies. I would also like to acknowledge the clinicians who worked with me, especially Robert C. Knowlton and Kenneth D. Laxer. Thanks to all my colleagues at the Laboratory for Radiological Informatics who served as mentors and friends over the years.

University of California San Francisco

and

University of California Berkeley

Abstract

DESIGN OF MEDICAL IMAGE DATA WAREHOUSE FOR EPILEPSY DIAGNOSIS AND RESEARCH

by Kent Soo Hoo, Jr.

Chairperson of the Thesis Committee: _____

Professor Randall A. Hawkins
Department of Radiology

There exists a need for a systematic software engineering approach to create medical information systems that support clinical diagnostic patient studies and biomedical imaging research. The purpose of this research is to create a formal design framework to describe medical image information systems and derive design patterns for solving problems within that framework. The framework is implemented as a prototype image data warehouse that supports epilepsy research and patient care. The goal of this system is to enable more efficient and effective utilization of medical images, laboratory tests, psychometric tests, and textual data in epilepsy research and care than what is currently supported by Picture Archiving and Communication Systems.

TABLE OF CONTENTS

LIST OF TABLES

LIST OF FIGURES

LIST OF EQUATIONS

Chapter 1

BACKGROUND

1.1 Introduction

Medical imaging is an essential component of medical services. It is one of the most dynamic and crucial technologies in modern medicine. Medical images are at the core of patient diagnosis, surgical planning, therapy treatment, outcome assessment, medical education, and research. By providing clinicians with vivid pictures of body organs and tissues, medical imaging enables them to better detect, monitor, and treat illnesses. Advances in non-invasive imaging techniques now allow physicians to locate and identify the nature of a brain tumor or lung nodules, well before planning any medical treatment. This also reduces the frequency and morbidity rate of conventional invasive procedures in diagnosis and treatment planning. The last two decades have seen the proliferation of many digital imaging modalities, including MRI, X-ray CT (Computed Tomography), PET (Positron Emission Tomography), MEG (Magnetoencephalography), and MRS (Magnetic Resonance Spectroscopy) [1-3]. These new modalities represent a tremendous leap forward in the quality and diversity of information obtained from medical images while reducing patient radiation dose and examination trauma.

Currently, digital modalities comprise 30% of all medical images captured today while the other 70% are done in conventional X-rays or computed radiography (CR) [4]. Different kinds of film digitizers are routinely used to convert plain X-ray films into digital format [5]. The amount of digital images captured per year in the United States is estimated on the order of petabytes, i.e., 10^{15}, and is increasing rapidly every year [6]. Physicians and researchers are confronted with the

time consuming task of integrating and accessing vast amounts of image and textual data from diverse sources with very limited information management tools. The integration of medical images with patient data raises many unresolved questions in image database management [6,7].

The new digital modalities have generated a large volume of multimodality image data such that traditional methods employed by the clinicians and health care providers to manage their data with papers and films are no longer adequate. Therefore, the classical way to deal with these data has appeared often sub-optimal with respect to their quality and to their medical objective, which often tend to exclude complementation information from other clinical information systems

Also, by permitting early diagnosis and targeted treatment of illness, diagnostic imaging helps reduce the costs of prolonged treatments, surgery, redundant tests, and hospital stays while maximizing the chances of recovery for the patients. Furthermore, the aging of the population is another important demographic factor that underlines the need for early and effective diagnostic imaging equipment, as this population will be at larger risk of contracting age-related diseases. These diseases include cancer, notably breast and prostrate cancer diseases, and cardiovascular diseases. Medical imaging modalities are well positioned to provide early detection of diseases and help reduce hospital and treatment costs.

Because of their high cost to purchase and operate, the majority of these imaging machines are dispersed unevenly in medical centers and prosperous suburbs that can afford them, and today's cost-conscious health-care environment won't permit the dissemination of these cutting-edge technologies to every hospital. The medical imaging equipment market alone represents over $16 billion in revenues in 1997, excluding the revenues from medical consultation and services that depend on the operations of this equipment. Cost-effectiveness, upgradability,

interconnectivity, digitization, and data management constitute major technology trends in biomedical imaging equipment today.

1.2 Categorization of digital imaging modalities

On November 8, 1895, an experimental physicist was investigating the properties of cathode rays when he noticed that a cardboard screen lying several feet away glowed whenever the cathode ray tube was activated. He was puzzled by the luminescent phenomenon because neither cathode rays nor any other rays he could think of could account for the glow coming from the screen coated with barium platinocyanide, a fluorescent material used to develop photographic plates at the time. Wilhelm Conrad Roentgen had stumbled upon evidence of a new class of electromagnetic radiation: X-rays. Over the next several weeks as he explored the phenomenon in some detail, Roentgen lay down the foundation of modern medical imaging [8]. Reportedly, one of the first X-ray radiographs ever taken was of his wife's hand, revealing a picture of the living skeleton. Over the next 50 years, the technology of peering into the human body would be refined as physicians went on to image the structural and physiological state of internal organs like the stomach, intestines, lungs, heart, and brain.

A revolution in medical imaging occurred during the last two decades when the convergence of the imaging physics and computers produced new digital imaging modalities: film scanners, diagnostic ultrasound, CT, MRI, digital subtraction angiography (DSA), single photon emission computed tomography (SPECT), PET, and MEG. Most of these modalities are routinely being used in clinical applications, and they allow *in vivo* evaluation of physiology and anatomy in ways that conventional X-ray radiography could never achieve.

A two-dimensional (2-D) medical image has a size of M × N × k bits, where 2^k equals the gray level range. Table 1 lists the average number of megabytes (MB) per examination generated by medical imaging technologies, where any 12-bit image is represented by 2 bytes in memory. The plain X-ray films of images of the higher resolution requirement can be digitized by 4K × 4K × 12-bit digitizers. The size of an image and the number of images taken in one patient examination vary with modalities. Except for Digitized Electronic Microscopy and Digitized Color Microscopy which are pathologic and histological images of microscopic tissues, all the other modalities are generally classified as radiological images and are used for diagnosis, treatment and surgery planning purposes. A radiological image is generally represented in monochrome, with the exception of Doppler ultrasound and pseudo-color nuclear medicine images. Each radiological examination involves a well-defined procedure. One examination

Modality	Image Dimension	Gray level (bits)	Average size/exam
Nuclear Medicine (PET & SPECT)	128 x 128	8 or 16	1 ~ 2 MB
Magnetic Resonance Imaging (MRI)	256 x 256	12	8 MB
Ultrasound (US)	512 x 512	8	5 ~ 8 MB
Digital Subtraction Angiography (DSA)	512 x 512	8	4 ~10 MB
Computed Tomography (CT)	512 x 512	12	20 MB
Digitized Electronic Microscopy (DEM)	512 x 512	8	Varies
Digitized Color Microscopy (DCM)	512 x 512	24	Varies
Digitized X-rays	2048 x 2048	12	8 MB
Computed Radiography (CR)	2048 x 2048	12	8 ~ 32 MB
Digitized Mammography	4096 x 4096	12	32 MB (one image)

Table 1 Medical images sizes (unit: MB = megabytes). The vast volume of biomedical images generated by these digital imaging modalities renders traditional methods employed with papers and films inadequate. The traditional methods have appeared sub-optimal with regard to their quality of services and to their medical objective, which often tend to exclude complementary information from other clinical information systems. Furthermore, these manual recording systems incur additional costs and loss of productivity due to missing records, misplaced files, duplicated studies, and large filing space required.

(about 40 image slices) of X-ray CT with uniform image slice size of 512 × 512 × 12 bits is around 20 MB while one image of digital mammography usually generates 32 MB of data.

Figure 1 shows the categorization of major biomedical imaging modalities according to structural and functional contents of the image data they generated. The structural or anatomical imaging modalities include MRI, CT, diagnostic ultrasound, projectional radiograph, and microscopy. The functional or physiological imaging modalities cover functional and spectroscopic magnetic resonance, magnetic source imaging, and nuclear medicine imaging. In addition, the pharmaceuticals and medical image management systems category of diagnostic imaging equipment market also includes diagnostic imaging contrast media, picture archiving and communication systems (PACS) and teleradiology.

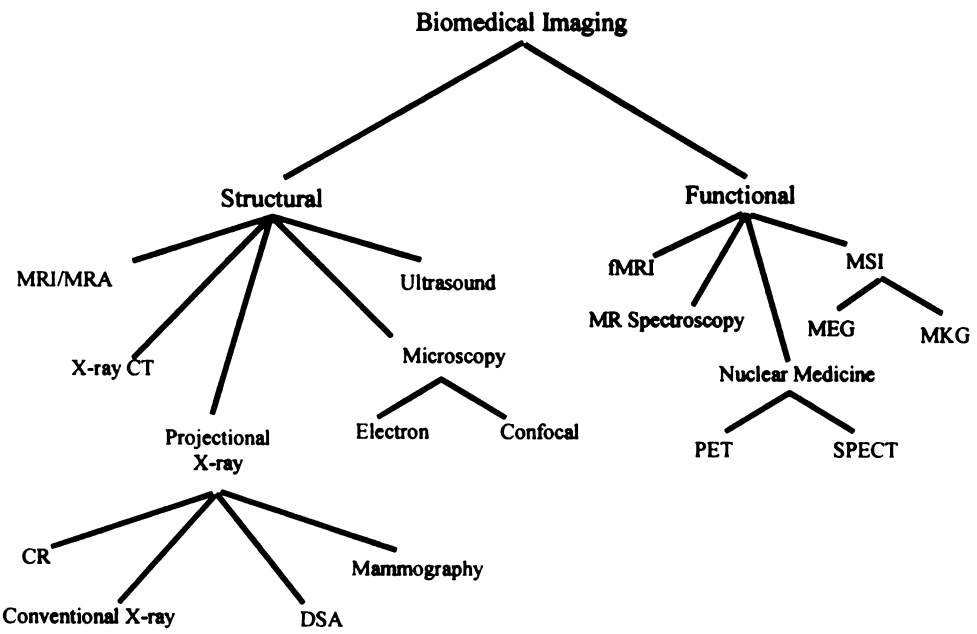

Figure 1 Classification of biomedical imaging modalities. Biomedical imaging modalities can be broadly divided into two groups distinguished by what kind of information they reveal about the body, structural or functional.

1.3 Projectional X-ray imaging

1.3.1 X-ray radiography and fluoroscopy

An X-ray, also known as Roentgen ray, is an electromagnetic radiation of shorter wavelengths than visible light. When used in radiography, X-rays are projected through organs or structures of the body onto a photographic plate. Since certain tissue, such as bone, is more radiopaque, allowing fewer X-rays to pass through, than other tissue, such as skin or fat, a shadow is created on the plate that is the image of a bone or of a cavity filled with a radiopaque substance. This category of imaging modalities generally includes chest X-ray units, mammography scanners, and non computer-based tomographic systems. Mammography, the X-ray imaging of the breast, is used to detect breast cancer and is often treated separately because of its high requirement and its use as a mass-screening tool for asymptomatic women.

X-ray radiography is a relative mature technology and the world X-ray market traditionally has a stable revenue growth rate. The technology has evolved over the years to increase spatial resolution and signal to noise ratio while at the same time reducing patient dose. Contrast agents as we know them today were first developed in 1923 to permit the opacification of internal hollow organs and are currently used to visualize blood vessels, gastrointestinal structures, and other anatomy. Without the use of contrast agents, these fluid filled structures would blend into the surrounding soft tissue because they have similar radiographic density. The use of fluorescent screens to enable direct viewing of the X-ray image by a dark-adapted viewer was introduced in 1899, and this process called fluoroscopy became widely available in the 1920s.

Film subtraction angiography took this a step further by taking positive and negative film images before and after injection of the contrast agent to yield images containing only vascular structures affected by the contrast injection. Such subtraction eliminates the superposition of extraneous

anatomy onto the final film such as bone. In 1950 the image intensifier revolutionized radiology by allowing ordinary movie cameras to capture moving pictures of fluoroscopic images from the new, extremely bright, scintillating screen. An image intensifier was also introduced to enlarge and brighten the image before it is passed through a TV camera to a monitor where it can be viewed by the physician or the operator. Fluoroscopy images are used to diagnose cancers of the urinary tract, bowel, and gastrointestinal system. Today fluoroscopy provides a low-cost, real-time imaging modality to study the motion of certain organ systems including gastrointestinal and vascular. Combined radiography/fluoroscopy units are an important part of the X-ray equipment market.

Despite the plethora of new computer-based digital imaging systems available today, conventional X-ray projection radiography is still the most commonly used diagnostic imaging procedure. In its most common form an X-ray tube generates X-rays, which exit the tube in a fan-shaped beam toward the patient. Lead panels are placed to control the lateral extent and size of the radiation beam. Behind the patient is a metal cassette housing a photosensitized film. The cassette prevents exposure of the film to outside light and contains a fluorescent screen, which converts the X-rays to light. Both the direct effect of the X-rays as well as the indirect effect of the fluorescence exposes the film inside the cassette. The areas of the body imaged include the chest, the abdomen, upper extremity, lower extremity, spine, and skull and head.

The resulting film contains a 2-D superposition of a patient's three-dimensional (3-D) anatomy, and the film's optical density is directly proportional to the attenuation coefficient of the X-ray path through that part of the body. The four basic optical densities on the film are: air which appears black, fat which appears dark gray, soft tissue which appears light gray, and bone which appears white. Spatial resolutions up to 50 microns can be achieved on today's high-resolution

mammography systems. The disadvantage of this technique is its use of ionizing radiation which can cause direct damage such as radiation burns, fibrosis, necrosis, and sarcomas as well as indirect damage such as leukemia, increased incidence of cancer, shortened life span, genetic damage, and chromosomal aberrations. The cost of acquiring, storing, and disposing of the chemicals used in developing the radiographic films is high. The antiquated paper-based filing systems used to store conventional X-ray films are not only inefficient but are also ill suited to store the digital images of the new digital imaging modalities.

1.3.2 Film digitization

Although the trend of medical imaging is toward digital, currently about 70% of all radiographic procedures still use film as the output medium. Film scanners are being used to convert the films into digital format for storage in PACS. The function of film scanners is to quantize the 2-D radiographic film into a 2-D array of gray level values. The film is sampled according to the sampling theorem, which states that:

> If the Fourier transform of the image $f(x,y)$ vanishes for all u,v where $|u| \geq 2f_n$, $|v| \geq 2f_n$ then $f(x,y)$ can be exactly reconstructed from samples of its non-zero values taken $\frac{1}{2f_n}$ apart or closer, the frequency $2f_n$ is called the Nyquist frequency.

The theorem implies that if samples are taken more than $\frac{1}{2f_n}$ apart, then it is impossible to reconstruct completely the images from these samples, resulting in an image with aliasing artifacts. Film scanners come in several types: video scanning system, rotating drum, solid-state (linear motion) camera, and laser scanner.

A video scanning system consists of three major components: a scanning device (e.g. television camera) that scans the X-ray film, an analog to digital converter (ADC) that converts the analog video signals from the camera into digital gray level values, and memory to store the digital values from the ADC.

A drum scanner is a mechanical device consisting of a rotating drum, a light source, and a photo detector. An X-ray film is clamped around the cylindrical surface of the drum. A light source inside the drum shines through the film and into a photo detector, which converts the transmitted light into a gray level value. Most drum scanners have spatial resolutions from 25 mm to 400 mm and can convert the optical density of film to 256 gray levels. Solid-state cameras have three major components: a photo detector, ADC, and memory. A light box is used to illuminate an X-ray film and the photo detector measures the transmitted light photons, converting them into an electric signal. The ADC converts the electric signal into a digital image for storage in the memory. There are two types of photo detectors in use: photodiodes array and charge-coupled devices. Finally, the laser scanner utilizes a low-power laser beam (usually Helium-Neon) to scan across a single line of the X-ray film in a light-tight environment. The optical density of the film is measured from the transmission of the laser through the radiograph using a photomultiplier tube and logarithmic amplifier. Again, an ADC digitizes the analog signal for storage in memory. The photomultiplier detects light transmission one pixel at a time, and spatial resolutions of up to 50mm can be achieved.

1.3.3 Computed radiography

Currently, X-ray film is by far the most important recording medium for projection imaging. Non-film based digital detectors are rapidly encroaching upon this film-based domain. Computed radiography is one such technology. Both conventional X-ray and computed

radiography (CR) use X-ray beams as the source of energy. In conventional X-ray, the image obtained is projected onto a photographic plate of a fluorescent screen. Computed radiography is actually not a new imaging modality, but a new method of handling the data. CR uses an electron radiation image detector and adds computer capability to digitize, manipulate, display, and store the data. Available detectors include photostimulable phosphors, Charge-coupled device (CCD) sensors coupled to conventional phosphors, and solid-state semi-conductor materials such as selenium and silicon.

Technology for these detectors is advancing rapidly and will likely provide array sizes of 4000 ´ 4000 elements soon to match the capabilities of screen/film systems for both static and dynamic projectional imaging [9]. Recent reductions in system costs, improved throughput, and the inevitable movement to an all-digital radiology department of the future have made computed radiography an attractive alternative to the conventional screen/film detector.

1.3.4 Digital subtraction angiography

Angiography involves the imaging of blood vessels to determine blockage caused by the narrowing of the vessels. An iodine-based contrast agent is taken orally or intravenously into the vessels to create a shadow in order to help physicians visualize the blood flow. Angiography also enables the recording of the arterial pulse by use of sphygmograph. A sphygmograph is an instrument used for recording the shape and force of the pulse wave. Angiography is also used to help close off a blood supply to abnormal tissues and organs.

Diagnostic angiography film-screen systems developed into the principal modality for vascular imaging. In subtraction angiography an image is acquired before introduction of contrast agents into the arteries or veins. This initial image is called the mask, and subsequent images taken after introduction of the contrast agent are enhanced when the mask is subtracted. This subtraction

results in an image that is devoid of extraneous background anatomy, leaving just the images of the vascular structures containing the contrast agent. This technique produces excellent images of the vascular structures but can be adversely affected by patient motion. Patient movement, respiratory motion, bowel motion, and swallowing are some of the kinds of movements that can significantly degrade the image quality.

In the early 1970's, subtraction was attempted using video TV systems and analog storage screens, but the technique had poor reliability and image quality. Digital subtraction angiography (DSA) using digital acquisition and processing became a reality by the end of this decade, with Mistretta and co-workers at the University of Wisconsin and Ovitt and co-workers at the University of Arizona detailing their work in applications of intravenous studies [10, 11]. DSA enables the performance of angiography digitally, allowing a radiologist or cardiologist to zero in on the point of interest by digitally eliminating unnecessary detail from the area. First, an image of the organ is taken without the contrast material and is stored on the computer. The contrast material is then injected and a second image is taken digitally. The first image is then subtracted from the second one. The resulting image shows only those areas where the contrast material is present. The first image is referred to as the mask. The final one is the subtracted one.

DSA is gradually taking over conventional angiography and has become the method of choice for imaging the vascular system. Its advantages over screen-film angiography include reduced examination times and lower film costs. Digital images are available for review immediately after the operation and images can be printed out as films as needed. The digital subtraction technique also reduced radiation exposure to a patient by a factor of two. In many institutions, film angiograms are being phased out entirely.

State of the art digital angiography systems include 1000 x 1000 image matrices, a full suite of quantitative packages for geometric and densitometric analysis, and integration of physiologic signals, e.g., EKG (Electrocardiography), among other components. Also complementing and, sometimes, replacing conventional and digital X-ray angiography is CT angiography and MR angiography, as described in the sections on CT and MR in this chapter.

1.4 Computed tomography

X-ray Computed Tomography (CT or CAT) was the first radiological technique that allowed the generation of tomographic images of every part of the human body without the superimposition of adjacent structures. CT produces very detailed pictures of bones and cartilage, but even more significantly, CT images have a contrast resolution high enough to allow the differentiation of soft tissue within the highly attenuating skull. First demonstrated in London in 1971, CT scanners have evolved through four generations to become a clinical fixture in many of today's hospitals. CT scanners send collimated beams of X-rays through the body to arrays of detectors, which then send these "projections" to computers for reconstruction into the final images.

A CT image is a digitized view of the cross section of the body where each pixel has a number known as the CT number or Hounsfield number. This number is determined by the X-ray attenuation through the body and is directly proportional to the electrons per unit volume. When a beam of monochromatic X-rays passes through a homogenous object, they are attenuated according to the equation:

$$I = I_0 e^{-\int a dx} \tag{1}$$

Where I is the X-ray intensity behind the object, I_0 is the X-ray intensity without the object, x is the length of the X-ray path through the object, and a is the linear attenuation coefficient of the material for the X-ray energy employed.

The human body is not homogeneous, so the equation describing the attenuation becomes:

$$I = I_0 e^{-\int a(x)dx} \tag{2}$$

In order to generate a 2-D CT image, the X-ray attenuation is measured along a number of different of lines within a plane perpendicular to the long axis of the patient with the goal of reconstructing a map of the Hounsfield numbers (expressed in HU) a for this plane. These numbers are often expressed with reference to water:

$$a(\text{in HU}) = 1000\frac{a_{\text{patient}} - a_{\text{water}}}{a_{\text{water}}} \tag{3}$$

First generation CT systems have a single, or perhaps dual, X-ray source and a single detector that moves slowly in planes around the subject. Collimators are employed to limit the pencil X-ray beam to only a part of the detector (Figure 2). Technicians have to translate and rotate the entire linkage around the patient for each plane, resulting in very long study times. Scan-time for one scan is almost 5 minutes.

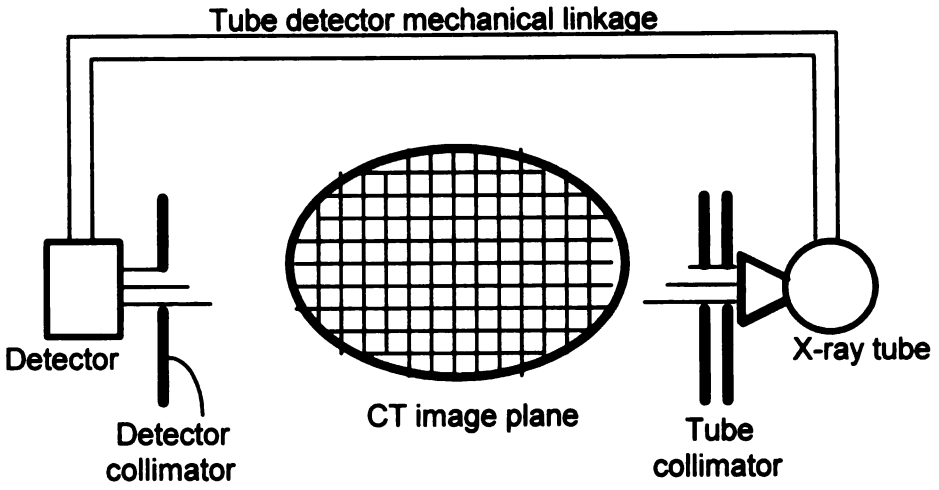

Figure 2 This figure approximates the first generation of CT scanners. The image plane consists of a grid of voxels through which X-rays are projected. The detector measures the transmission along the particular path from the X-ray tube to the detector, and many such transmissions are needed at different angles to reconstruct the attenuation values of each voxel.

Intensity values are obtained from series of transmission measurements taken as a function time.

The projected intensities as a function of position at various angles are found (Figure 3).

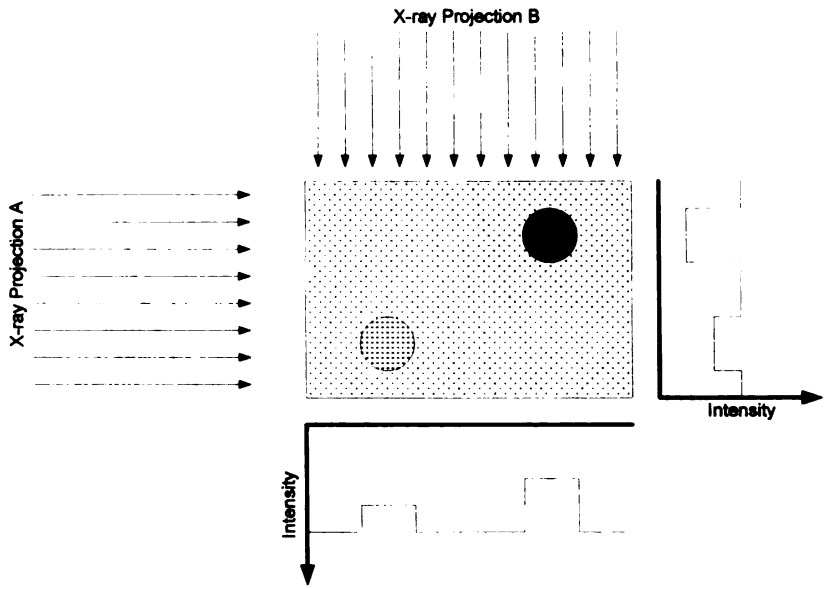

Figure 3 Two projections through a phantom containing a low density region and high density region. The intensity of the X-rays exiting from the phantom decrease in the areas of the two regions of interest. The magnitude of the intensity reduction in the low density region is one-half that of the intensity reduction in the high density region. Projection A X-rays have to penetrate a longer path through the phantom, resulting in a lower intensity profile compared to Projection B.

Subsequent generations of CT systems were developed to reduce scan times and are based on a fan beam geometry in which several detectors are utilized all at once (see Figure 4). Second-generation scanners use either a fanlike X-ray beam or multiple beams and multiple detectors, and a gantry that moves in larger steps, collecting more information in less time. Multiple detectors in the plane of the cut permit the simultaneous acquisition of transmission measurements along a number of non-parallel rays in second-generation systems. The fan-shaped X-ray beam is utilized at several projection angles to acquire the intensity profiles. The image is reconstructed by either rearranging the projections into groups of parallel projections or more directly by using the original projections with a modified fan beam reconstruction algorithm. Third generation systems use a beam wide enough to cover the entire cross-section

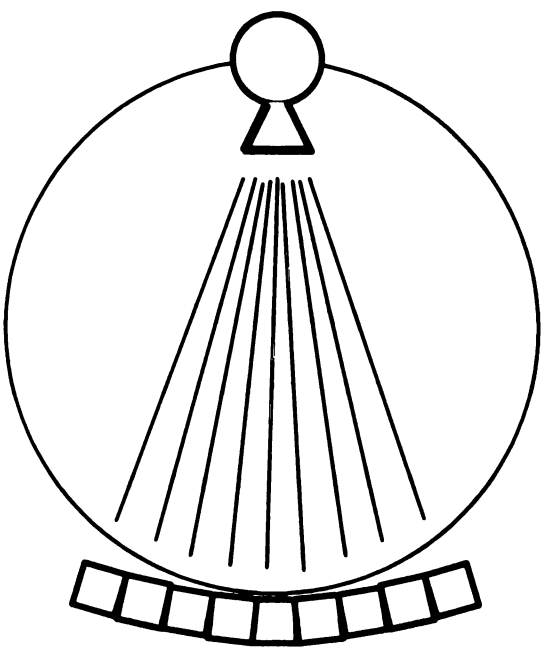

Figure 4 Basic fan-beam geometry of X-ray CT systems. The X-ray source is at the top, and array of detectors is located at the bottom. The intensity profile detected at each of the detectors contributes to the overall intensity profile of the object being imaged.

while the whole X-ray tube and detector array assembly rotate concentrically around the patient, resulting in scan-times of seconds rather than minutes. Although they were fast, the third-

generation systems suffered from artifacts produced by the circular motion of the rotating tubes and detectors. Thus, the fourth-generation CT was designed and had a complete ring of fixed detectors while rotating only the X-ray tube.

CT development continued through the 1980's with the "Imatron" scanner and spiral CT. Douglas Boyd, a physicist at the University of California, San Francisco, developed a super fast CT system known as "Imatron" which has no moving parts and can obtain a picture in 50 to 100 milliseconds. Such speed is adequate to image the heart between beats, so it has been especially useful in coronary checkups. The "Imatron" can also acquire images in seven planes simultaneously, allowing for a variety of perspectives. The first spiral CT system entered the market in 1989. Spiral CT acquires data continuously over a large volume of the body instead of taking a series of separate, parallel slices as in conventional CT. Slip-ring technology adopted from radar enables the continuous motion of the X-ray tube and detectors, resulting in a spiral motion during which the patient is moved swiftly through the gantry as data is constantly acquired. The volumetric data can be processed into cross-sections of arbitrary thickness, as thin as four millimeters, or reconstructed into 3-D renderings. Spiral CT is usually used without any contrast media, saving money and possible allergic reactions on the part of the patient.

Also, the introduction of spiral CT scanning has ushered in the development of minimally invasive spiral CT angiography. CT angiography combines the rapid, volumetric acquisition of the spiral CT scanner with an accurately timed high-flow peripheral intravenous injection of iodinated contrast material. The resulting images are rendered into 3-D images of the vasculature.

1.5 Magnetic resonance imaging

Magnetic resonance imaging (MRI), also referred to as nuclear magnetic resonance (NMR), techniques were first described in the late 1940's by Bloch of Stanford and Purcell of Harvard [12, 13]. Their combined theoretical work led to the use of MRI in the analysis of chemical compounds, based upon the ability to magnetize certain nuclei in a strong magnetic field, excite them with the absorption of a specific radio wave frequency, and detect the emitted weak signal upon return to equilibrium. Chemical shift studies and MR spectroscopy evolved over several years.

To elaborate in greater detail, MRI excites the molecules of the body with radio-frequency (RF) range radiation, and then the molecules themselves emit a type of fluorescent radiation, weak signal, that is measured. The signal source is the macroscopic spin magnetization **M** from nuclei with an odd number of neutrons and/or an odd number of protons, such as hydrogen (^{1}H), nitrogen (^{14}N), sodium (^{23}Na), and phosphorus (^{31}P). A nucleus has spin and therefore angular momentum, and when it is place in a magnetic field, the magnetic dipole of the nucleus experiences a torque, which causes it to precess around the magnetic field line (see Figure 5).

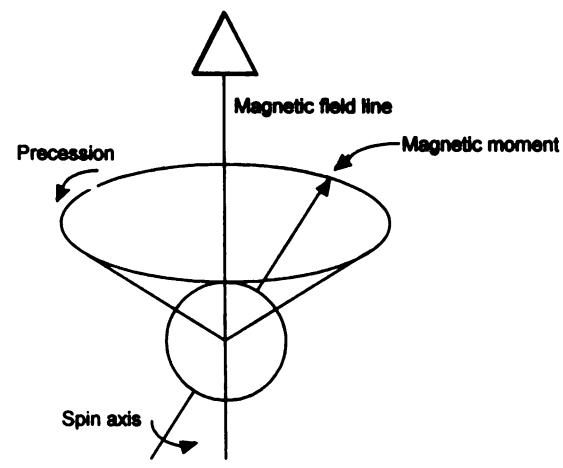

Figure 5 When a spinning nucleus is placed in a magnetic field, the resulting torque induces the nuclear spin axis to precess about the magnetic field lines.

The hydrogen nucleus has two possible orientations of spin with respect to external magnetic fields, parallel and anti parallel. These two orientations are referred to as spin *up* (parallel) and spin *down* (anti parallel). The spin *up* orientation has a lower energy state since it is closer to being aligned to the field, and when an external magnetic field is applied, the lower energy state is favored. More nuclei are oriented *up* when the magnetic field is strong and the temperature is low.

Each individual nucleic magnetic moment is broken down into longitudinal and transverse components with respect to the applied magnetic field. The transverse component is oriented at right angles to the applied magnetic field and precesses at the Larmour frequency. For time spans on the order of seconds, the transverse component averages out to zero. The longitudinal magnetization, on the other hand, remains constant over time provided the nucleus does not change orientation. A material consists of many nuclei, and the cumulative effect of their individual magnetizations is referred to as bulk magnetization. Since most nuclei will align spin *up* in the presence of an external magnetic field, there will be a net magnetization in the direction of the magnetic field.

The MRI signal is created by the changing in direction of the transverse component of the bulk magnetization. First, external energy in the form of a rotating magnetic field ($\mathbf{B}_1$) is applied in addition to the static magnetic field ($\mathbf{B}_0$). The nuclei are promoted into the higher spin *down* energy state. After this excitation the nuclei rapidly change back to the spin *up* energy state in a process called free-induction decay (FID) in which energy is released. Disregarding the longitudinal component, the radiation emitted by the re-alignment of the transverse component is detected as the MRI signal.

The magnetic field rotates at the Larmour frequency to create resonance and is a circularly polarized RF field. The change in angle of the bulk magnetization, due to the circularly polarized RF field, is proportional to the strength of the RF magnetic field, the gyro magnetic ratio, and the duration for which the RF magnetic field is applied. The RF field is usually applied for the time needed to rotate the bulk magnetization either 90 degrees or 180 degrees.

The rate at which the system returns back to its stable orientation after application of the excitatory rotating magnetic field is expressed in terms of the time constant in the exponential relationship, called the relaxation time:

$$\mathbf{A} = \mathbf{A}_0 e^{\frac{-t}{\tau}} \tag{4}$$

where $\mathbf{A}_0$ is the initial amplitude, t is the time, and τ is the characteristic time of relaxation.

There are two physically distinct modes of relaxation. The first is T1 and refers to the longitudinal or spin-lattice relaxation time. T1 is the time it takes the longitudinal magnetization to reach a steady state after excitation and involves interaction of nuclear spins with the lattice. This spin-lattice interaction is tissue specific, and the T1 of muscle or soft tissue organs is much shorter than that for blood and cerebrospinal fluid.

The other relaxation time is called the transverse or spin-spin relaxation and is denoted by T2. In steady state there is no net transverse magnetization where the nuclei are randomly oriented, but one can be created by a 90-degree rotation of the bulk magnetization. After excitation more nuclear magnetic moments are pointed in phase in the one direction than the other. The relaxation of nuclei from the excited, in-phase state to the random, steady state involves interactions between nuclei and is a longer-range interaction than the spin-lattice interaction. Like T2, T1 is also tissue-specific; for example, the T2 values of cancerous tissue are considerably

longer than for the normal tissue. T1 and T2 contribute independently to the contrast between different tissues.

The motion of the magnetization vector of uncoupled spins, such as those for protons in water, is described in terms of the phenomenological Bloch equations:

$$\frac{d\mathbf{M}}{dt} = \gamma\mathbf{M} \times \mathbf{B} - \frac{M_{xy}}{T_2} - \frac{M_z - M_0}{T_1} \tag{5}$$

where $\mathbf{B}$ is the effective field, M_0 the equilibrium magnetization, and T_1 and T_2 the relaxation times. The gyro magnetic ratio (γ) is the fixed ratio between the angular momentum and the magnetic moment of a given nucleus. This ratio is unique to each and every nucleus; thus, the speed of precession is characteristic for the nuclide given a particular magnetic field strength. This speed or the number of precessions completed per second is the Larmour frequency:

$$\omega_0 = \gamma\mathbf{B}_0 \tag{6}$$

where $\mathbf{B}_0$ is the magnetic field strength. In the presence of magnetic fields on the order of 1 Tesla (10,000 Gauss), the Larmour frequencies range from a few megahertz to a high of approximately 42.5 megahertz for ordinary hydrogen (^{1}H).

Rather than sampling in object space as in CT, the MRI signal is sampled in the spatial frequency domain. The most common technique involves alternate application of two or three orthogonal gradients. A one-dimensional readout gradient is applied to detect and sample the signal, producing a rectilinear grid of data from which the image pixel amplitudes are obtained by the discrete Fourier transform. Data acquisition time was drastically shortened with the development of 2-D and 3-D Fourier transform techniques, as well as the multi-slice data

acquisition methods introduced by Crooks and co-workers at University of California, San Francisco [14].

NMR imaging hit the clinical mainstream by the mid 1980's and the name was changed to magnetic resonance imaging (MRI) to avoid any public misconceptions about the word "nuclear." It was once thought that MRI would never be as fast or have as high a spatial resolution as CT scans. That has been disproved with the development of extremely fast echo planar imaging, where an image can be acquired in as little as 50 milliseconds per slice, and MR microscopy capabilities with resolution down to tens of microns.

MRI and MR spectroscopy techniques and applications continue to progress rapidly, with new pulse sequences, intravenous contrast agents, and fast image acquisition. Besides the anatomic imaging with spin-echo and inversion recovery pulse sequences, MRI is capable of producing non-invasive angiographic images approaching the quality of X-ray angiograms, quantifying velocity and flow of blood, selectively exciting small volumes of tissues for non-invasive MR spectroscopy of several elements, and performing functional imaging scans of the brain [15].

1.6 Nuclear medicine imaging

Nuclear medicine radionuclide imaging involves the use of unstable atoms, which disintegrate to release energy in the form of γ-rays. Hevesy pioneered the creation and manipulation of biologically safe and useful radioactive tracers when he demonstrated that radioisotopes fed to laboratory rats had affinities for particular organs [16]. This demonstration triggered the creation of radioactive isotopes that home in on and label specific organs. At the same time, Ernest Lawrence at the University of California's Radiation Laboratory in Berkeley used a cyclotron to

produce a radioactive isotope of sodium, which could be introduced harmlessly into the body, and over next several years, he manufactured seventeen other biologically useful radioisotopes.

When these radioisotopes are attached to substances that undergo normal physiological processing in a patient, selected organ systems can be imaged. For example, given that damaged red blood cells accumulate in the spleen, red bloods cells are extracted from the patient, damaged, and tagged with a radioactive substance to yield a radioactive-labeled pharmaceutical (radiopharmaceutical). This radiopharmaceutical is reintroduced into the bloodstream of the patient, and as it accumulates in the spleen, an image of the organ is captured on a screen or film. Most radiopharmaceuticals used in nuclear medicine are labeled with radionuclides that emit γ-rays or photons and have to be swallowed, inhaled, or injected into the body. Although it is possible to evaluate almost any organ in the body in nuclear medicine, the liver, spleen, bones, urinary tract, lungs, heart, thyroid, and brain are the organs most frequently imaged. The resulting images highlight "hot" or "cold" areas of the body, depending on the functional or anatomic state.

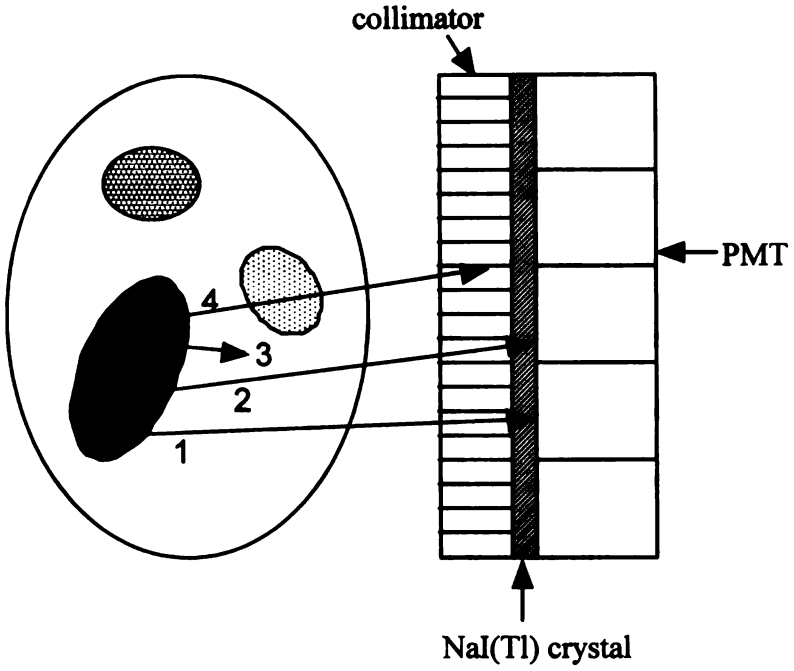

Figure 6 The typical nuclear medicine imaging system consists of a collimator, NaI(Tl) crystal, and photomultiplier tubes (PMTs).

A scintillation camera is commonly used to capture the 2-D projection image of the 3-D radiopharmaceutical uptake within the patient. A lead collimator allows photons traveling in certain directions to pass through a large-are scintillator (usually NaI(Tl) crystal) that converts the energy of γ-ray photons to lower-energy photons which are in turn converted into electric signals by the photomultiplier tubes (PMTs) (Figure 6). The electric signals are processed to yield information about the position at which a photon interacts with the crystal.

1.7 Single Photon Emission Computed Tomography

Single photon emission computed tomography (SPECT) is a medical imaging technique that is based on conventional nuclear medicine imaging and tomographic reconstruction methods. SPECT had its origins in the early work of Kuhl and Edwards [17]. In 1968 SPECT evolved from Kuhl's first system for mapping photon emission from internal radioactive substances, single photon emission tomography (SPET), which used fixed cameras to record single lines of

photons as the patient was rotated. By adding a computer and rotating camera with an immobile patient, Kuhl turned SPET into SPECT.

SPECT provides tomographic images by detecting and reconstructing γ-ray emissions from radiopharmaceuticals injected into the body. A scintillation camera system is used as the imaging device and consists of a lead collimator that allows only those photons traveling in given directions to pass through a large-area scintillator. By utilizing methods of image reconstruction from different projections, SPECT takes the conventional 2-D nuclear medicine images acquired at different views around the patient and provides an estimate of the 3-D activity. SPECT systems are relatively inexpensive and easy to operate in a clinical setting, and they are the most frequently used emission-scanning technique used all over the world.

There are three basic categories of SPECT systems: those that use (1) arrays of multiple scintillation detectors, (2) one or more scintillation cameras, or (3) hybrid scintillation detectors combining the first two approaches. Multiple-camera-based SPECT systems have increased the detection efficiency over single-camera systems (Figure 7). The three-camera design allows 360 degree sampling in period as short as 5 s.

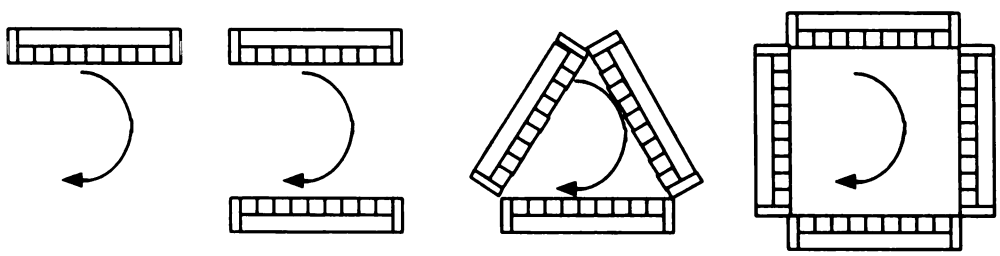

Figure 7 These multiple-camera-based SPECT systems increase the detection efficiency by surrounding the patient with cameras.

SPECT assesses the functional aspects of a patient in real-time and is being employed to image bone cancer, blood flow in the heart, brain and liver, and acute myocardial infarction despite

several disadvantages. SPECT's major drawback compared to the other major nuclear medicine imaging modality, PET is its quite poor spatial resolution, only half that of PET.

The most common collimator design used in nuclear medicine and SPECT consists of parallel holes, and in such collimators the detection efficiency can be increased only at the expense of a concurrent degradation of spatial resolution. Two special SPECT collimator designs that don't have such a trade-off are fan-beam and cone-beam geometries, providing about 1.5 to 2 times the detection efficiency of a parallel-hole collimator with the same spatial resolution. Furthermore, SPECT exposes the whole body to small doses of radioactivity for periods as long as days. This length of exposure is due to the use of isotopes that can be economically generated at a central location and shipped to hospitals.

1.8 Positron emission tomography

Positron emission tomography (PET) differs from SPECT in its use of positron rather than gamma ray emitting isotopes. Positrons, the positive antiparticles of electrons, were first detected in 1932, and in the early 1950s the medical imaging potential of a particular class of positron-emitting radioactive substances was first realized. The first scans of the brain tumors occurred in 1952 by Brownell and Sweet, but PET did not become a tomographic modality Hounsfield's publication of his description of EMI's CT scanner in 1973 [18, 19]. The reconstruction formulas of *transmission* tomography --passing X-rays through the body - were finally applied to *emission* tomography - tracking the radioactive source within. The last twenty years have seen the greatest strides made in PET systems; since 1975 spatial resolution has increased from 14 mm to 4 mm, number of detectors from 64 to 19,000, and data per study 4 kilobytes to 4 megabytes.

A PET imaging study commences with the injection of a radiopharmaceutical tagged with a positron-emitting isotope such as ^{11}C, ^{13}N, ^{15}O, or ^{18}F. The now-tagged biological molecule then accumulates in the particular area of the body for which it has an affinity. For example, a glucose analog labeled with ^{18}F accumulates in the brain or in tumors, where glucose is the primary source of energy. The radioactive nuclei then decay, emitting their positrons. The positrons never make it to the detectors, however, because each one almost instantaneously combines with a nearby electron. The two particles annihilate each other, and in the process produce two photons that fly away from each other at a 180-degree angle. The combined masses of the electron and positron are converted to energy, and this energy is equally divided to yield the pair of 511keV photons. These high-energy γ-rays emerge from the body and are detected by the detectors that surround the patient (Figure 8).

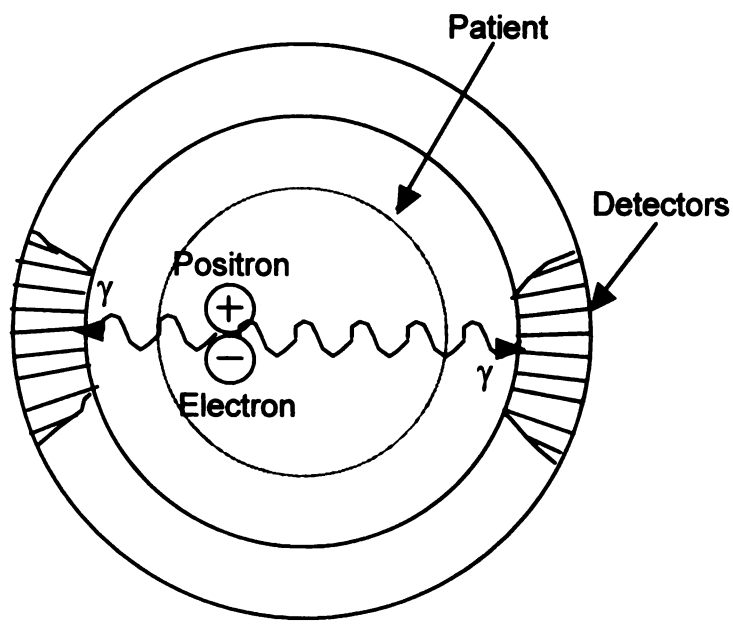

Figure 8 A radioactive nucleus decays, emitting a single positron. The positron immediately annihilates with a nearby electron, releasing two γ-rays which fly away from each other at a 180 degree angle. The circular arrangement of the PET detectors detects the simultaneous incidence of the two co-linear 511keV γ-rays.

This "coincidence" phenomenon is the key to how a PET scanner reconstructs the 3-D radiopharmaceutical distribution. When a pair of detectors records the simultaneous incidence of two γ-rays, the annihilation event that produced the pair of γ-rays must have occurred somewhere along the line connecting the two detectors. If one of the γ-rays was scattered, the line of coincidence will be incorrect. The tracer distribution is calculated using tomographic reconstruction procedures after at least 100,000 annihilation events are detected:

$$P = e^{-\int a(s)ds} \int f(s)ds \tag{7}$$

where P is the projection data, $a(s)$ is the linear attenuation coefficient for 511-keV γ-rays, and $f(s)$ is the isotope distribution. This equation ignores the effects of scattering, which is significant in a subset of PET imaging situations. The exponential factor accounts for the attenuation of the two γ-rays inside the patient's body.

PET reconstructs a 2-D image from the acquired one-dimensional projections at various angles. 3-D reconstructions are also obtainable from 2-D projections at various angles (Figure 9). After correcting for the attenuation and scatter of the γ-rays, the resulting images provide a quantitative measure of the radioactive tracer distribution, and hence the physiological state of that area of the body. PET can be used to qualitatively evaluate areas of the body where unusual tracer accumulations occurs such as in tumors.

Clinical applications of PET include studies of epilepsy, Alzheimer's disease, Parkinson's disease, and coronary artery disease, and recent developments have seen success in applying PET to locate tumors and metastatic disease in the brain, breast, lower gastrointestinal tract, lung, and other areas of the body. The advent of whole-body PET in the 1990s has enabled the tracking

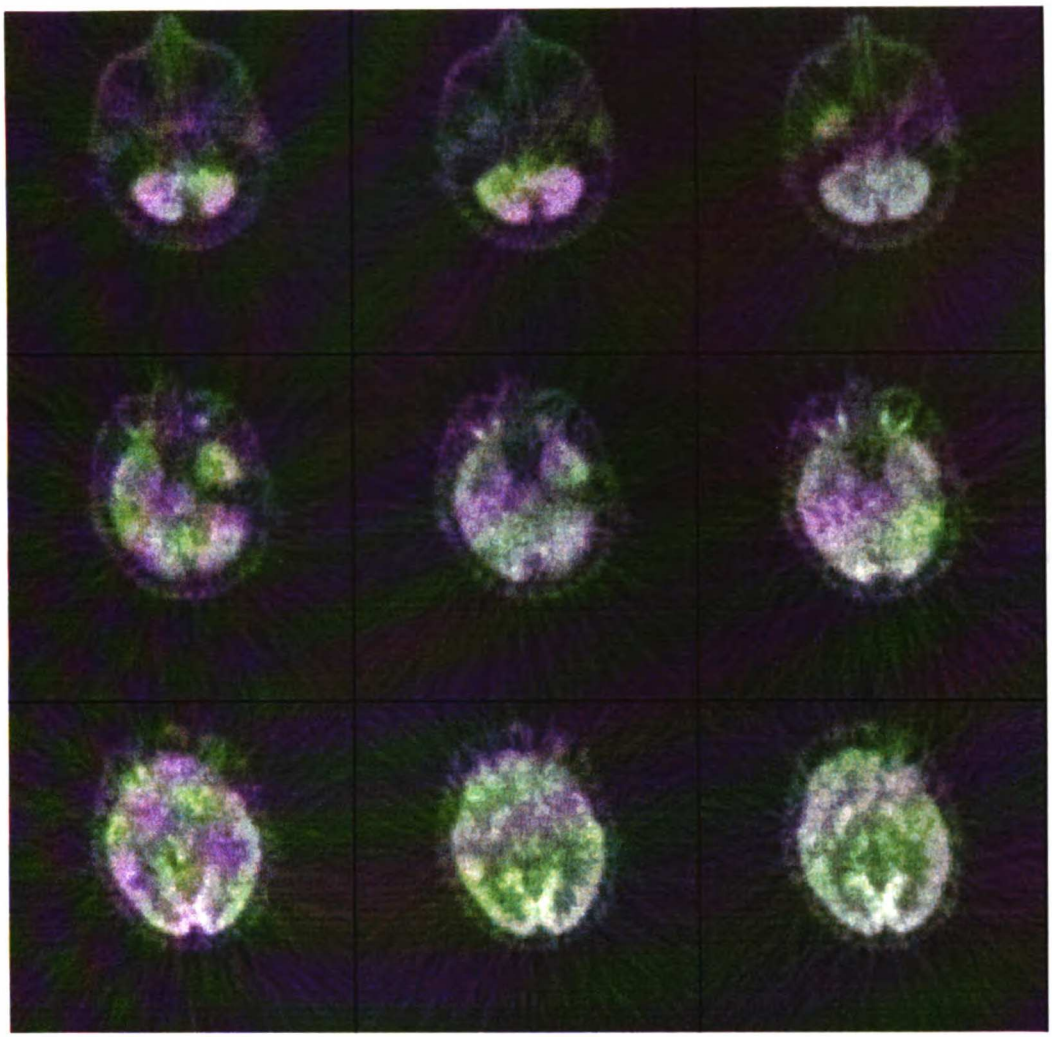

Figure 9 2-[^{18}F]fluoro-2-deoxy-D-glucose PET image slices. These image slices have been reconstructed from the original scanner data contained in the sinogram files and represent a subset of the complete image series for this scan. Areas of high signal intensity correspond to areas of higher glucose uptake.

of the functional development of cancers. Moreover, PET can assess the success or failure of chemotherapies as the various drugs are introduced into the body, rather than waiting weeks for symptoms to appear. Basic research into the changes in metabolism, blood flow, and oxygen utilization has benefited handsomely from PET systems. PET is vastly more sensitive than other cross-sectional imaging modalities like MRI and CT in its ability to quantitatively detect radiopharmaceutical tracer concentrations in the nanomolar range. Unfortunately, PET is a high-cost, research-oriented imaging modality. SPECT image quality and capabilities has begun

to approach that of PET, with much lower equipment and associated operating costs. The future of PET is therefore potentially limited.

1.9 Ultrasound

Ultrasound refers to sound beyond the normal range of human hearing, which is below 20,000 hertz. Galton's production of the first high-frequency sound waves in 1880 predates Roentgen's discovery of the X-ray, but unlike the X-ray, the medical imaging potential of ultrasound waves would have to wait many decades before it was exploited. In fact, it wasn't a medical application but a need to detect submarines using sonar during the first two world wars, which motivated research in the development of ultrasound devices. Early work on medical uses and imaging applications of ultrasound occurred in the late 1940's [2]. The ultrasound devices developed in the 1950s required immersion of the patient in a tank of water, but development did away with this requirement and now only the tip of a moistened cylinder need touch the patient.

The most common type of ultrasound scanner is the B-mode scanner (B-mode stands for brightness modulation), which provides 2-D representations of the reflecting surfaces. The user holds a cylindrical transducer against the skin of the patient. The transducer has an array of individually pulsed piezoelectric elements, which launch an ultrasonic pressure pulse of about 1 microsecond into the patient's body. The pulse propagates until it is reflected by boundaries between mediums having different acoustic impedances. In this way the pulse is scattered and reflected inside the body, and the scattered pressure wave is detected by the transducer array, which converts the mechanical wave into electrical signals via the piezoelectric effect. The resulting signals are used to make an image, which represents the region of the body from which the pressure pulse was reflected.

Ultrasonography is a low-cost, noninvasive, real-time imaging modality with applications in imaging the head and neck, heart, breast, and abdomen. Early ultrasonographers employed echoencephalography to image the intracranial midline structures of the brain looking for evidence of unilateral mass lesions such as brain tumors or subdural hematomas. M-mode (motion) scanning is a dynamic form of B-mode imaging used in investigations of the heart. Evaluation of the heart using ultrasound yields a variety of information regarding valvular mobility, myocardial contractility and cardiac anatomy. Breast masses greater than 1 cm in diameter can be detected with ultrasound. Virtually all of the intra-abdominal organs lend themselves to ultrasonic investigation. The disadvantages of ultrasonography are that areas around the lungs cannot be imaged and the images are not clear.

In recent years, Doppler techniques and color flow imaging devices represent a major area of future expansion in ultrasound, including the ability to perform ultrasound angiography. The increased sensitivity of "power Doppler" technique combined with the use of ultrasound contrast agents may allow the future ability to quantitate organ function with fill and wash-out curves generated by ultrasound angiography, similar to nuclear medicine studies [21, 22]. Ultrasound imaging will continue to expand and flourish in medical imaging due to the unique acquisition capabilities, low cost, and relative safety of these techniques in patient care.

1.10 Magnetic source imaging

The fundamental functional unit in the human brain is the neuron, consisting of a cell body, one or more dendrites, and a single axon. Action potentials are the electrical signals that propagate down the axon. These action potentials are transient changes in the potential (voltage) of the axon membrane. Action potentials are caused by ion flows across axon membranes, and ion channels embedded in the axon membrane regulate these flows. Electroencephalography (EEG)

detects action potentials from the surface of the scalp. EEG has been an important tool in studying brain function for 50 years, but the insulating effects of the skull and tissues seriously hampers its accuracy.

Neuronal electrical currents also induce magnetic fields, which are not, theoretically, distorted by the intervening tissues and skull. These magnetic fields are extremely small, on the order of several pico Tesla (10^{-12} Tesla), and require sensitive superconducting quantum interference device (SQUID) magnetometers [23]. The resulting signals can be analyzed mathematically to yield locations of brain activity as it happens on a millisecond time scale. The estimation of the electric sources on the basis of magnetic field measurements is called magnetic source imaging or MSI. Other terms for the same method include magnetic field tomography and biomagnetic computed tomography. The study of the magnetic fields of the brain is called magnetoencephalography (MEG). In addition to brain activity, magnetic signals can be detected from the heart (magnetocardiography or MKG), from muscles, and from many other body organs.

The first biomagnetic measurements were performed in 1963 on the human heart using an induction-coil magnetometer [24]. The introduction of the SQUID magnetometer by Zimmerman and co-workers brought a vast improvement in sensitivity and allowed the construction of compact sensors [25]. In the seventies, SQUID magnetometers were used for detecting magnetic fields evoked by visual, somatosensory, and auditory stimuli. Starting from the 1980s, SQUID have been applied clinically for non-invasive diagnosis of epilepsy and stroke patients. A SQUID consists of a superconducting niobium ring with a very thin gap to capture the magnetic flux, immersed in liquid helium at 4.2K.

In addition to SQUID technology, several techniques are employed to increase the signal to noise ratio of MSI. Environmental noise from wall power lines or electrical equipment are on the order of 10^5-10^6 times larger than the amplitude of the spikes under study, so the patient must be shielded from such extraneous magnetic fields by conducting MEG or MKG in a magnetically shielded room. The use of inductive coupling of the SQUID to various detector coils and special coil geometries also help to reduce the effects of environmental noise. Patients with low signal to noise ratios of the spontaneous activity or high noise from metallic artifacts such as electrode connectors can be analyzed with event averaging.

Event averaging of the MEG waveforms synchronized to EEG spikes follows these steps: 1) selection of an EEG spike template, 2) selection of all EEG spikes with a similar morphology, 3) alignment of EEG and MEG based on calculation of correlation coefficients for each event (waveform fit with respect to template), and 4) averaging of the MEG waveforms for an event window of 100 msec. EEG is almost always simultaneously recorded with MEG, so that artifacts, such as eye-blinking, heart-beating (electrocardiogram), and other sources of biological magnetic fields can be filtered visually by a trained physician, isolating the epileptiform epochs containing spike or seizure discharges.

Detecting the tiny extracranial magnetic fields is only half the problem. The other half is in localizing the sources of activity by inversely calculating the configuration of the source(s) based on the detected magnetic fields. The solution to an inverse problem is generally not unique and therefore requires constraints and assumptions about the sources of the extracranial field. The single equivalent current dipole (SECD) model is used, assuming that all the magnetic activity measured originates from a single source [26]. The SECD model performs calculations based on the extracranial magnetic fields to determine the 3-D location of a single dipole source which

would generate such fields, taking into account the location, size, and direction of current flow as well as the composition of the brain tissues and skull intervening between the dipole and detector coils. However, the model assumes that the spatial extent of the source is infinitesimally compact, and therefore is prone to larger errors as the size of the source increases or in the presence of multiple sources as is often the case in neurophysiology. Despite these limitations, the SECD model is useful in detecting localized events when brain activity is dominated by a single compact source and is the most rapid and reliable approach for localizing focal magnetic fields of the brain.

The clinical use of MEG has required the development of biomagnetometers using large arrays of detectors to coherently sample the magnetic field pattern over a large portion of the scalp. These large-array systems are commercially available from several commercial manufacturers. One configuration utilizes two 37-channel sensors to simultaneously record magnetic fields from both hemispheres of the brain. One sensor is floor-mounted while the other is suspended from a gantry on the ceiling. Magnetic fields can be recorded from three to four regions on each side of the head for a total of six to eight recording positions. The raw MEG signals resemble the voltage fluctuations of conventional EEG, but unlike EEG, these signals are analyzed by software. Each channel captures a unique profile of the magnetic field, depending on its spatial location relative to the source. The spatial pattern provides the information required to localize the intracranial source of the activity by modeling the source of the activity as a single equivalent current dipole. The program iteratively calculates the parameters of a dipole source, which could have produced the detected magnetic field until a "best dipole fit" is found. This source localization process has millisecond time resolution, enabling the tracking of brain functions with characteristic frequencies greater than 1 kHz.

By having a coordinate transformation from the biomagnetic measurement system and the MRI, it is easy to project all or parts of the reconstructed dipole pathway into a multislice or 3D-MR image of the patient. In biomagnetic source localization, the combined use of the biomagnetic measurement device and an imaging method for the presentation of anatomical structures, e.g., MRI or CT, is of high value. Figure 10 shows an example of MEG dipoles superimposed on anatomical MR image of the epilepsy patient for detecting the source of seizure foci.

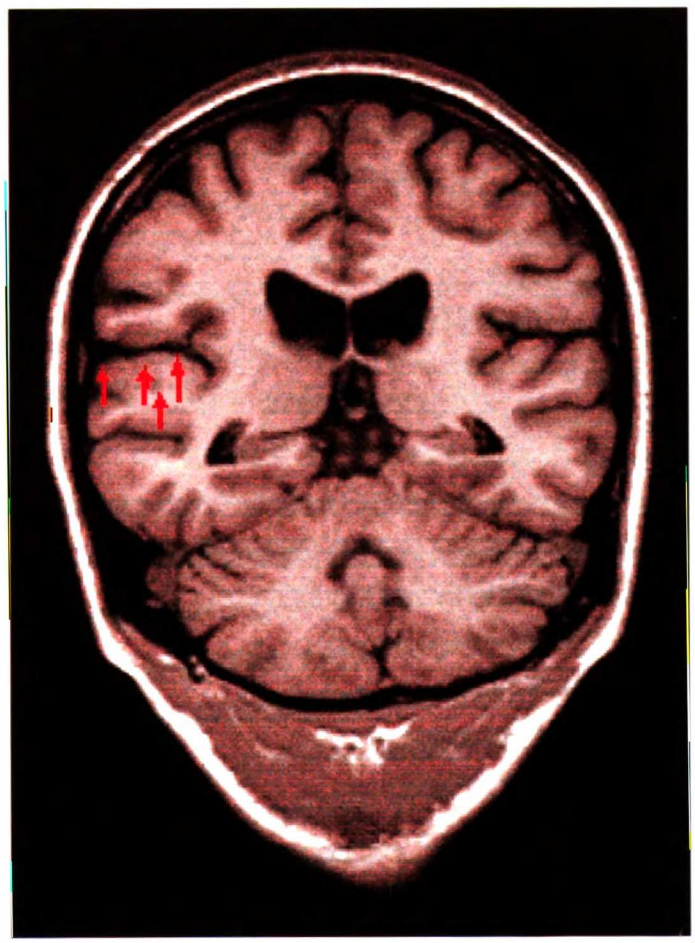

Figure 10 A tight cluster of MEG dipole moments superimposed on a MRI slice. The MEG dipoles correspond to suspected areas of epileptogenic activity in the temporal lobe.

1.11 Summary

This chapter provides an overview of the technical developments of major medical imaging modalities. The major developments include the introduction of X-ray radiography about a century ago and the rapid adoption of other imaging techniques in the past decades, such as computed tomography, various forms of MRI, digital subtraction angiography, digital radiography, nuclear medicine imaging, ultrasound, and magnetoencephalography. These imaging modalities have revolutionized the practice of modern medicine and provide non-invasive means for diagnosis, treatment planning, and disease management.

Chapter 2.

EXTENDING IMAGING SERVICES BEYOND RADIOLOGICAL READING

2.1 Introduction

The trend in medical imaging is increasingly digital and multimedia [27]. The motivation is to represent medical images in digital form supporting image transfer and archiving and to manipulate visual biological information in useful and novel ways, such as image enhancement, therapy planning, and biomedical research. The vision of all digital radiology environments in hospitals pushes for electronic acquisition, storage, communication, and display of large volumes of biomedical images. Meanwhile, the rise of managed care has reduced payments for imaging services. Computer systems promise more efficient operations, thus addressing the need to do more with less. They allow elements of care to be geographically dispersed and support growth of telemedicine and regionalized healthcare. Increasing interest from information systems managers and hospital administrators to consolidate and integrate various medical information systems to curb operating costs while providing better medical services. Smaller hospitals are becoming now dependent on regional imaging centers to provide access to specialized radiological services such as MRI and PET, and PACS serves as the storage and distribution center of the medical images over wide area networks, internet, and phone lines to the other hospitals.

2.2 Definitions and challenges in managing medical images

Broadly speaking, an image database system is a database management system (DBMS) that can access and manipulate any features or regions of interest in images defined in an image data

model as a relational database system today does for any portions of data defined in records or tables. A medical image database system (MIDS) is an image database system that manages a large amount of multimodal, heterogeneous, changing, pictorial, and symbolic data and provides a means to query and manipulate these medical data in an efficient manner to facilitate optimal decision making in a health care environment. A properly organized imaging database can compensate for limitations in human memory and in film recording, and open up many new vistas to improve patient care, biomedical research, and education.

Considerable effort has been spent on developing textual medical databases. However, the fusion of medical images with other patient data in imaging databases raises many new challenging issues, owing to fundamental differences between information acquired and represented in images and in text. In what follows, I describe the key issues; some of them have recently been explored in a National Institutes of Health workshop on medical imaging databases [7].

2.2.1 Multimodality

A plethora of digital modalities now available generate medical images containing different biomedical information, e.g., anatomical, biochemical, physiological, geometrical, and spatial, of different body organs, e.g., brain, heart, chest, and liver. Features and information obtained in multimodal images are diverse and interrelated in complex ways that they are not always easy to interpret. Geometric considerations, such as location and volume, are as important as organ functionality, such as heart and liver. Physiological changes, such as the rate of cerebral blood flow, may have subsequent effect on body biochemical activities, such as the intensity level of neural metabolites.

2.2.2 Data heterogeneity

Medical image data are heterogeneous in how they are collected, distributed, and displayed. Images are acquired from the scanners of different modalities and in different positions, represented in internal data formats that are varied with modalities and manufacturers, and displayed in divergent appearance, orientation, and spatial resolution. Scans of PET and CT look entirely different from one another, and also distinct from other modalities, such as MRI, computed radiography (CR), and ultrasound. PET scans different body parts from that of mammography images. Even within the same modality and for the same anatomy, two sets of medical images can vary greatly in slide thickness, dataset orientation, scanning range, and data representation. It is worth noting that diagnostic images are acquired and displayed in gray scale. Color images are edited only for illustration purposes; physicians rarely use color images in diagnosis and therapy workups.

2.2.3 Structural and functional contexts

Structural information in a medical image contributes essential knowledge of the disease state and clinical decisions. For example, the location of a tumor, as well as its adjacent anatomical structures, has profound implication in therapeutic planning (spatial context), whereas monitoring of growth or shrinkage of that tumor is an important indicator of the patient's progress in therapy (geometric context). What distinguishes medical images from other types of digital images, however, is the representation of functional information, e.g., biochemistry and physiology, of body parts, in addition to their anatomical contents and structures. As an example, temporal lobe hypometabolism exhibited in SPECT scans if not coincide with the tissue atrophy of the suspected region shown in MRI images may indicate that a different epileptic focus as otherwise would be concluded.

2.2.4 Large data sets

Another characteristic of medical images distinct from textual records is their large data sizes. Images acquired in one examination can range from one or two megabytes of nuclear medicine modalities to around 32 megabytes in mammograms and digital radiographs. Medical images accumulated in a major hospital are on the order of a terabyte a year [28]. These digital modalities generated such a large volume of image data that traditional methods employed in textual databases for information management are inadequate. These large data sets call for more advanced algorithms to manage multimodal images and their complementary textual information for database processing.

2.2.5 Imprecision

Images contain information that is often imprecise and can only be expressed informally. This phenomenon applies to entire data sets as well as features within individual images. The boundary of a tumor, for example, may be fuzzy, depending on the resolution of the imaging modality that is used. Yet, the accurate delineation of a tumor is an essential first step for curative therapy. Worst, the imprecision of image resolution is often compounded by the vague description of features extracted from the images or ambiguous coding of disease classification in diagnostic reports. For instance, the diagnosis "acute myocardial infarction, anterior wall" imparts a sense of certainty and specificity, and can be linked to ICD-9 (International Classification of Diseases, ninth revision) code 410.10. On the other hand, for the diagnosis "left ventricular aneurysm," an agreeable definition has yet to reach within the medical community. New, more expressive data/knowledge models that can cope with such imprecision are needed.

2.2.6 Temporal

Staging of the disease state and the monitoring of patient progress over time are fundamental to diagnostic and therapeutic decisions and to outcome assessment in long term follow up. The ability to define and tract temporal relation in the medical image sets of a patient taken at different periods, together with the medical history of that patient, is an essential component of medical image databases. As the database expands to incorporate a large mass of similar patient data, tools developed for the intra-subject temporal monitoring can also be extended to inter-subject temporal comparison to improve prognostic and diagnostic outcomes.

2.2.7 Infrastructure support

The accessibility to heterogeneous images, patient data, and medical reference materials from diverse sources in the clinical decision making process presupposes the existence of a communication infrastructure. The reality, however, is that most databases and information systems in hospitals today are disjoint, are under control of different medical sections and departments, and often do not communicate with external reference database networks as well [29]. The isolation creates many technological and administrative barriers that make the gathering of information cohesively from different medical images to extract objective, medically relevant, and statistically valid disease knowledge extremely difficult. This lack of supporting infrastructure causes the concept of multimedia data integration far from practical deployment.

2.2.8 Security

Along with the multimedia data integration comes a new issue: How does one establish integrity and privacy in medical images and records that exist only in the easily altered digital storage of computers. This issue is especially prominent when an image database framework is connecting to national and international medical database networks. An insecure information system is

unlikely to be acceptable by the conservative medical community due to legal-medical complications. The effort of applying cryptographic techniques to medical images, without noticeably effect on system performance, is just in the beginning [30].

2.3 Clinical information systems

The modern hospital relies on several information systems for managing clinical and administrative data. The hospital information system (HIS) keeps track of patient demographic data, admission/discharge records, laboratory test results, and diagnostic reports. The radiological information system (RIS) manages the scheduling of patients for radiological services and stores the resulting radiological reports. The picture archiving and communication system (PACS) stores, distributes, and displays medical images to support diagnostic analysis. The image data warehouse builds on top of these information systems, leveraging the archived data while adding additional services not supported by these systems.

2.4 Picture archiving communication systems

To meet the challenges of acquiring, archiving, communicating, and displaying medical images, PACSs were developed during the last decade as image management systems [4]. A PACS is a system integration of many components, including image acquisition devices, computers, communication networks, image display workstations, and database management systems. PACS have been the prevalent means for acquisition, storage, communication, and display of digital images related to radiological practice during the last decade [31]. PACS operations can be summarized as follows: (i) Digital images generated in an examination are captured by an acquisition computer and sent immediately to a central database for long term archive; (ii) these images then will be retrieved later from the central archive and transmitted to display at a remote

medical display station automatically or upon the user's request; and (iii) diagnostic findings of viewing these images are appended to the images at the central archive.

First generation PACS was designed to support direct radiological softcopy readings, but were not intended to integrate other related textual information sources of radiological practice [27]. Several hundred of the first generation systems are currently deployed in hospitals worldwide. The subsequent development of the second generation PACS, also known as HI-PACS or Enterprise PACS [32, 33], has included the integration of PACS with heterogeneous information systems like HIS and RIS, the migration to an open client/server system architecture, and the implementation of recognized industrial standards in image and data format, i.e., DICOM and Health Level 7 (HL7) [34]. This integration trend continues as PACS takes its place in the enterprise effort to provide more efficient and cost-effective access to all medical data to support patient care [35]. HI-PACS are more expensive in deployment, usually costing a few to tens of millions dollars for deployment.

A PACS manages the flow of images from the imaging scanner to the display workstation (Figure 11). Digital images of an imaging scanner generated in an examination are captured by an acquisition computer and sent immediately to a central database for long-term archive. These

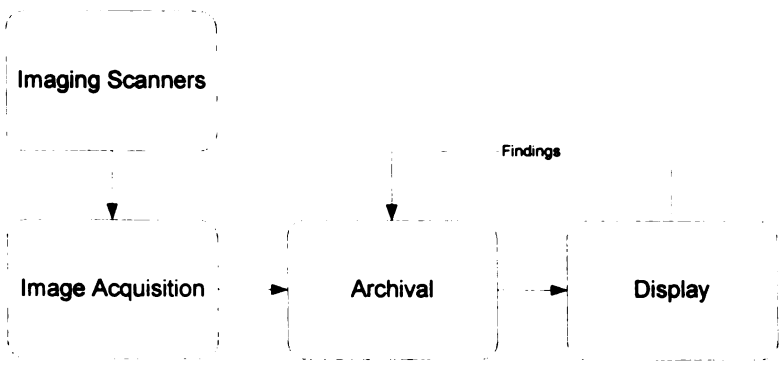

Figure 11 The basic operational flow of PACS illustrates how PACS acquires images from the imaging scanner, communicates the images to display stations, and stores the images in the permanent archive.

images then will be retrieved later from the central archive and transmitted to display at a remote medical display station automatically or upon the user's request. Diagnostic findings of viewing these images are appended with the images at the central archive.

Depending on the application, a PACS can be a simple or complex system. For example, a PACS for an intensive care unit can be a simple system comprising a video camera for digitization of radiographs, a broadband video system to transmit the images, and a video monitor to receive and display images. On the other hand, a departmental PACS is comprehensive and requires careful planning and large capital investment. During the past decade, several large-scale picture archiving and communication systems have been developed and are in clinical trial and use [31, 36-39].

In spite of these technological advances, widespread availability of the medical imaging record still relies on the hand-carried film jacket. Fundamental system integration and operational issues have not yet completely been resolved. The notable issues include the absence of data exchange and protocol standards for different imaging devices and of cost effective means for multimedia networking and storage.

Recently, the HI-PACS aims to remedy the shortcomings of first generation PAC systems [27, 33, 40]. Figure 12 shows a schematic diagram of the HI-PACS installed in the University of California at San Francisco (UCSF). The implementation of this HI-PACS emphasizes recognized and implemented standards, open systems connectivity, hierarchy memory management, database integration, and security. The PACS fiber-optic backbone has been installed interconnecting four major facilities in UCSF, i.e., Moffitt and Long hospitals, ambulatory care clinic, and campus library, to provide a fully connected data bank that links various clinical databases, imaging devices, and medical reference sources. The HIS and RIS are interfaced to the HI-PACS through the use of the HL7 standard for text data and TCP/IP (Transmission Control Protocol/Internet

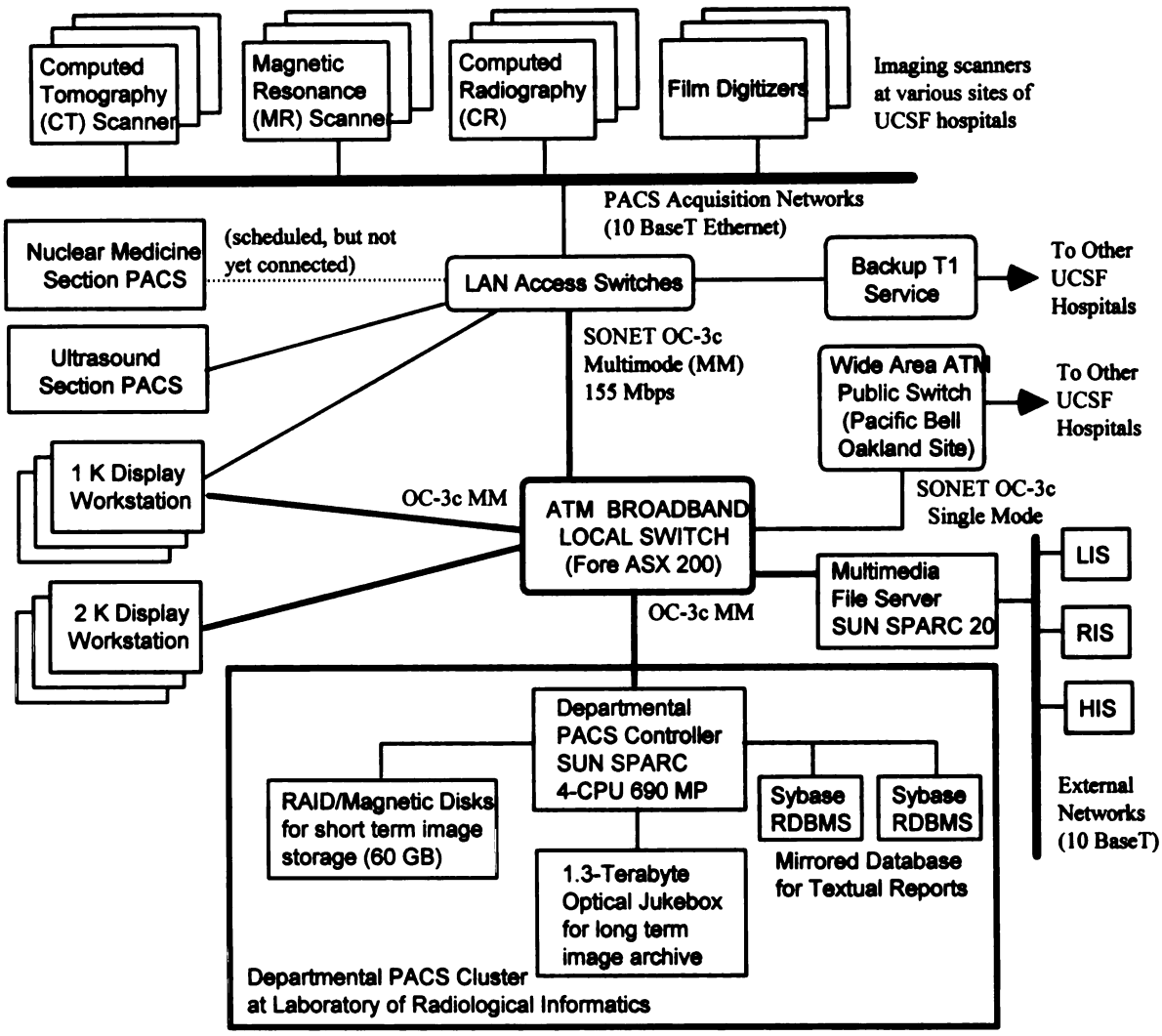

Figure 12. Schematic diagram of the HI-PACS at UCSF. The data sources include the digital imaging modalities CT, MRI, CR, film digitizers, and ultrasound. The PACS has both low and high resolution (1K and 2K) display workstations located throughout the radiology wards as well as the emergency room and intensive care unit.

Protocol).

RIS manages the workflow of the radiology department and stores alphanumeric patient information, such as patient demographics, diagnostic reports, and image study worklists. HIS is run by the hospital information technology department and supplements additional clinical and administrative information of a patient not captured by RIS. The integration of these three

information systems provides a comprehensive view of imaging workflow in the hospitals as well as image-related information of a patient. As the framework evolves, HI-PACS will integrate more clinical databases into its networks, i.e., laboratory information systems.

The original intent of picture archiving and communication systems is to provide management and distribution of image files in a digital radiology department. Recent effort is to gather images of different modalities and coupled them with the information carried in the patient reports for better correlation of diagnosis findings [33]. The file system management only handles query by artificial keys, such as a patient's name or a hospital ID, and lacks the means to organize, synthesize, and present medical images and associated text to the users in a structured way for database applications. Not only is the analysis and archiving of images for any single patient not well addressed, but there is little effort to gather data from images of different patients and couple them with the information carried in the clinical text reports for the purpose of obtaining relevant disease knowledge.

The vast storehouse of multimodal images and textual data consolidated in a HI-PACS overcomes many administrative and technological barriers of gathering scattered and fragmented medical images and textual data and loading them into the epilepsy data warehouse. The formation of the data warehouse may be hypothetical and shallow without a rich multimedia data bank as a foundation. Consequently, the database research would not have any practical relevance. On the other hand, HI-PAC systems represent the most advanced communication and networking environment found in hospitals today and thus can serve as a ready-made infrastructure to support imaging database experiments that are difficult to simulate or evaluate in isolation.

PACS is being widely implemented in radiology departments today to support daily clinical diagnosis. PACS is designed to enable efficient communication, archival, and display of medical images and related textual data. Images are visualized on radiology display workstations that have easy and fast access to the PACS. It is difficult to access the PACS images and associated data outside the radiology department for image visualization and analysis, and there is a need for a sophisticated means of managing the data derived from image analysis in a way that is accessible and modifiable by remote clinicians.

2.5 New imaging services

Despite the broad range of digital imaging applications in diagnosis, therapy, and prognosis, tools for archiving, communicating, classifying, organizing, and retrieving medical images to take full advantage of their rich information content are virtually nonexistent [7]. The lack of mechanisms to manage and distribute complex, interrelated, diagnostic images and text data hinders the effective use of primary imaging modalities in routine medical practice, research, and education. During the last decades, individual investigators of medical imaging have been working on their own modalities in isolation, and, on the other hand, the medical informatics community focused primarily on textual information processing [41, 42]. Recent advances in computers and networks, demands for cost-effective delivery of health care, and the presence of recognized and implemented standards, bring together the imaging and informatics professionals in the effort of integrating primary digital modalities and clinical databases into digital radiology. This effort also aims to facilitate the "mining" or extraction of the rich information embedded in medical images in a way that exceeds the individual sum of each of the imaging technologies.

Clinicians and researchers outside the radiology department want to have as easy access to the medical images stored in PACS, as do the radiologists themselves. Currently deployed PACS

display workstations are expensive, have limited image-processing capabilities, and have no utilities for storing results of analysis besides textual diagnostic reports. These display workstations are also heavily used by radiologists and are difficult to access by researchers and clinicians not conducting routine diagnostic readouts. Although the operation of PACS has led to the accumulation of vast stores of multimedia medical data files including raw images, patient data, and diagnostic reports, accessing and analyzing these images outside the scope of daily clinical operation is a long and tedious process.

What is the current practice of analyzing images for research and diagnosis today? Clinicians and biomedical researchers employ powerful computer workstations to retrieve digital images from PACS and other image sources, store images on local disk, visualize multiple image sets simultaneously, and apply image processing routines such as segmentation, quantitation, and registration. All of the patient images and text data derived from such analysis are stored on the local disk.

The drawbacks of using such computer workstations are many. The data is inefficiently managed via flat files on hard disk, and there is no redundancy to ensure data integrity. The analysis work must be done on a single machine; collaborative research between multiple individuals is inhibited. The workstations are themselves expensive and not easily accessible. Such obstacles hinder the ability of clinicians outside the radiology department to collect and analyze medical images when preparing diagnostic workups of patients for epilepsy surgery and determining decision thresholds.

For example, the Northern California Comprehensive Epilepsy Center of UCSF utilizes several neuroimaging modalities as well as other textual and signal data in the diagnosis of patients with intractable temporal lobe epilepsy. Neurologists and neuroscientists spend a great deal of time,

often weeks, gathering data from disparate information systems and paper records before sitting down to do the actual diagnostic workup or data analysis. The UCSF protocol for epilepsy pre-surgical evaluation involves multiple major neuroimaging modalities, i.e., MRI, PET, MEG, and MRS, and many neurological data types such as surface and intracranial EEG, physical and neuro exams, and patient history.

Chapter 3.

OBJECT-ORIENTED ANALYSIS AND DESIGN

3.1 Introduction

The choice of methodology used to create an information system is very important in order to produce a system that will be usable by the customers, feasible with the current technology, and maintainable by the technicians. This methodology encompasses the assessment of the customer's needs, the translation of those needs into designs, and the implementation of the design in a software and hardware solution. Designers often make the mistake of taking shortcuts when it comes to following a rigorous analysis and design methodology, undermining the success of the information systems they build.

3.2 Motivation for object-oriented analysis and design

The current approach to designing medical image information systems such as PACS does not employ formal languages for modeling the system before design. The advantages of using a formal language such as Unified Modeling Language (UML) are support for iterative development process and creation of encapsulated software modules that can be re-used in the future. For example, HL7 version 3 and CORBA-MED are adopting the UML as a formal language for modeling.

The creation of an information system begins with analysis and design before any code is written or equipment purchased. A description of the problem and requirements to be addressed by the system is needed – what the problem is about and what the system must do. *Analysis* emphasizes an investigation of the problem. *Design* emphasizes the creation of a high-level logical solution to

the problem based on the knowledge gained from analysis – how the information system fulfills the requirements and solves the problem. After these two phases have been completed, the implementation of the logical solution in software and hardware can proceed.

Object-oriented analysis and design (OOAD) emphasizes viewing the problem domain and the logical solution as a framework of interconnected objects [43]. For example, in the case of a medical problem domain, some objects might be image datasets, clinicians, and hospitals. During object-oriented analysis, the goal is to find and describe objects – or concepts – in the problem domain. These objects have attributes and methods. To illustrate, in the MMIS, an image dataset software object may have a modality attribute and a visualize method. During object-oriented design, the emphasis is on defining the logical solution in terms of software objects that will ultimately be implemented in an object-oriented programming language.

3.3 Iterative analysis and design Process

The differences between a data warehouse and an operational information system occur at the very fabric by which these technologies are woven. System Design Life Cycle (SDLC) is the common methodology used to build any operational system [44]. For most operational systems one can gather the correct requirements with proper analysis in the beginning. With the analysis completed, one beings construction of the development plan and modeling the operational system. A high likelihood exists that the model so developed will become the finished product, unless a major mistake is discovered during the development. The process continues until the system is complete. Typical enhancements are adding simple new features or changes to reports. One would not rethink the core functionality of this system. Because the requirements are clear, it needs not be an iterative process to be successful.

With a data warehouse project, it is difficult, if not impossible, to do anything other than iterative analysis (Figure 13). The end users often do not yet know how they will analyze the data; it is impossible to start by gathering all requirements. The goal of a data warehouse is to be flexible enough to deal with the changing needs of the business so that when "What if?" questions are posed, it is possible to mine deeper and deeper into the warehouse. Each question probes the information in new ways, and implemented correctly, the warehouse provides the answers.

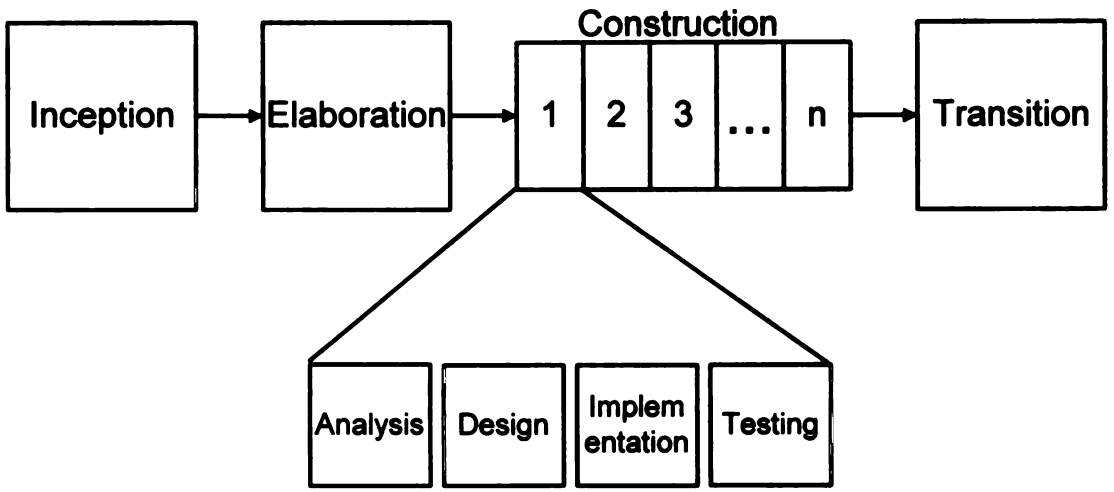

Figure 13 The iterative development process consists of four main phases: inception, elaboration, construction, and transition. During the construction phase analysis, design, implementation, and testing occurs within each iteration. By proceeding in such a fashion, the designer can fine-tune the system between iterations as he systematically adds functionality to the system during construction.

Therefore, an object-oriented analysis and design (OOAD) process is followed to create a logical and iterative model of the software solution [45]. This process transforms real world concepts such as medical images, medical records, lab tests results, phenotype and genotype information, doctors, neuroscientists, patients, and transforms them into a logical model on paper. Use cases are created to summarize operational scenarios of clinicians using the system to complete certain tasks such as image registration [46]. After the use cases are prioritized, a spiral development process is followed to incrementally build computer services to support each use case. The spiral

development process consists of multiple development cycles, each of which has its own analysis, design and construct phases.

The UML is used to describe the object-oriented concepts of the system throughout the software analysis and design process. The UML is a formal language for describing object-oriented concepts and relationships. The language is visual and communicates everything from the requirement analysis all the way up to describing methods and objects to be implemented in code. This means that throughout the analysis and development process, the system documentation is generated in parallel with the artifacts of the process. Figure 14 illustrates the important UML building blocks and how they flow into the technical documentation. The advantages of using a formal language such as UML are support for

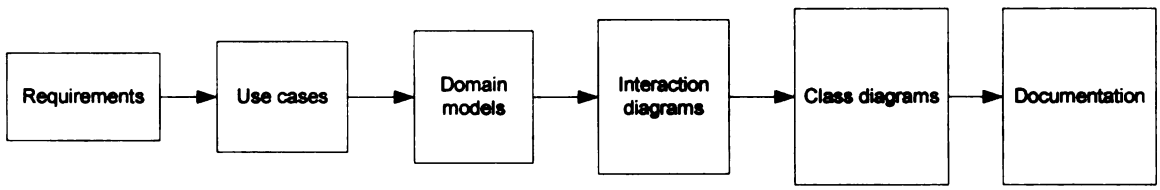

Figure 14 OOAD artifacts. The OOAD process results in the creation of certain artifacts that describe system processes. The UML building blocks above flow into the documentation.

iterative development process and creation of encapsulated software modules that can be re-used in the future. UML has the advantage of existing independently of any programming language, and arguably of any implementation methodology. Therefore, the logical model described by UML can be re-used as technologies advance. Another advantage of UML is that it creates a communication standard and a consistent method to create incremental documentation [47]. For example, the healthcare information standards, such as HL7 version 3 and CORBA-MED, adopt the UML as a formal language for modeling.

A use case is a narrative document that describes how an external actor uses the system to complete a specific task. The domain models are constructed based on the use cases to illustrate how the system would function on a logical level in order to complete all the tasks specified by the use cases. The use case is written in plain English so that the user (i.e. the neurologist or the imaging specialist) and the designer can agree on how the system will solve the problem at hand. The use case not only serves as the basis for design, but also is used for evaluating how well the system fulfills customer expectations. Figure 15 illustrates an example of a leaf use case.

LEAF USE CASE

Name: Retrieve image files
Actors: Clinical researchers and technicians
Goal: Select and retrieve patient image files for offline visualization and analysis.
Overview: A clinician sits down at the client computer and selects patient image files for retrieval. The clinician also selects a file format for the image files. The formatted image files are downloaded onto the client computer's hard drive.
Priority (user): high
Rank (analyst): high
Preconditions:

The clinician's identity and access privileges have been validated.
The PACS is accessible.

Description:
Primary Path

Actor Action	System Responsibility
Clinician enters a patient name or patient medical record.	Display list of image studies.
Clinician selects a study.	Display radiological series/sequence list for that study.
Clinician selects which series/sequences to retrieve.	Transfer selected series/sequence to client computer.

Alternative

Actor Action	System Responsibility
The clinician can clear the patient name or patient medical record number anytime before committing it and reenter a new name or number.	Clears the patient name field and places input cursor in the patient name field.

Exception

Actor Action	System Responsibility
The clinician enters an invalid patient name or medical record number.	Issues error message, clears the input field, and asks clinician to reenter the patient name or medical record number.
Clinician enters patient, but there are no image studies.	Issue error message.

Postconditions:

1. The image series/sequences transferred are noted in the system log.

Future additions:

1. Enable the selection of individual image slices from the sequence.

Thumbnail viewing of image slices.

Figure 15 This use case details how the user interacts with the system to accomplish the task of retrieving images. Note that the use case is organized by the actions the user takes and the responsibilities of the system to fulfill his requests. Primary, alternative, and exception scenarios take into account the variability of system responses. Use cases are useful for communicating the functionality of the system to end-users.

Once all of the use cases have been determined, a use case diagram is generated to demonstrate the relationship between the external actor and the use cases. As an example, in Figure 16, the clinician user interacts with one of five use cases, visualize image dataset, register two image datasets, segment image features, visualize lab test results, and psychometric test scores visualization. The three use cases visualize image dataset, visualize lab test results, and psychometric test scores visualization access the use case validate user. The design phase develops a logical solution based upon the object-oriented paradigm. The main task of this phase is to create interaction diagrams that illustrate how objects will communicate in order to fulfill the requirements. The creation of interaction diagrams requires the application of principles for assigning responsibilities and the use of design patterns. The single most important step in OOAD is the judicious assignment of responsibilities to software components and is usually accomplished with design patterns [48]. A design pattern is a named description of a problem, solution, when to apply the solution, and how to apply the solution in new contexts. Skillful use of design patterns can improve the understandability, reusability, and flexibility of the software system.

With the completion of interaction diagrams, the last step in the design phase is translating the interaction diagrams and conceptual model into software classes and methods. Design class diagrams are created to illustrate the specifications for software classes and interfaces in an application. In contrast with a conceptual model, a design class diagram illustrates software entities rather than real-world concepts.

The design class diagrams are mapped into an object-oriented programming language by writing source code for class definitions and method definitions. A good development effort is characterized by a significant amount of analysis and design modeling before coding begins.

Rushing to code creates systems that are harder to understand, extend and maintain, and does not support a successfully repeatable process. However, there will be instances where unexpected insights are gained during the construct phase and will be integrated in the next development cycle of the spiral development process.

When an expert has fine-tuned a solution to solve a particular design problem, he will use it again and again in the future. Thus, object-oriented systems contain many recurring patterns of classes and communicating objects. These design patterns solve specific problems and make object-oriented designs more flexible, elegant, and ultimately reusable. They allow designers to create successful systems based on prior experience. The smart designer knows that it's not always smart to solve a problem from first principles when someone else has already solved the problem with a simple and proven design pattern.

Design patterns make it easier for the designer to reuse successful designs and architectures from the past. By documenting such successful solutions, the patterns can be applied in new contexts by designers of new systems. Design patterns not only help the designer make the right choices in creating reusable, efficient systems, but also help the designer to document and maintain the existing systems by providing a vocabulary for describing the system in terms of its underlying patterns. Especially in large software systems, the number of objects, relationships, and interactions can be overwhelming, and patterns simplify the system description because the seasoned designer will comprehend the functionality based on the design pattern.

UML is a formal language for describing object-oriented concepts and relationships. The language is visual and is used to describe the logical framework of the MMIS. The language communicates everything from the requirement analysis all the way up to describing methods and objects to be implemented in code. This means that throughout the analysis and

development process, the system documentation is generated in parallel with the artifacts of the process.

A use case is a narrative document that describes how an external actor (the clinician) uses the system to complete a specific task. The domain models are constructed based on the use cases to illustrate how the system would function on a logical level in order to complete all the tasks specified by the use cases. Interaction diagrams illustrate how objects interact with each other to fulfill these tasks. These objects are then translated into class diagrams that lead to the classes of implementation. UML has the advantage of existing independently of any programming language, and arguably of any implementation methodology. Therefore, the logical model described by UML can be re-used as technologies advance. Another advantage of UML is that it creates a communication standard and a consistent method to create incremental documentation [47].

3.4 Plan and elaborate phase

The first OOAD phase is the plan and elaborate phase that involves gathering real-world information from the application domains to define an overview statement, goals, system functions, system attributes, and use cases. Use cases are narrative descriptions of how a user interacts with the system to accomplish a task. This information is gathered by conducting interviews with clinicians and researchers. The use cases are ranked and scheduled into development cycles for analysis, design, and construction.

Once all of the use cases have been determined, the use case diagram is generated to demonstrate the relationship between the external actor and the use cases (Figure 16). The clinician interacts with one of five use cases, visualize image dataset, register two image datasets, image segmentation, lab test results visualization, psychometric test scores visualization. The

three use cases visualize image dataset, lab test results visualization, and psychometric test scores visualization access the use case validate user.

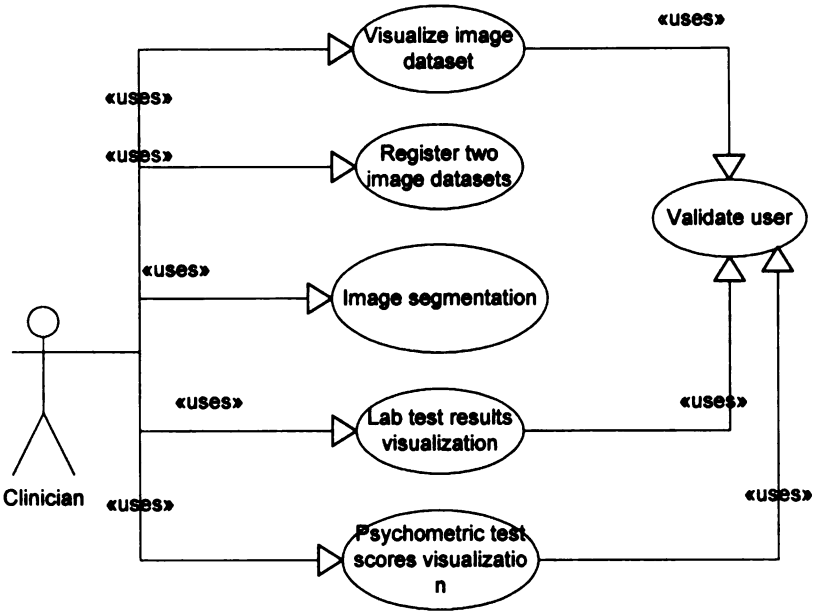

Figure 16 Use case diagram illustrating the relationship between the external actor (clinician) and use cases. Each use case illustrates a high-level interaction in which an external actor uses the system to complete a task. The use case diagram provides a visual diagram of the functionality of the system and the basis for designing the system itself.

The analysis phase of development emphasizes an understanding of the requirements, concepts, and operations related to a system. The information gathered in the plan and elaborate phase is abstracted into an object-oriented conceptual model to describe concepts, associations between concepts, and attributes of concepts in the problem domain. It is the most important step during object-oriented analysis as it serves as the analytical view the real-world problem domain that will be addressed by the system. Armed with an understanding of the problem, system sequence diagrams are created to identify system events and system operations. Their creation is dependent on the prior development of the use cases. System sequence diagrams define system behavior, i.e. what a system does, without explaining how it does it. Contracts are written to characterize system operations from the system sequence diagrams.

The design phase develops a logical solution based upon the object-oriented paradigm. The main task of this phase is to create interaction diagrams that illustrate how objects will communicate in order to fulfill the requirements. The creation of interaction diagrams requires the application of principles for assigning responsibilities and the use of design patterns. The single most important step in OOAD is the judicious assignment of responsibilities to software components and is usually accomplished with design patterns. A design pattern is a named description of a problem, solution, when to apply the solution, and how to apply the solution in new contexts. I use design patterns to define problem-solving algorithms in the neuroinformatics domain. Skillful use of design patterns can improve the understandability, reusability, and flexibility of the software system.

With the completion of interaction diagrams, the last step in the design phase is translating the interaction diagrams and conceptual model into software classes and methods. Design class diagrams are created to illustrate the specifications for software classes and interfaces in an application. In contrast with a conceptual model, a design class diagram illustrates software entities rather than real-world concepts.

3.5 Construct phase

The design class diagrams are mapped into an object-oriented programming language by writing source code for class definitions and method definitions. A good development effort is characterized by a significant amount of analysis and design modeling before coding begins. Rushing to code creates systems that are harder to understand, extend and maintain, and does not support a successfully repeatable process. However, there will be instances where unexpected insights are gained during the construct phase and will be integrated in the next development cycle of the spiral development process.

Chapter 4.

PRESURGICAL MULTIMODALITY NEUROIMAGING ANALYSIS FOR SURGICAL CANDIDATES WITH TEMPORAL LOBE EPILEPSY

4.1 Introduction

Epilepsy refers to a tendency toward recurrent seizures, i.e., paroxysmal derangement of cerebral function due to uncontrolled, excessive discharges from an aggregate of neurons. As a population, patients with epilepsy are undereducated, underemployed, and have a life span approximately 10 years less than their peers. The total cost of epilepsy taking into account unemployment, underemployment, excess mortality, long-term treatment, residential care including institutionalization, costs of drugs, vocational rehabilitation, and special education at the time of the epilepsy commission, is estimated at between 3 and 4 billion dollars per year [49].

4.2 Surgical treatment of temporal lobe epilepsy

Despite the advances made in anti-epileptic drugs, about 25% of epilepsy patients have seizures uncontrolled by medical treatment, i.e., medically refractory. Approximately half of these patients are candidates for surgical treatment. Surgical planning of epilepsy requires the accurate identification of the area of the brain responsible for seizure onset, known as the epileptogenic zone. It has been estimated that approximately 125,000 patients of medically refractory epilepsy in the United States may be suitable candidates for surgical treatment [50], and an estimated 5,000 per year are added to this patient population.

The importance of surgical treatment was recently confirmed by an NIH (National Institutes of Health) consensus conference [50]. The best surgical outcomes are obtained when the various

preoperative localizing examinations, e.g., video electroencephalography telemetry (VET) and MRI, are concordant, implicating the same brain region as the epileptogenic zone. Unfortunately, a number of patients have either discordant or non-conclusive imaging data.

Currently, intracranial electroencephalography (EEG) recording is the gold standard for evaluating surgical candidates of medically refractory epilepsy. An intracranial EEG study is an invasive surgical procedure, which requires placing electrodes directly on the surface of the brain or within the brain itself for recording brain electrical activity during spontaneous seizures to determine where they originate. This array of electrodes remains in the patient from a week to a few weeks for seizure onset monitoring. There are definite risks (6% to 8% morbidity rate) and considerable costs associated with such an invasive procedure ($40,000 to $80,000 per study which includes intracranial EEG monitoring in the hospital).

These invasive and expensive procedures are not performed unless the results of noninvasive studies permit formulation of a reasonable guess about the possible lateralization or location of a resectable epileptogenic region. Usually, the noninvasive presurgical evaluation must identify lateralization choices before invasive testing can be planned.

Technological advances in medical imaging bring forth many new noninvasive techniques that not only help to lateralize the epileptogenic region with reasonable certainty before invasive EEG recording is performed, but can also eliminate or reduce the frequency of such invasive testing. The technological revolution began with PET scanning and the ability to display regional metabolic dysfunctions associated with epileptogenic zones. MRI followed, providing unsurpassed anatomic detail to detect structural abnormalities. Research studies utilizing PET and MRS separately have demonstrated noticeable metabolic abnormalities in the epileptogenic zone.

Multiple imaging methods are available to aid in lateralizing complex partial seizures. To reduce the need for intracranial electrodes and to localize the epileptogenic zone with a higher degree of confidence, 2-[^{18}F]fluoro-2-deoxy-D-glucose PET (FDG-PET) and MRI are used to provide confirmatory localizing information. Relative temporal lobe (TL) hypometabolism on FDG-PET and hippocampal atrophy or prolonged T2 on MRI reliably predict lateralization of the epileptogenic zone [51, 52]. FDG-PET may demonstrate diminished glucose uptake associated with epileptogenic substrates even when the MRI is unremarkable. MRI-PET findings, however, may be non-localizing when structural and metabolic disturbances are widely distributed or equivocal, or when no abnormality is revealed. ^{1}H-MRS has been used to detect unilateral and bilateral metabolite abnormalities in patients with epilepsy [53]. Unlike EEG, which provides direct evidence of the origin of seizures, MRI, PET, and ^{1}H-MRS provide only indirect evidence of potential epileptogenic zones. Unfortunately, scalp-recorded EEG does not always yield clear localization of the epileptogenic zone either, and the relationship of EEG-detected abnormalities to structural lesions may be ambiguous. The significance of many structural and functional imaging abnormalities cannot be interpreted in isolation.

This study compares FDG-PET, MRI, and ^{1}H-MRS in patients suffering from complex partial seizures. The high resolution FDG-PET is compared with quantitative MRI techniques and ^{1}H-MRS in the lateralization of the epileptogenic zone. The analysis of imaging data is carried out on a computer-assisted diagnostic workstation developed in our laboratory.

4.3 Diagnostic workup of epilepsy

Figure 17 outlines the general diagnostic workup for presurgical epilepsy diagnosis [54]. Patients entering this protocol must satisfy one of two conditions: (1) they are medically refractory; their seizures are not controllable by anti-epileptic drugs or (2) they experience intolerable side effects

from anti-epileptic drugs. The goal of the protocol is to determine whether or not the patient is a good surgery candidate. EEG and MRI are routinely used to classify seizures and localize the epileptogenic zone. MRI provides visualization of brain anatomy with detail greatly surpassing that of any imaging modality, including X-ray CT. The spatial resolution provided by MRI has greatly improved the detection of most mass lesions or tumors. Good surgery candidates have their epileptogenic focus localized using the various clinical, EEG, and neuroimaging examinations. The successful finding of concordance among the non-invasive imaging modalities precludes the necessity to perform invasive intracranial EEG monitoring from surgically implanted electrodes [55].

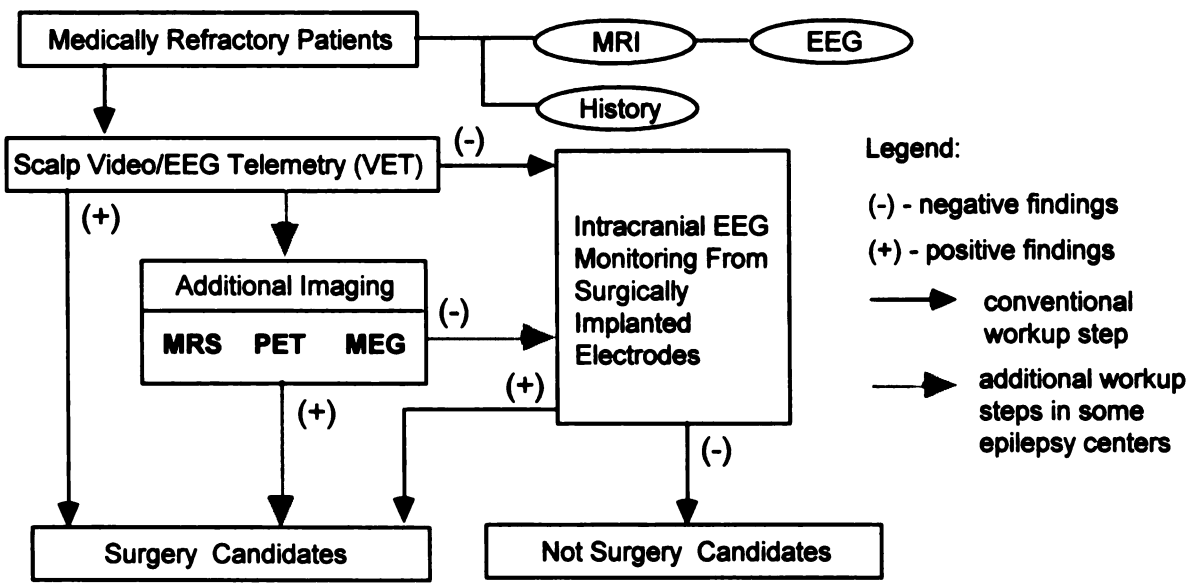

Figure 17 Diagnostic workup of epilepsy surgical candidates. Neuroimaging modalities are being applied to noninvasive surgical planning of patients with complex partial seizures in hopes to minimize the need for invasive intracranial EEG tests; this contributes major savings in cost, reduced patient risks, and increased center capacity. Multimodal data analysis will help to identify more medically refractory patients for surgery treatment than the current means and to determine quantitative decision thresholds for non-invasive tests.

Detection of structural lesions in epilepsy makes surgical evaluation relatively straightforward. Many epilepsy cases, however, do not exhibit structural abnormalities in MR images. Further,

paroxysmal abnormalities occur intermittently and may not be easily captured in EEG recordings. Prolonged inpatient recording with video EEG telemetry (VET) is necessary to capture spontaneous seizures.

Positive results from MRI and VET in localizing the epileptogenic zone typically indicate an outcome of becoming seizure free by surgery. Non-concordance between MRI and VET almost invariably requires invasive EEG recordings with either one or more of the following: subdural strips, arrays, and stereo tactically inserted depth electrodes. For example, approximately 35% to 40% of medically refractory epilepsy patients in the Northern California Comprehensive Epilepsy Center operated on at the University of California at San Francisco (UCSF) require invasive intracranial EEG monitoring. The average cost of intracranial EEG is about $60,000 per evaluation and amounts to about $2 million to $3 million per year in the UCSF Epilepsy Center alone for performing this pre-operative procedure.

The UCSF Epilepsy Center currently performs additional imaging examinations, i.e., ^{1}H-MRS, and PET, on selected epilepsy patients before coming to invasive evaluation. These additional imaging tests cost about $3,000 to $4,000 per patient, a fraction of the cost (< 10%) of an intracranial EEG study. All neuroimaging studies of these patients are collected for computer analysis. The use of combined noninvasive tests to reduce the number and improve the accuracy of intracranial EEG recordings will help to reduce the cost of presurgical evaluation, minimize patient risk, and improve surgical outcome. In addition, a better understanding of decision thresholds from multimodal imaging analysis should improve the selection of candidates for surgery by increasing the identification of patients with previously unlocalized seizure origination.

4.4 Data collection

Considerable effort is expended in setting up the mechanisms to gather data from several departments including Radiology, Neurology, Neurosurgery, Psychology, and Pathology. The data can be broadly categorized into neuroimaging modalities, diagnostic reports, psychometric tests, patient demographics, laboratory tests, surgical findings, neuropathological findings, and postoperative outcomes six months, one year, and two years after surgery.

Patients undergo a series of examinations under well-defined protocol at the Northern California Comprehensive Epilepsy Center. The image datasets are transferred from the imaging scanners to the PACS archive. Radiologists review the image datasets and write diagnostic reports of their findings. These diagnostic reports along with the image datasets are retrieved from the on line PACS archive and inserted into the Epilepsy data warehouse. Each image dataset contains a DICOM header which itself contains textual data regarding the patient name, modality, scanning parameters, date, attending physician, etc. (Table 2). The extraction and composition of textual data from the diagnostic reports and the DICOM (Digital Imaging and Communications in Medicine) header fields are automatic, whereas the segmentation and extraction of medical images often are done interactively.

Group, Element	Name of field	Example of contents
0008, 0008	ImageType	ORIGINAL\PRIMARY\OTHER
0008, 0016	SOPClassUID	1.2.840.10008.5.1.4.1.1.4
0008, 0018	SOPInstanceUID	1.2.840.113619.2.5.1762534004.1335.936889707.261
0008, 0020	StudyDate	19990909
0008, 0030	StudyTime	161428
0008, 0031	SeriesTime	161428
0008, 0033	ImageTime	161429
0008, 0050	AccessionNumber	3063531
0008, 0060	Modality	MR
0008, 0070	Manufacturer	GE MEDICAL SYSTEMS
0008, 0080	InstitutionName	UCSF MR3
0008, 0090	ReferringPhysicianName	BARBARO^NICHOLAS^M
0008, 1010	StationName	GEMROW
0008, 1030	StudyDescription	MR BRAIN UN &EN
0008, 103e	SeriesDescription	SAG T1
0008, 1060	PhysicianReadingStudy	stufflebeam
0008, 1070	OperatorName	bmm
0008, 1090	ManufacturerModelName	GENESIS_SIGNA
0010, 0010	PatientName	DOE^JOHN^^^^
0010, 0020	PatientID	10284628
0010, 0030	PatientBirthDate	19530120
0010, 0040	PatientSex	M
0010, 1010	PatientAge	046Y
0010, 1030	PatientWeight	74.843
0010, 21b0	AdditionalPatientHistory	SEIZURE
0018, 0020	ScanningSequence	SE
0018, 0022	ScanOptions	SAT_GEMS\NPW \SP
0018, 0023	MRAcquisitionType	2D
0018, 0050	SliceThickness	4
0018, 0080	RepetitionTime	500
0018, 0081	EchoTime	14
0018, 0083	NumberOfAverages	0.5
0018, 0084	ImagingFrequency	638643090
0018, 0085	ImagedNucleus	H1
0018, 0087	MagneticFieldStrength	15000
0018, 0088	SpacingBetweenSlices	5
0018, 0093	PercentSampling	53.125
0018, 0094	PercentPhaseFieldOfView	100
0018, 1050	SpatialResolution	1.145833
0018, 1250	ReceivingCoil	HEAD
0018, 1251	TransmittingCoil	HEAD
0020, 000d	StudyInstanceUID	1.2.124.113532.192.9.54.60.19990907.122709.1410095
0020, 000e	SeriesInstanceUID	1.2.840.113619.2.5.1762534004.1335.936889707.260
0020, 0010	StudyID	1359
0020, 0011	SeriesNumber	4
0020, 0013	ImageNumber	32
0020, 0032	ImagePositionPatient	35.000000\ -110.000000\110.000000
0020, 0037	ImageOrientationPatient	0.000000\1.000000\0.000000\0.000000\0.000000\ - 1.000000
0020, 0052	FrameOfReferenceUID	1.2.840.113619.2.5.1762534004.1356.936889677.316
0021, 0010	Zoom	GEMS_RELA_01
0028, 0030	PixelSpacing	0.859375\0.859375
0032, 1030	ReasonForStudy	LUCY X2-6241 NO AUTH NEEDED. V# 2634052

Table 2 Data element tags from the DICOM image header. All of the above fields are automatically loaded into the appropriate data warehouse tables. The goal is to efficiently store all of the above information for future queries.

The clinical and laboratory tests include complete blood count, electrolyte panel, liver function enzymes, thyroid function, and medication. The test results are retrieved from the on line HIS via HL7 gateway. Software modules automatically extract the test results from the HIS reports and insert them into the Epilepsy data warehouse.

The Neurosurgery database resides on a standalone Windows-based personal computer running Microsoft Access. The data is exported to an excel file and automatically loaded and transformed into the data warehouse. The psychometric test results are manually entered into the database from the paper records using the Web browser front ends.

4.5 Neurological Tests and Data Types

VET. EEG is one of the most efficient tests used to localize the epileptogenic focus [56]. The video EEG telemetry unit in the UCSF Epilepsy Center is a four bed inpatient unit. Each room has the capability of simultaneously recording eight hours of the patient's behaviors with 32-64 channels of EEG on a single videocassette. The EEG is analyzed by a computerized spike and seizure detection program. VET applies to both scalp and implanted EEG, i.e., intracranial EEG monitoring. Data collected includes video clips of VET and selected epic of associated EEG recordings. Currently we have not included VET into the data warehouse yet, only textual descriptions and findings.

MRI. The MRI examinations have been shown to provide very good diagnosis of hippocampal sclerosis in patients with medically refractory temporal lobe epilepsy [57]. The imaging examination consists of the coronal whole brain heavily T1-weighted spoiled gradient recalled 3D volume sequence (TR < 600, TE min, slice thickness 1.5 mm.), voxel dimension 0.97 mm x 0.97 mm x 1.6 mm; followed by coronal T2-weighted spin echo sequence (TR > 2000, TE 35) which includes cardiac gating and flow compensation gradients; and a proton density weighted axial

whole brain sequence. Interpretation of mesial temporal abnormalities was based on signal, morphological, and volume changes.

T2 relaxometry. Thirteen of the 25 patients had hippocampal T2 measured using a procedure similar to that reported by Jackson et al. and Grunewald et al. [58, 59]. A multi-spin echo sequence (16 echoes) with TR 2000 ms and TE 22.5, 45...360 ms from a 8mm thick slice of the anterior hippocampus was performed. Two independent operators placed circular regions of interest (ROI) within the margins of the hippocampal body. The average of the two T2 relaxation times was calculated to obtain a final measurement for T2 of the corresponding hippocampus.

FDG-PET. The PET examinations allow clinicians to measure the glucose uptake of neuronal cells between seizure episodes (interictal). Patients with medically refractory temporal lobe epilepsy will usually have both the PET and MRI examinations localize the epileptogenic focus to the same region of the brain. Interictal studies are performed with 2-[^{18}F]fluoro-2-deoxy-D-glucose using a 47 level CTI/Siemens 961 HR EXACT scanner that has a FWHM (full width at half maximum) in plane resolution of 3.5 mm and 4.0 mm axially. Forty-seven slices are acquired with voxel dimensions of 2.404 mm x 2.404 mm x 3.12 mm. Patients are scanned in the unstimulated, but non-sensory-deprived state. Axial, coronal, and sagittal planes are reconstructed for visual interpretation.

^{1}H-MRS. Twenty-four of the patients were studied with ^{1}H-MRS. These spectra were acquired on a 1.5 T Magnetom VisionTM (Siemens, Erlangen, Germany) using a standard circularly polarized head coil according to the method previously reported by Ende et al. [60]. Quantitation of the metabolites, N-acetyl-aspartate (NAA), choline (Cho), and creatine (Cr), is based on the use of the unsuppressed water signal obtained in a second MRS examination with otherwise

identical measurement parameters. The concentration of NAA is used to determine metabolite abnormality and lateralization in ^{1}H-MRS.

MEG. Interictal MEG data are recorded with a 74-channel biomagnetometer. Scalp EEG is performed simultaneously. Magnetic fields are recorded over three to four regions on each side of the head for a total of six to eight recording positions. Visual analysis of both the EEG and MEG waveforms are performed to limit dipole analysis to epochs of data indicating epileptiform activity. A single equivalent current dipole is used to obtain localization of spike sources.

Neuropathological Images. We have also gathered pathological samples from surgery on the selected patient population of temporal lobe epilepsy. The samples are sliced, stained, and digitized using a SPOT II digital camera. The aim is to analyze the brain structure and function from several levels of detail for clinical research and outcome analysis.

Medical Records and History. Neurological history and examination, image diagnosis reports, neuropsychological test data and surgery results of the selected patients are collected. The patient history includes patient age, sex, education, previous drug treatments, and intermittent symptoms and signs, while neurological examination cover mini-mental status examination (MMSE), physical examination, laboratory tests, and neuropsychological test reports.

Image interpretation and analysis. The PET images are interpreted for evidence of focal hypometabolism by two investigators. Five temporal lobe ROIs were selected - temporal pole, anterior medial, posterior medial, anterior lateral, and posterior lateral cortex - and scored for relative hypometabolism. The sum of the five regions was used to provide a qualitative measure of the degree of hypometabolism. An asymmetry index (AI) is used to measure the degree of

asymmetry for MRI hippocampal volume, FDG-PET glucose count, and ^{1}H-MRS NAA concentration:

$$AI = \frac{right - left}{\left(right + left/2\right)} \times 100 \qquad (8)$$

An effective means to access, manipulate, and correlate large, heterogeneous multidimensional medical images was lacking. We thus developed a computer-aided diagnostic (CAD) workstation for epilepsy surgical planning to fulfill this need. This neurodiagnostic workstation aims to provide an environment for optimal interpretation of multiple non-invasive image modalities by combining functional information of PET and ^{1}H-MRS with structural MRI anatomy, both qualitatively and quantitatively. Since there is currently little knowledge about the patient populations with positive and negative findings of various imaging and intracranial EEG studies, the data extracted will also be essential for outcome analyses to identify inefficient or duplicative evaluation procedure.

Chapter 5.

EPILEPSY DATA WAREHOUSE DESIGN

5.1 Introduction

This research applies industrial standards and methods to develop the image data warehouse framework for multimedia data management, analysis, research, and access services. The framework is a complete description of the problem that abstracts the many aspects of epilepsy research and care to a high level of visual understanding. It can be modified and expanded to provide new services or support new application domains. The design patterns used in the framework will be useful in solving problems in different medical domains. The entire design process is use case driven.

5.2 Image data warehousing approach

Up to now, the primary purpose of most database systems was to meet the needs of operational systems, which are typically transactional in nature. Hospitals today generate and collect vast amounts of data in the ongoing process of providing care. Classic examples of operational systems in hospitals include: patient registration and order entry (HIS), image reports and scheduling (RIS), and image display and reading (PACS). Operational systems by nature are primarily concerned with the handling of a single transaction and are optimized and normalized for transactional updates. Normalization is a term for a process the data modeler goes through to avoid the traps and pitfalls easily encountered when the network of entities, attributes, and relationships that make up a relational data model that is commonly used in today's database systems. A data modeler goes through the process of normalizing a database in order to avoid

traps and pitfalls easily encountered in a network of entities, attributes, and relationships that make up a relational data model that is commonly used in today's database systems. Most of the time, the needs of an operational system do not change much.

On the other hand, a data warehouse application is different as a typical transaction deals with large amounts of data, which is aggregate in nature. The operational entities are often denormalized in the data warehouse, a process whereby the structure of the tables from the operational environment is changed to allow faster processing in the data warehouse.[9] The data stored in the data warehouse undergoes little if no update activity. Its main purpose is to be read by users while they make decisions or verify hypotheses. Under today's competitive managed care environment, the healthcare decision makers must be able to interpret trends, identify factors, or utilize information based on clearly, timely data in a meaningful format. The biomedical researchers would use the data warehouse to verify scientific hypotheses and deal with "What if?" questions in various aspects of disease management and treatment.

In Figure 18, I illustrate the process flow for developing medical image data warehouses. The data warehousing process consists of five elements: (1) Prepare the data; (2) Acquire the data; (3) Transform and extract the data; (4) Archive the data; and (5) Analyze and mine the data. The major tasks in each process element are described in the figure.

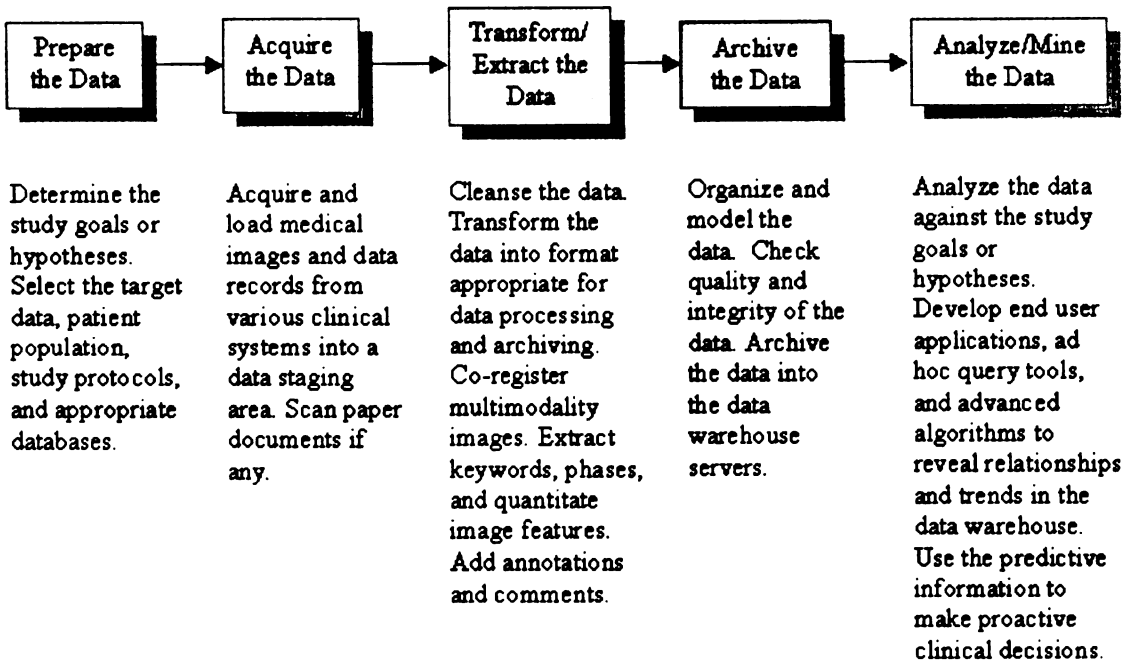

Figure 18 The basic elements of image data warehousing solutions.

There are several distinctions of medical image warehousing systems compared to data warehousing systems in other business organizations or industries. These include:

1. The medical imaging data warehouse would be more efficiently built in a PACS or digital radiology environment in which massive volumes of images and associated reports are acquired and archived centrally. The availability of message exchange standards such as DICOM and HL7 also help in reducing the complexity of data preparation and acquisition.

2. The medical imaging data warehouse involves sophisticated effort of image processing, registration, extraction and Quantitation of image features. It also requires the modeling of multimedia data of various forms, including free and structured texts, planar and volumetric images, signals, spectroscopic data, graphics, and scanned paper records; rather than simply textual data as in most business data warehousing systems.

3. The image data warehouse emphasizes the preparation and acquisition of data with pre-defined or prospective protocols, rather retrospective analysis or mining of data. The emphasis is due to the predominant paradigm adopted in biomedical research and study today.

4. The image data warehouse develops analytical tools to support a verification-based approach in which the user hypothesizes about the specific data relationships and then uses the tools to verify or refute those hypotheses. This follows the hypothesis-driven paradigm adopted in most biomedical research endeavors. Data mining, in contrast, uses what are called discovery-based approaches in which pattern matching and other algorithms are employed to determine the key relationships in the data. The ability to automatically discover important information hidden in the data and then present it in the appropriate format is a critical complementary technology to verification-based approaches. Since the goals are exploratory in nature, data mining systems would normally require a much larger data size than data analysis systems. In addition, discovery-based tools and techniques are relatively immature compared to verification-based tools and often is a research topic on its own.

5.3 Neuroimaging data warehouse architecture

The neuroimaging data warehouse framework is based on a three-tiered architecture that separates the graphical user interface (GUI) presentation, business logic components, and backend database services into distinct layers. The middleware layer consists of several CORBA and Web components (please see Figure 19) that fulfill requests from the user interface layer by sending commands to the backend servers. CORBA is a popular and standardized component-based architecture developed by the Object Management Group. Its architecture consists of

interoperating objects that provide access to services such as laboratory test data retrieval or image registration. It separates service from actual implementation, enabling the integration of existing services on legacy computer systems.

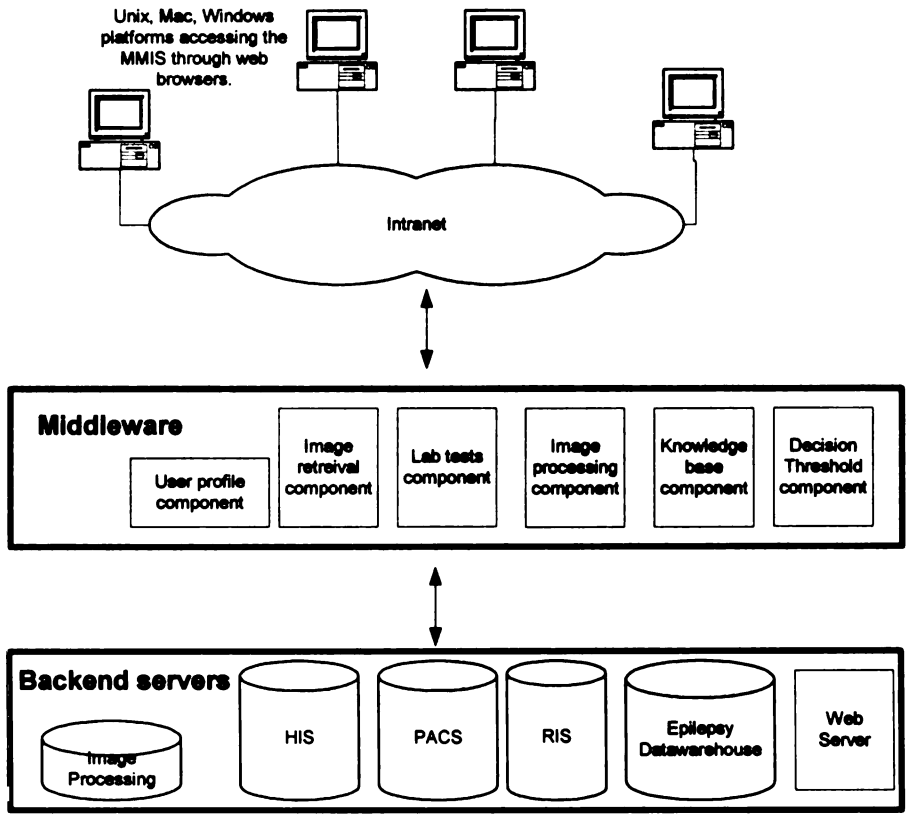

Figure 19 3-tiered data warehouse architecture. The backend servers include the various sources of raw data: HIS, PACS, RIS, and other specialty information systems. The middleware contains the business logic for applications such as decision threshold and image processing analysis. The top tier consists of the actual workstations where clinicians interact with the system.

The middle-tier server layer includes several application servers and middleware service components. The application servers include the image database server, Web application server, CORBA application server, and image processing server. The image data warehouse stores data of various image features, keywords, thumbnail pictures and annotated images into an object-relational database (Oracle 8i) and raw or processed multimodal images in a RAID 5 system. The images include MRI of various protocols, PET, as well as other brain images such as MRSI

(magnetic resonance spectroscopic imaging) and MEG, which is currently not archived in PACS. The middleware service components manage, integrate, and distribute the data of multiple clinicians, neuroimaging specialists, and neuroscientists working in concert on complicated research and clinical projects. The middleware functions of each service component are as follows:

The Database Engine contains a collection of objects and a set of operations that they can perform. Data models are devised to classify, organize, and represent classes of different images and text to support information retrieval by image content for various medical applications. The database engine treats system components and multimedia data of the entire database framework as a logical conglomeration of distributed, interacting objects of various levels of granularity.

The data model is centered on the patient since the data naturally lends itself to such an organizational basis and query of the database is often by patient name or ID. For example, tables 3 and 4 illustrate the Studies and Series tables respectively. When a patient goes into the radiology department for an imaging study, often times several imaging series are captured, and each series consists of a 3D stack of image slices. Each study done on a patient corresponds to one row in the study table, and each series done corresponds to one row in the series table. Each row in the study table corresponds to at least one row in the series table. All of the fields of these tables are automatically extracted from the image datasets' DICOM header and inserted into the database. Queries can be constructed based on any arbitrary combination of fields.

	Column name	Oracle type	Length	Keys
1	MRN	varchar2	8	Foreign Key
2	Lastname	varchar2	30	
3	Firstname	varchar2	30	
4	Middlename	varchar2	30	
5	Specific_Character_Set	varchar2	20	
6	SOP_Class_UID	varchar2	60	
7	Study_Date	date		
8	Study_Time	time		
9	Accession_Number	number	12	
10	Modality	varchar2	10	
11	Manufacturer	varchar2	40	
12	InstitutionName	varchar2	40	
13	Referring_Physician_Name	varchar2	60	
14	Station_Name	varchar2	20	
15	Study_Description	varchar2	60	
16	Physician_Reading_Study	varchar2	60	
17	Operator_Name	varchar2	20	
18	Manufacturer_Model_Name	varchar2	40	
19	Additional_Patient_History	varchar2	60	
20	Study_Instance_UID	varchar2	60	Primary Key
21	Study_ID	varchar2	4	
22	Study_Priority_ID	varchar2	10	
23	Reason_For_Study	varchar2	60	

Table 3 This is the database table named "Studies". It has one primary key, Study_Instance_UID, and one foreign key, Medical Record Number. One entry in the studies table corresponds to one or more series in the "Series" table.

	Column name	Oracle type	Length	Keys
1	MRN	varchar2	8	Foreign Key
2	StudyInstanceUID	varchar2	60	Foreign Key
3	Image_Type	varchar2	50	
4	Series_Time	time		
5	Series_Description	varchar2	60	
6	Scanning_Sequence	varchar2	10	
7	Sequence_Variant	varchar2	10	
8	Scan_Options	varchar2	20	
9	MR_Acquisition_Type	varchar2	4	
10	Sequence_Name	varchar2	10	
11	Angio_Flag	number	1	
12	Slice_Thickness	number	4	
13	Repetition_Time	number	5	
14	Echo_Time	number	4	
15	Inversion_Time	number	4	
16	Number_Of_Averages	number	4	
17	Imaging_Frequency	number	15	
18	Imaged_Nucleus	varchar2	4	
19	Echo_Number	number	2	
20	Magnetic_Field_Strength	number	7	
21	Spacing_Between_Slices	number	4	
23	Percent_Sampling	number	7	
24	Percent_Phase_Field_Of_View	number	3	
25	Spatial_Resolution	number	15	
27	Receiving_Coil	varchar2	10	
28	Transmitting_Coil	varchar2	10	
29	Phase_Encoding_Direction	varchar2	10	
30	Flip_Angle	number	3	
33	Patient_Position	varchar2	10	
34	Distance_Source_To_Source_Side_Collimator	varchar2	15	
35	Series_Instance_UID	varchar2	60	Primary Key
36	Series_Number	number	3	
37	Image_Orientation_Patient	varchar2	70	
38	Frame_Of_Reference_UID	varchar2	60	
39	Zoom	varchar2	20	
40	Photometric_Interpretation	varchar2	20	
41	Pixel_Spacing_X	number	11	
42	Pixel_Spacing_Y	number	11	
43	Bit_depth	number	4	

Table 4 This is the database table named "Series". It has one primary key, Series_Instance_UID, and two foreign keys, Medical Record Number and Study_Instance_UID. One entry in the series table corresponds to one or more images in the "Images" table.

The medical knowledge base component controls the high level interaction between the user and the servers, encodes medical rules for decision aids, and provides interactive workup models of different epilepsy categories. Rule-based modules that encode general and specific medical rules for decision making, case-based modules that aid the navigation of database through similar or reference imaging cases, and model-based modules that provide interactive work-up models of different disease categories closely involving physicians making joint decisions.

The user profile and audit trail component manages the customizable user interface for individual clinicians depending on their personal preferences. After requests for information are processed by other middleware components, the processed data is sent to the user profile component for formatting before it is sent to the presentation layer. The service component also provides user authentication and audit trail capabilities.

The image retrieval component keeps information on image classes, search algorithms, image features, keywords, pictures of interest, and their association to support content-based retrieval of medical images.

The image processing component engine provides and selects image processing algorithms for image filtering, co-registration, enhancement, feature extraction, quantitation, and structural/functional mapping. The lab test retrieval component provides access to laboratory tests from the HIS and other specialty database systems.

The image and data analysis component contains algorithms for searching the data warehouse to analyze image data and associated clinical and laboratory findings. For example, the user can invoke the service component to calculate and analyze clinical thresholds for structural volume and glucose metabolism that indicate lateralization of the epileptogenic focus.

There are also data load, transformation, and cleansing components that interface and acquire relevant patient information from various clinical systems, e.g., PACS, RIS, HIS, imaging scanner consoles, neurological database system, pathologic database system, and other legacy systems (using DICOM, HL7, JDBC, etc.). The data are first archived into an intermediary database for subsequent transforming and cleansing by the specialists before archiving into the image data warehouse.

The Epilepsy data warehouse system consists of a heterogeneous collection of hardware platforms and operating systems each of which is optimized to deliver specific services. The image data warehouse is implemented on a dual-Pentium II processor Dell PowerEdge Server running Windows NT 5.0 Server operating system and Oracle 8.1.7 database management system, and with clustering another Dell PowerEdge server for back up purpose. A database management system provides centralized storage of all multimedia epilepsy data so that clinicians are not tied down to using a particular workstation and so that the data of multiple clinicians working together may be managed, integrated, and distributed. The image processing server is implemented on a high end SGI Onyx Workstation (Silicon Graphics, Inc., Mountain View, CA) running Irix 5.3 and containing two Reality Engines for rapid image visualization and an Apple PowerMac G4 running the BrainImage software from Stanford University. The image registration software, Automated Image Registration from UCLA, runs in a Solaris environment on a Sun Ultra10 workstation. The PACS DICOM gateway and the HIS HL7 gateway reside on a SUN Enterprise 2 computer and an IBM RISC Computer, respectively. The network consists of 10 and 100 BaseT Ethernets.

Money and development effort are saved through more efficient utilization of existing computing resources and moving the user interface to less expensive personal computers while maintaining accessibility to more powerful workstation servers in the middleware layer that provide CPU-intensive services such as image processing and data analysis functions. The data warehouse front end includes both web browser access and dedicated multimedia GUI client on either Unix or PC platforms. The current set up is to have the web browsers access the image data warehouse via Intranet or HTTP over SSL (Secured Socket Layer) for users outside UCSF campuses.

5.4 Design pattern implementation

A design pattern is a named description of a problem, solution, when to apply the solution, and how to apply the solution in new contexts. A design pattern is expressed as objects and interfaces. Normally, a design pattern is tested and modified many times over before it becomes accepted as a truly reusable design pattern, and once it has achieved such a status, it successfully captures the experience gained from designing previous systems in a way that can be utilized easily in future designs. Design patterns not only leverage experience from previous work, but also help to visualize, specify, construct and document the artifacts of a software-intensive system. Design patterns make software systems easier to understand because they organize the overwhelming number of objects and relationships into recognizable, functional components. There are three main classifications of design patterns: (1) Creational patterns abstract the instantiation process; they help make a system independent of how objects are create, composed, and represented. (2) Structural patterns are concerned with how classes and objects are composed to form larger structures, and (3) Behavioral patterns are concerned with algorithms and the assignment of responsibilities between objects; they describe patterns of communication between objects or classes.

One structural pattern that has found use in the medical image information system is the Composite pattern (Figure 20).

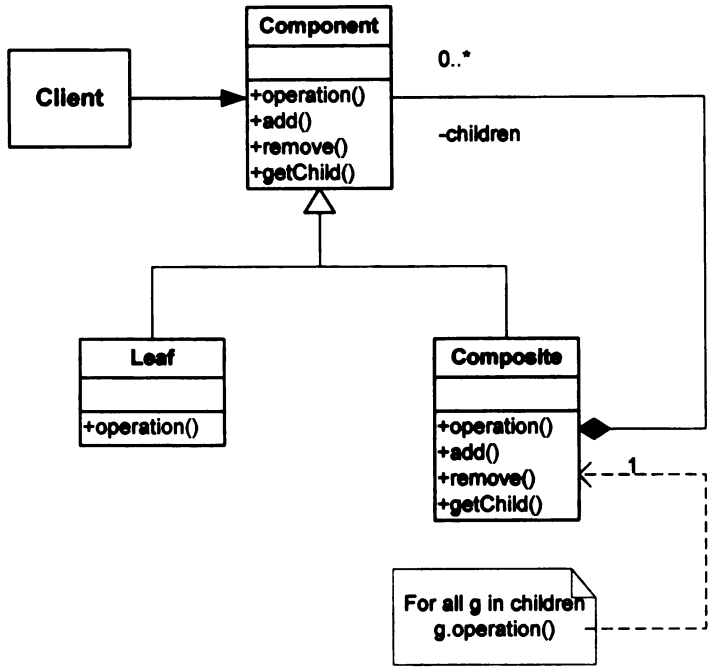

Figure 20 The Composite pattern consists of Component, Leaf, and Composite objects. This pattern enables the structuring of primitive objects and composite objects in a way that enables clients to manipulate uniformly.

The intent of the composite pattern is to organize objects into tree structures to represent part-whole hierarchies. Composite lets clients treat individual objects and compositions of objects uniformly. This pattern is useful for organizing region of interest objects, which can take the form of polygons, arrows, rectangles, and textual labels. All of these primitive objects are classified under the Component "Graphic" (Figure 21). Polygons, arrows, and text are drawn for each image slice and can be structured using the Composite pattern.

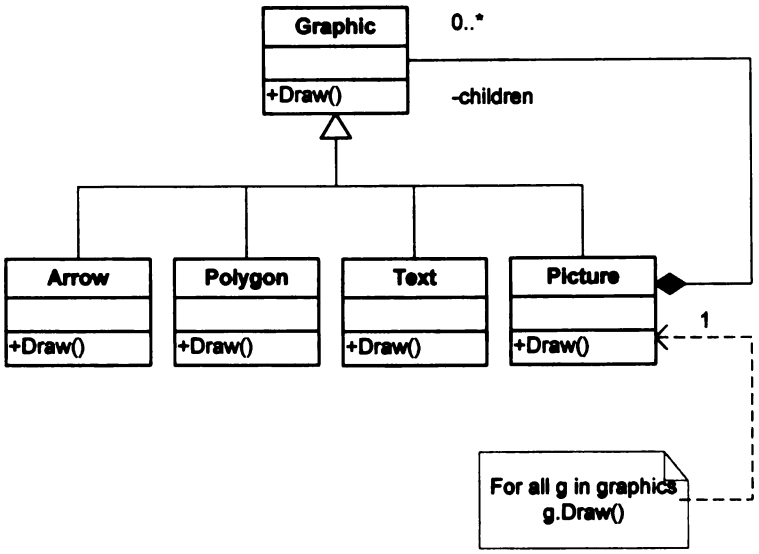

Figure 21 Application of the Composite pattern to structurally organizing region of interest objects that are drawn on a 3D image dataset such as MRI. These regions of interest graphics take the form of the textual labels, polygons, and arrows draw on the MRI dataset and PET datasets.

Another design pattern I applied in the medical image information system is the observer pattern, which defines a one-to-many dependency between objects so that when one object changes state, all its dependents are notified and updated automatically [48]. This pattern is useful for abstracting the underlying application data from the GUI presentational widgets (Figure 22). The Observer pattern provides for messages to be sent to the various presentational widgets to update themselves when the application data has been changed. For example, when the user changes the value in the text field, the slider widget is automatically updated with the new value. In this case, the subject is the new value in the text field and the observer is the slider widget. A subject can have any number of dependent observers, and all observers are notified whenever the subject undergoes a change in state. This kind of interaction is also known as publish-subscribe.

The subject knows its observers and provides an interface for attaching and detaching observer objects. The Wisconsin defines an updating interface for objects that should be notified of

changes in a subject. The *ConcreteSubject* stores state of interest to *ConcreteObserver* objects and sends a notification to its observers when its state changes. The *ConcreteObserver* maintains a reference to the *ConcreteSubject* objects and implements the Observer updating interface to keep its state consistent with the Subject's.

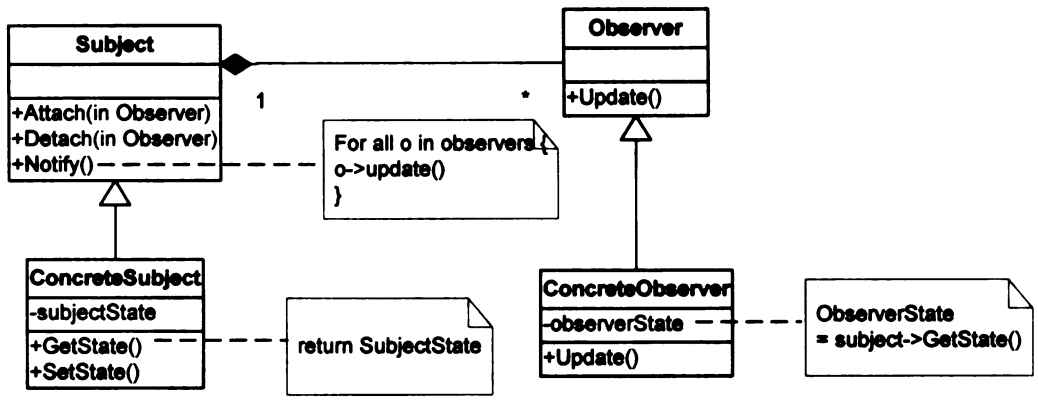

Figure 22 The data model and/or business logic reside in the Subject. All the "view" functionality is delegated to the decoupled and distinct Observer objects. The Observers register themselves with the Subject when they are created. Whenever the Subject changes, it broadcasts to all registered Observers that it has changed, and each Observer queries the Subject for that subset of the Subject's state that it is responsible for monitoring. The Observer pattern allows the changes made in the subject to be reflected in the observers that are dependent on its state.

5.4 Workstation design and implementation

A neurodiagnostic workstation is developed to serve as the basic computing platform for clinicians to access the data warehouse, perform data and image analysis, synthesize the findings from multiple diagnostic resources, and isolate the epilpetogenic focus for surgical treatment. The strategy of neurodiagnostic workstation development is to use, modify, and integrate off-the-shelf computing hardware and software to enable rapid prototyping and to better focus on user interface design. The capabilities of this workstation include on-line access to the image and textual data from PACS and other image sources by patient name or hospital identification (ID), automatic image registration, 2D and 3D visualization, image processing, and persistent storage of extracted data. The workstation must be easy to use because this design feature ultimately

determines its usefulness and acceptance to the clinicians and therefore its ability to aid in supporting the localization of the epileptogenic zone.

The workstation's basic computing platform is a Sun Ultra 10 workstation running Solaris 2.6 operating system. The workstation's software routines access the centralized archive of the UCSF PACS by patient name and hospital ID and contain 3-D image visualization packages: 3DVIEWNIX (University of Pennsylvania) [61] and Volumetric Image Display and Analysis (University of Iowa) [62]. The following image processing routines reside on the SGI Onyx workstation: a set of automated image registration (AIR) programs based on Wood's algorithms [63], and region of interest (ROI) analysis tools from Lawrence Berkeley National Laboratory [64]. All of the above disparate software components are integrated into an easy-to-use neurodiagnostic workstation user interface based on the object-oriented Gain Momentum Multimedia User Interface (Sybase, Inc., Emeryville, CA). This GUI utilizes graphical widgets to present information, launch 3DVIEWINIX and VIDA, make calls to registration algorithms, and manage data contained in the relational database (Figure 23).

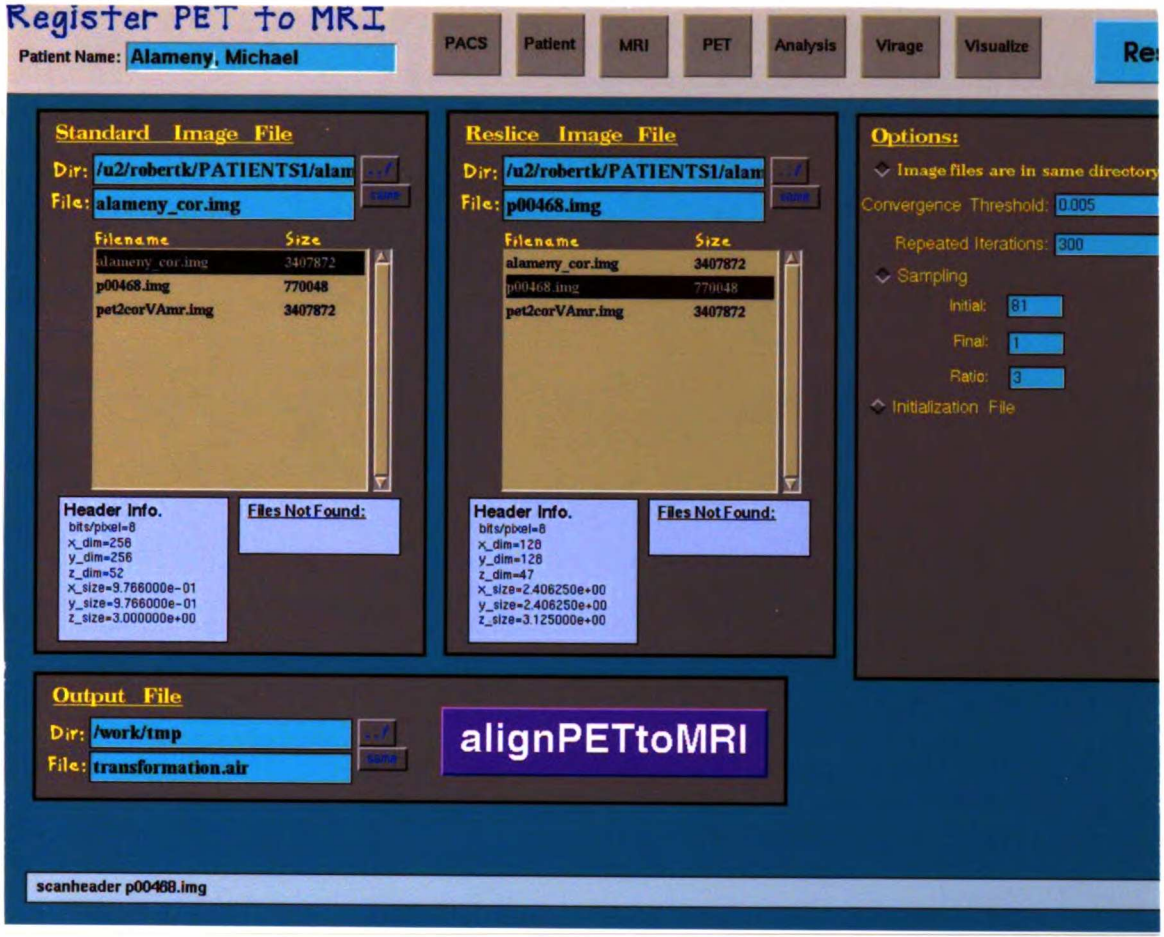

Figure 23. A screenshot taken from the neurodiagnostic workstation showing the registration of PET to MRI. The user selects the MRI file in the left most box, the PET file in the middle box, the options for registration in the right most box, and the output filename in the bottom box. Clicking the purple button "alignPETtoMRI" launches the AIR algorithm, calculating the transformation matrix for aligning the PET image dataset to the MRI datasets. The resulting PET dataset will be resliced into coronal slices corresponding to the MRI dataset.

Figure 24 shows the distributed system architecture of the neurodiagnostic workstation together with the computer-aided workup steps that the workstation supports. The neurodiagnostic workstation provides a multimedia user interface to: (1) access medical data stored in the PACS file archive and the neuroimaging database and (2) analyze the retrieved data for noninvasive surgical planning of epilepsy [6]. For security reasons, all user queries from non-daily clinical operations pass through a multimedia data file server, which acts as a "firewall" against unauthorized access to the PACS central archive. The multimedia user interface of the neurodiagnostic workstation is built on top of the Gain Momentum software package (Gain Technology Division, Sybase, Palo Alto, CA) and X window programming environment.

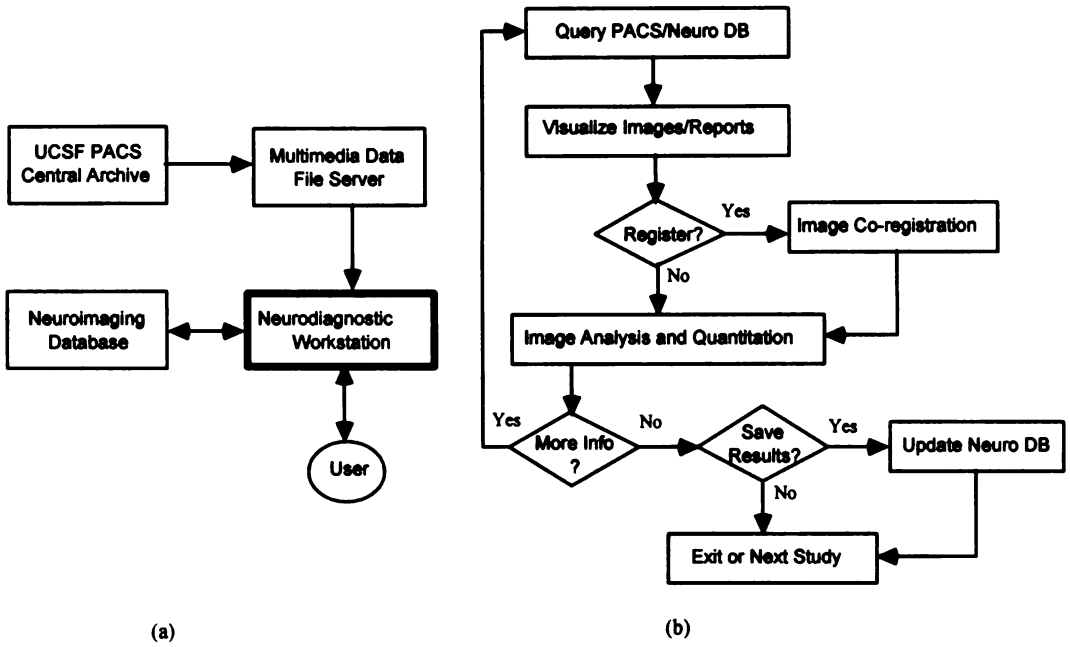

Figure 24 (a) Distributed system architecture of the computer-aided neurodiagnostic workstation, and (b) the computer-aided workup for epilepsy surgical planning that the neurodiagnostic workstation supports.

Chapter 6.

IMAGE ANALYSIS AND RESULTS

6.1 Introduction

Heterogeneous medical data retrieved from PACS and/or the neuroimaging data warehouse are combined and rendered into 2D or 3D images. Before any data combination and analysis, however, medical image registration is often required to geometrically align two or more brain image volumes so that voxels representing the same underlying anatomical structure may be superimposed or directly compared. A pair of image volumes might be from the same subject and the same modality (but taken at different positions or different scanning instruments), from the same subject but different modalities, or from the same modality but different subjects.

The structural and functional information contained in the medical images must be quantitatively extracted using a multi-step process involving expert domain knowledge and computer-assisted analysis. Structural information in a medical image contributes essential knowledge of the disease state and clinical decisions. For example, the location of a tumor and its adjacent anatomical structures has profound implications in treatment planning (spatial context); whereas monitoring of growth or shrinkage of that tumor is an important indicator of the patient's progress in therapy (geometric context). What distinguishes medical images most from other types of digital images, however, is the ability to represent functional information, e.g., biochemistry and physiology, of body parts. As an example, temporal lobe hypometabolism exhibited in SPECT scans, if not coincident with the tissue atrophy of the suspected region shown in MRI images, may indicate that a different epileptic focus as otherwise would be

concluded. The quantified structural and functional information serve as indexes to the image datasets themselves inside the data warehouse.

6.2 Registration and quantitation of images

Figure 25 illustrates the steps to extract image and textual features from the on line PACS data. The feature extraction is based on the *a priori* approach, rather than the dynamic and automatic feature extraction during user query as proposed in many non-medical image database applications [65, 66]. Co registration of functional PET and T1-weighted MR images is an essential step toward combining functional information from PET images with anatomical information in MR images [67]. Several co-registration algorithms have been published and are used in functional brain imaging studies. Image registration permits the combination of different types of functional (such as PET and MEG images) and structural information (such as MRI images), setting the stage for feature extraction. Our information system interfaces with the public domain Automated Image Registration package (AIR, Version 2.03) as well as several proprietary routines in commercial image analysis packages for registration of neuroimages including PET, MRI, MRS, and MEG [63, 68]. One study confirms that registration optimization based on measurement of the similarity of spatial distributions of voxel values is superior to techniques that do not use such information [69].

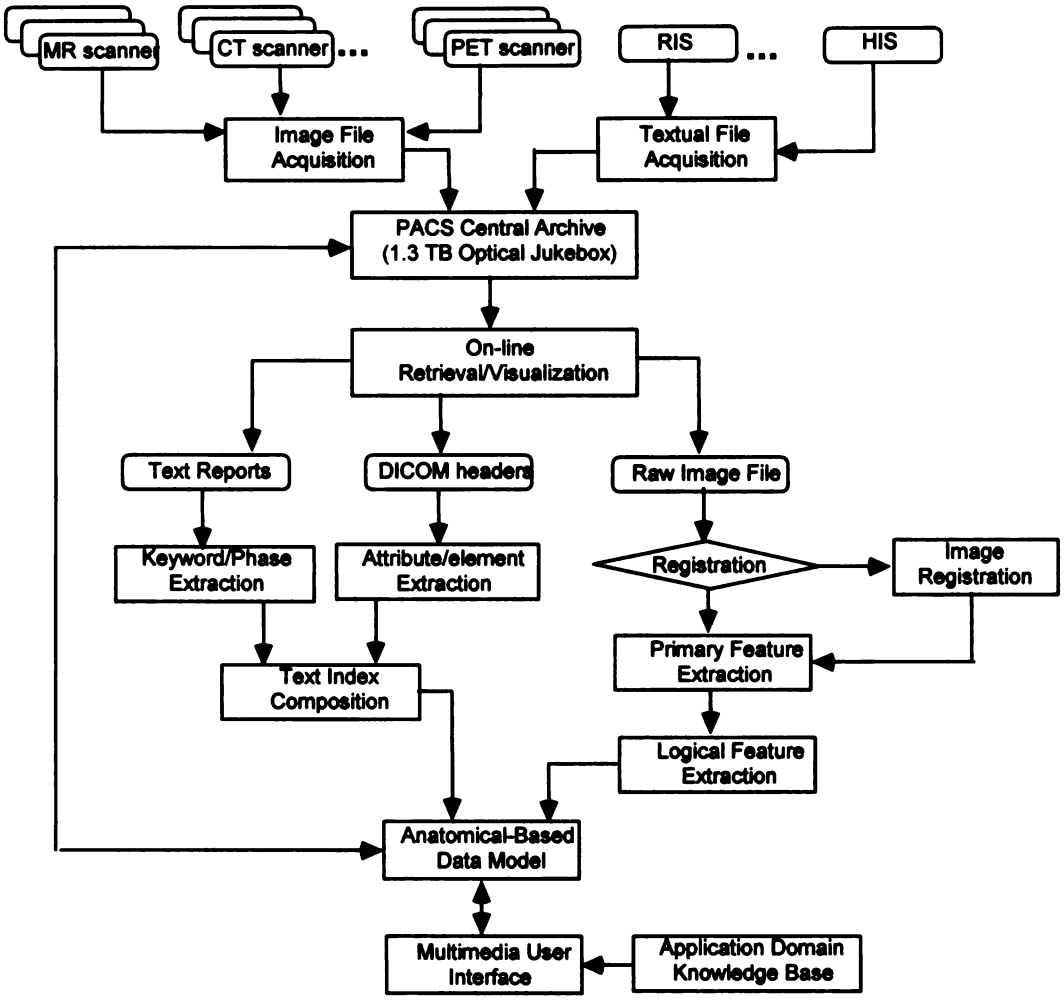

Figure 25 The operational flow of extracting image and text features into an anatomical based data model for subsequent content-based image indexing in the image data warehouse. Specific knowledge or heuristics is triggered to aid the query and navigation of the medical image database.

The AIR algorithm rests on a key assumption that voxels having the same intensity correspond to the same tissue type in the MR image. In order for this to be true, all non-brain voxels must be removed (i.e. their intensities set to 0) including the scalp and skull. This scalp and skull removal must be performed before co registration. The AIR algorithm is based on minimizing the intensity mismatch between the MRI and PET images. This intensity mismatch is calculated using a cost function, and a rigid body transformation T is determined by iterative, nonlinear minimization of this cost function. The algorithm uses a histogram segmentation to segment the

MR image into K voxel intensity partitions P_i and minimizes a weighted ratio of the standard deviations and means of the PET voxels corresponding to P_i by manipulating the transformation matrix T. The key formula of the algorithm is

$$f(\text{PET}, \text{MRI}, T) = \frac{1}{N}\sum_{j}^{K} n_j \frac{\sigma_j}{a_j} \tag{9}$$

where **PET** is the PET image, **MRI** is the MR image, T stands for the transformation matrix, n_j is the number of MRI voxels with an intensity of j, $N = \sum_j^K \frac{\sigma_j}{a_j} n_j$, a_j is the mean of all PET voxel values with a corresponding MRI voxel intensity in partition j, and σ_j is their standard deviation.

The two image datasets become coregistered when the right-hand side of the equation is minimized. This computation requires a nonlinear minimization method, because the additive components of the algorithm are not independent. The AIR algorithm uses Southwell's Relaxation Search, which is an iterative, univariate Newton-Raphson search [70]. The overall process consists of iterative steps, and each step produces a new transformation matrix T, which is subsequently used in the next Newton-Raphson iteration. When a global or local minimum in the parameter space of T is reached or when a prespecified maximum number of iteration steps is reached, the algorithm stop and returns the computed transformation matrix T.

The registration strategy is to have the high resolution, structural MRI dataset as the reference point for mapping across different imaging modalities. The MRI-MRS registration is straightforward: The MRS scans are performed immediately after the MRI examination of the patient using the same MR scanner (GE Signa or Siemens Vision) such that there is no change of the patient's head position. For the MRI-MRI, PET-PET, and MRI-PET image pairs, I employ

Wood's AIR algorithm [63]. The translation and rotation parameters are determined such that they minimized the voxel-by-voxel variance of the "ratio" image. The MRI volumes are stripped to remove the skull and scalp using BrainImage (the removal process is done semi-automatically) prior to calculating the ratio image for MRI-PET registration. The registration parameters are saved in the data warehouse for future reference.

Figure 26 illustrates a clinical case of volumetric visualization of MRI-PET registration. The top image of the figure presents a patient case of left mesial temporal lobe epilepsy with the registered PET slice superimposed onto the MRI volume, while the corresponding 2D MRI slice at the bottom showing very subtle hippocampal atrophy on the left temporal lobe.

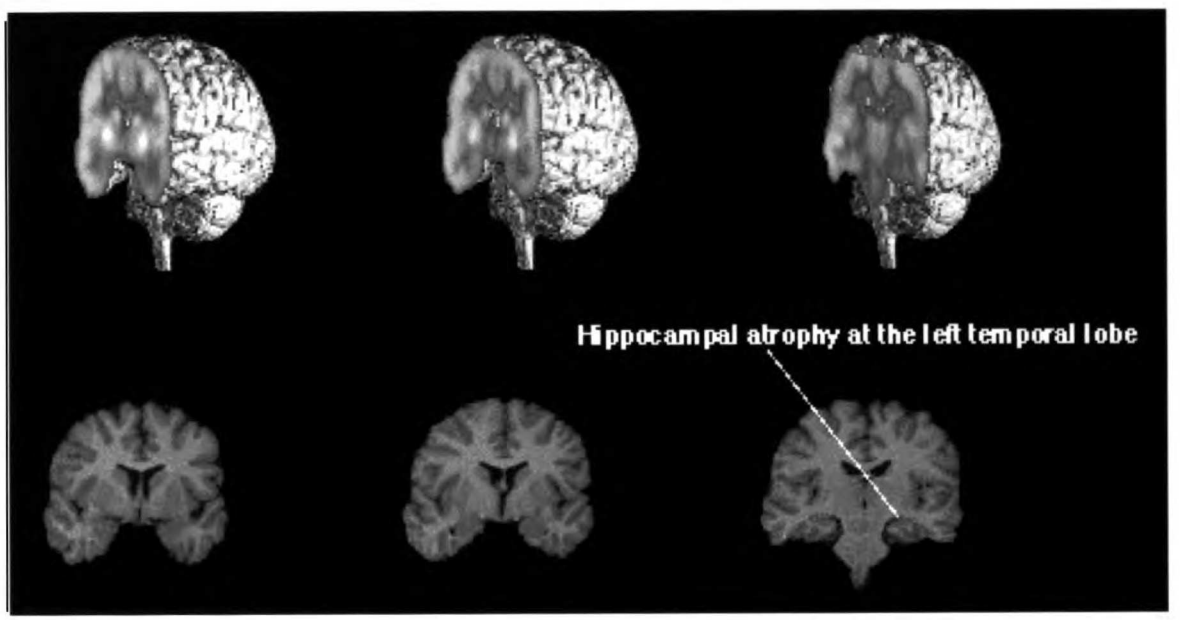

Figure 26 Top -- FDG-PET viewed on the cut surface of registered 3D MRI volume for a patient with left mesial temporal lobe epilepsy. Bottom -- the corresponding MRI coronal slice that the top PET slice replaced.

Once image pairs are registered into common space, their biomedical information can be combined, extracted, and quantitated to obtain important information about the location and nature of the epileptogenic zone. For example, the high-resolution MR image provides a basis

to anatomically map glucose metabolism. This allows the ability to identify metabolic rates in specific brain regions of interest. The algorithm incorporates a program developed at the Center of Functional Imaging, Lawrence Berkeley Laboratory [64] in conjunction with the VIDA project at the University of Iowa Medical College [62] to map regions of interest defined on the MRI to the PET sinograms for quantitation of glucose uptake. Figure 27 illustrates such an example taken from another partial epilepsy case. This figure marks down the values obtained from structural/functional image analysis on volumes and FDG-glucose update per unit volume of hippocampus and amygdala. Such quantitative data, which cannot be obtained in traditional workups, provide sensitive and objective localization information.

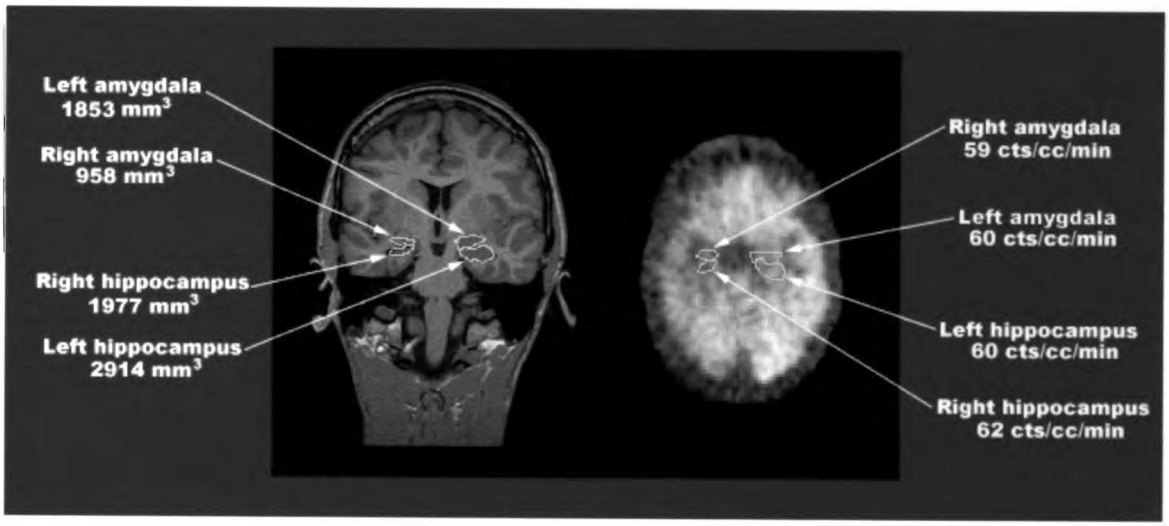

Figure 27 Quantitation of hippocampus and amygdala MRI regions and the use of MRI-PET co-registration to obtain FDG concentration per unit volume in FDG-PET (2-D original slices shown here).

The correlated image datasets are encoded into the targeted data model to serve as definitive indexing in image query. For example, registering the functional images of PET with the MRI images of the same patient, allows the intrinsically better spatial resolution of MR images to be used in quantitatively analyzing functional information (metabolic count of glucose consumption) of captured PET scans. In epilepsy surgical evaluation, neurologists are able to

pinpoint those parts of the brain with suspicious hypometabolic activity and compare their locations with the geometric location of neuronal cell loss in the MR images. The regions of interest derived from segmenting the MR images are transformed into the PET space for comparison.

6.3 Extraction of structural and functional information

The segmentation and extraction of medical images are done interactively using the volumetric image display and analysis (VIDA) environment [62] and BrainImage software (Stanford Psychiatry Neuroimaging Laboratory, Stanford University) [71]. Image features are stratified into different levels of detail: Image dataset → anatomical structures → pathological → microscopic. We divide the image features into primitive and logical. Primitive features are directly obtained from the medical images, such as volume, shape, and texture of certain organs in MR images or metabolic activities of brain tissue in PET scans. Regions of interest are semi-automatically outlined in the MR images to obtain anatomic volumes and co-registration with functional images allows quantitative analysis of functionality in the corresponding anatomic region. Logical features are abstract representations of images at various levels of detail and deeper domain semantics. For example, whether the volume of an anatomic structure is normal or whether certain brain tissue is hypometabolic in reference to certain established data. These logical features are synthesized from primitive ones and additional domain knowledge. All features extracted are entered into appropriate attributes of the objects defined in a data model to facilitate subsequent information query by content. In epilepsy, we have extracted MRI anatomical volume, PET glucose uptake count, MRS spectra, and MEG dipole polarization for the amygdala and hippocampus. I have also included pathological samples from surgery that

were digitized using a SPOT II digital camera. Therefore, we are able to analyze the brain structure and function from several levels of detail for clinical research and outcome analysis.

Once image pairs are registered into common space, their biomedical information can be combined, extracted, and quantitated to obtain important information about the location and nature of the epileptogenic zone. For example, the high resolution MR image provides a basis to anatomically map glucose metabolism. This allows the ability to identify metabolic rates in specific brain regions of interest. The neurodiagnostic workstation incorporates a program developed at Lawrence Berkeley Laboratory (Center of Functional Imaging, LBL) in conjunction with VIDA to map regions of interest defined on the MRI to the PET sinograms for quantitation of glucose uptake.

6.4 Image content indexing

A vital area of research for medical image databases is the development of techniques to retrieve image datasets by their content. Indexing images by their content allows a wealth of established database theory, methods, and tools can be readily applied for content-based access, creation, and manipulation of the teaching file. When creating a teaching file, the physician can execute at broad search to find all images that contain specific image features such as cancerous tumors in the frontal lobe of the brain, microcalcifications in the breast, small nodules in the lung, atrophic tissue in the brain, etc.

An image dataset consists of the image data and the associated textual header data. This research builds on the PACS indexing image datasets based on artificial keys, such as patient name or hospital ID. For content-based information query, the system must recognize and quantitate image content and merge the quantitated image data with textual patient data into a common data model. The content of a medical image includes three levels of abstraction: (i)

features or attributes, such as the texture pattern of an organ and the signal strength of brain metabolites; (ii) structural objects, such as image segments corresponding to anatomical regions; and (iii) semantic information, such as the types of relationships between two objects.

The automatic methods of creating textual content indices draw their information from the header portion of every image file as well as the diagnostic information contained in the textual reports stored in the RIS and HIS. The adoption of DICOM (Digital Imaging and Communications in Medicine) has standardized the structure and content of image headers, making the design of software routines to automatically convert the relevant clinical information into the pre-defined data model straightforward. UCSF HI-PACS image files all have the DICOM headers that contain patient and imaging exam information. The DICOM header is organized into sequential data element tags, each consisting of a group number and element number. For example, "SeriesDescription" is located in group 0008, element 103e (see Table 2). This value is automatically extracted and entered into the database column "Series_Description". In order to optimize the efficiency of the data warehouse, the information in the DICOM headers is inserted into three database tables, Studies, Series, and Images corresponding to the way in which DICOM images are organized in the HI-PACS system (See Tables 3 and 4). A study consists of one or more series, and a series consists of one or more individual images. For example, the typical MRI study consists of around 6 series, and each series usually has 50-144 image slices.

Certain keywords or phrases are automatically extracted from the physician textual reports for indexing purposes. More sophisticated software routines automatically search the textual patient reports for keywords to classify disease type, state, and outcome; support surgical, pharmaceutical, or radiotherapy treatments; etc.

The conversion of pixel-based image information into useful content indices is a much more complex undertaking due to the imprecise nature of medical images. The boundary of a tumor, for example, may be fuzzy; depending on the resolution of the imaging modality that is used. Yet, the accurate delineation of a tumor is an essential first step for curative therapy. State-of-the-art segmentation programs are being developed to improve the extraction of information from images of rigid bodies, such as hand bones and brain tumors, which have ideal image characteristics of relatively well-defined edges. Images of soft tissues like the heart and brain do not have ideal image characteristics and the available image processing routines perform poorly when applied. These soft tissue images are often imaged three dimensionally by CT, MRI, and PET and represent valuable anatomic and physiologic information.

We divide the image features into primitive and logical. Primitive features are directly obtained from the medical images, such as volume, shape, and texture of certain organs in CT images or metabolic activities of brain tissue in PET scans. Logical features are abstract representations of images at various levels of detail and deeper domain semantics. For example, whether the volume of an anatomic structure is normal or whether certain brain tissue is hypometabolic in reference to certain established data. These logical features are synthesized from primitive ones and additional domain knowledge. All features extracted are entered into appropriate attributes of the objects defined in an object data model to facilitate subsequent information query by content (Figure 28)

Figure 28 illustrates the operational steps taken to extract image features from the MRI and PET image datasets. The feature extraction is based on the *a priori* approach, rather than the dynamic and automatic feature extraction during user query as proposed in many non-medical image database applications [72]. Image registration permits the combination of different types of

functional (such as PET and SPECT images) and structural information (such as MRI images), setting the stage for feature extraction. For example, registering the functional images of PET with the MRI images of the same patient, allows the intrinsically better spatial resolution of MR images to be used in quantitatively analyzing functional information (metabolic count of glucose

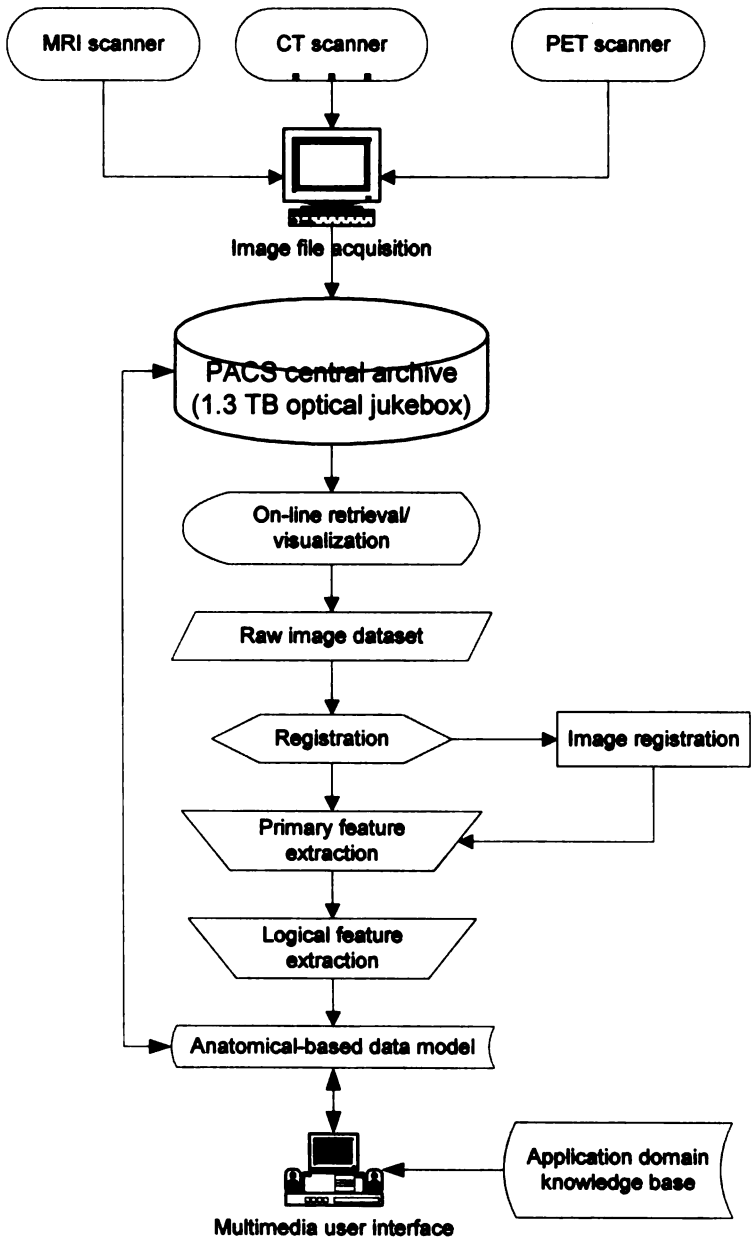

Figure 28 The operational flow of extracting image features into an anatomical based data model for subsequent content-based image indexing in digital imaging teaching file.

consumption) of captured PET scans.

The clinician saves the analyzed results of the workup in the object-oriented data model to serve as content indices to the images. The data model used in the database is based on the anatomical composition of the brain as illustrated in standard medical textbooks. An object in this data model of the brain consists of a unique anatomical name, a set of features or attributes, and a set of relations with other brain objects in the type hierarchy. For example, structural and functional information extracted as shown in Figure 27 are stored into the amygdala and hippocampus objects under the supertype of temporal lobe object. In epilepsy, I have extracted MRI anatomical volume, PET glucose uptake count, MRS spectra, and MEG dipole polarization for the amygdala and hippocampus.

A neurodiagnostic workstation prototype was developed using an object-oriented multimedia GUI builder. Thus, user-friendly interfaces for retrieving, visualizing, and analyzing PACS images, can be rapidly developed for specific domain applications. The following figures illustrate the content-based retrieval of medical images in presurgical planning in epilepsy and age assessment of pediatric bone images.

Figure 29 illustrates the use of content-based information query for assisting the presurgical evaluation of complex partial seizures. In this case, the user first specifies the structural, functional, and textual attributes of the MRI studies of interest. The sliders in the (MRI) "Structural Volume" and (PET) "Glucose Count" boxes are used to specify the range of the image attributes for the amygdala and hippocampus. The database returns with a list of seven patients satisfying the combined image and patient attribute constraints. The database returns a list of patients satisfying the query constraints and a set of representative pictures of interest of the image sets in thumbnail form. The user then clicks on one of the thumbnail images to zoom

it up to the full size or to retrieve the complete 3D MRI dataset for further study. After studying the retrieved images, the user can update the database with new pictures of interest, regions of interest, and image attributes, and textual reports. The multimedia user interface of the workstation is object-oriented and compositional, such that another interface format, tailored for different applications, can be rapidly implemented using the same set of graphical icons and tools.

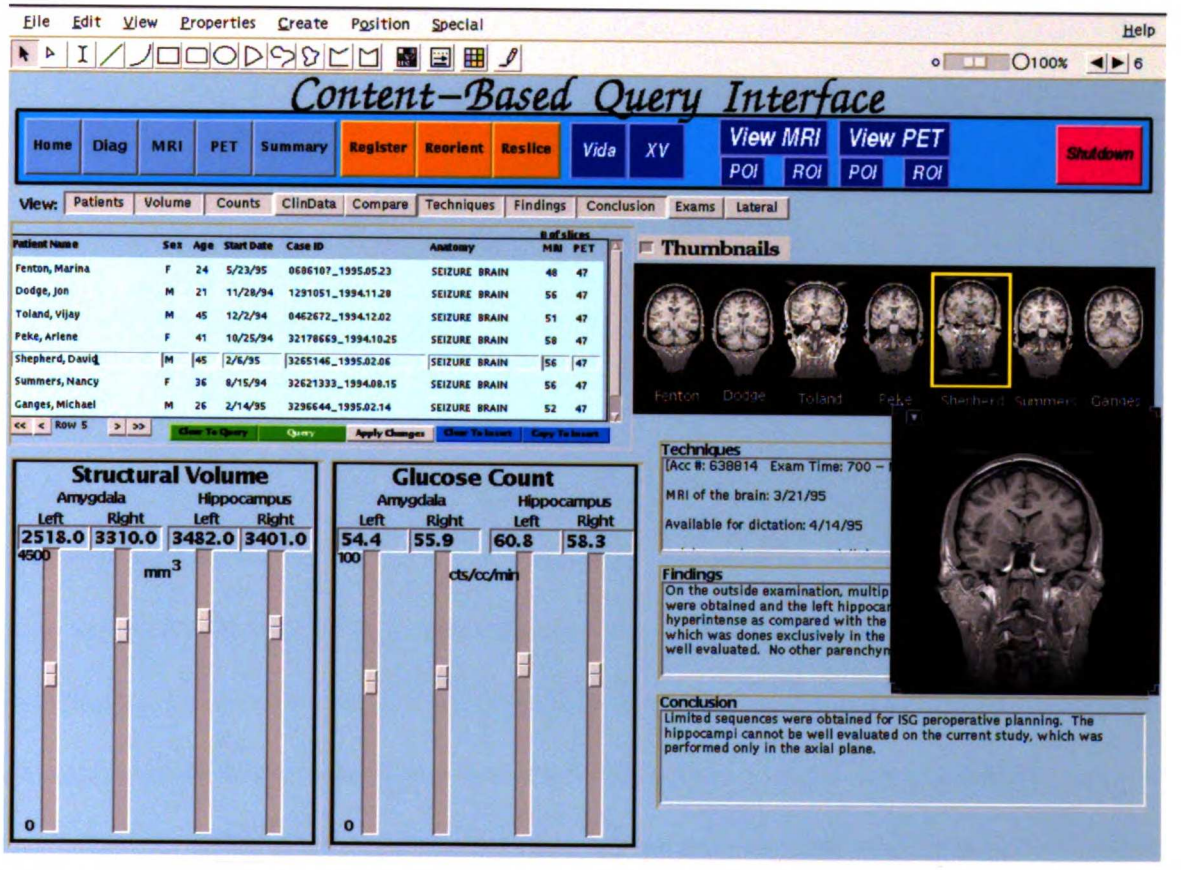

Figure 29 Content-based retrieval of MRI images based on ranges of structure/function attributes. The buttons across the top provide access to different types of data including diagnostic reports (Diag), MRI, and PET. The orange buttons correspond to windows for performing image registration (see Figure 23). Thumbnail images on the right provide a visual index to the image datasets. Using the sliders in the lower left inputs queries by structural volume and glucose count ranges.

The clinician can save the analyzed results of the workup into the neuroimaging database for future reference. For example, structural and functional information extracted as shown in

Figures 28 and 33 are stored into the neuroimaging database to enable flexible user query of multimedia medical data.

We are utilizing the neuroimaging data warehouse system in supporting several clinical care and research areas of seizure disorders. The following subsections describe some of these applications.

6.5 Diagnostic workup of seizure disorders

Diagnostic workup of neurological cases, such as epilepsy, often is a time consuming and laborious endeavor of gathering all relevant medical record and images in various information systems and paper filing systems. The collection and preparation of diagnostic workup may take weeks. The availability of an integrated multimedia database system capturing patient records and images for particular diseases allows a one-stop shopping solution to provide faster and more effective diagnostic workup.

When a clinician sits down at a client computer to initiate an analysis session, the first step is to retrieve image and textual data from PACS and other data sources. Figure 30 shows a screenshot taken during the retrieval of image and textual information from the PACS to the desktop workstation. In the upper left, the patient name is entered (the patient name and ID have been changed to maintain privacy). The system returns descriptions of the imaging studies corresponding to the specified patient name, and these items are displayed as rows in the upper scroll widget. Clicking on a row triggers the retrieval of the diagnostic report, and clicking on the "Retrieve Image" button triggers the retrieval of the selected image dataset. Software modules automatically convert the DICOM based image file to formats readable by the visualization packages on the desktop workstation. The PET, MEG, and MRS image datasets are retrieved

via file transfer protocol from the respective scanners. After retrieval the images can be visualized by launching either 3DVIEWNIX or VIDA from the GUI.

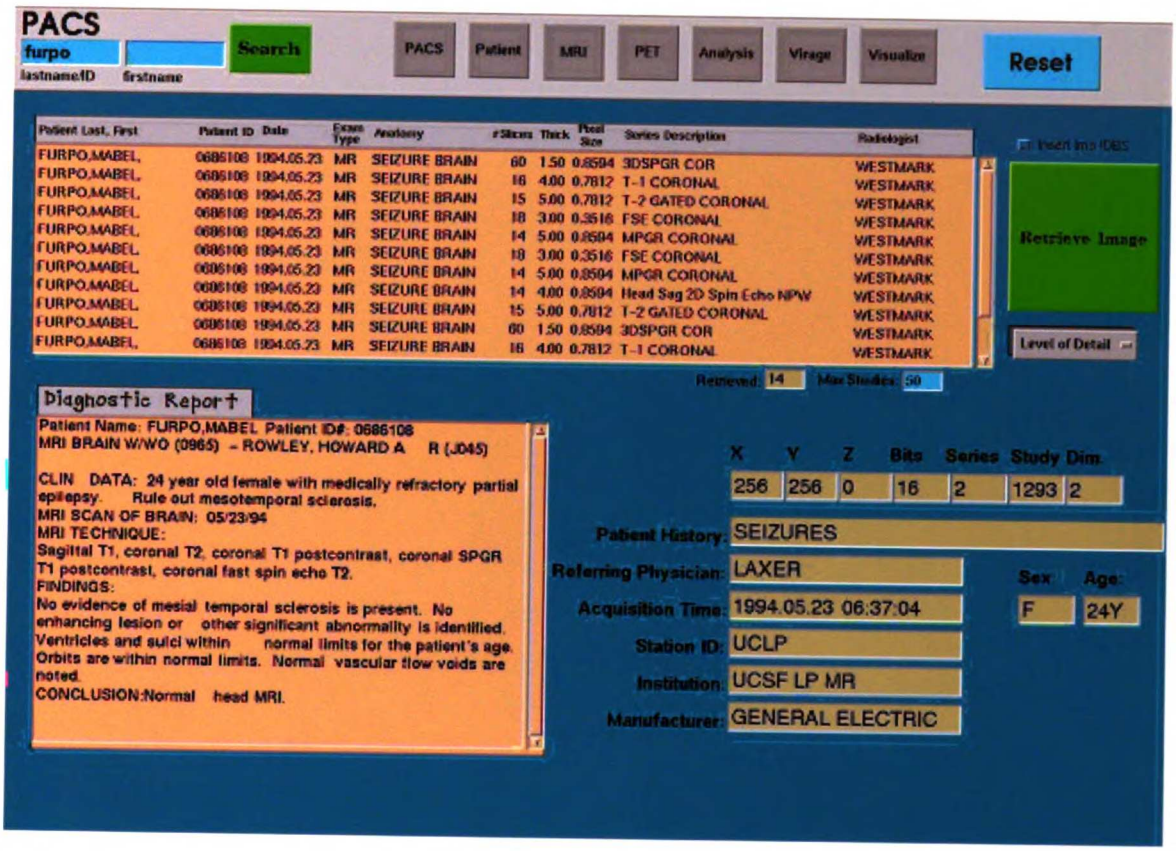

Figure 30 A screenshot taken from the neurodiagnostic workstation showing the textual information retrieval from the PACS central node. Note that the PACS lacks the sophistication of the image data warehouse query GUI as seen in Figure 29. PACS retrieval is by artificial keys instead of image features and thumbnail images.

With the imaging studies now reside on the workstation, biomedical information is quantitated, extracted, and combined in various ways to aid in the localization process. First, the non-brain structures, e.g. scalp and skull, are automatically segmented from the MRI dataset, and then, a transformation matrix is generated to co-register the volumetric PET with the newly processed MRI dataset. The user can set several registration parameters such as sampling, iterations, thresholds, and initialization files.

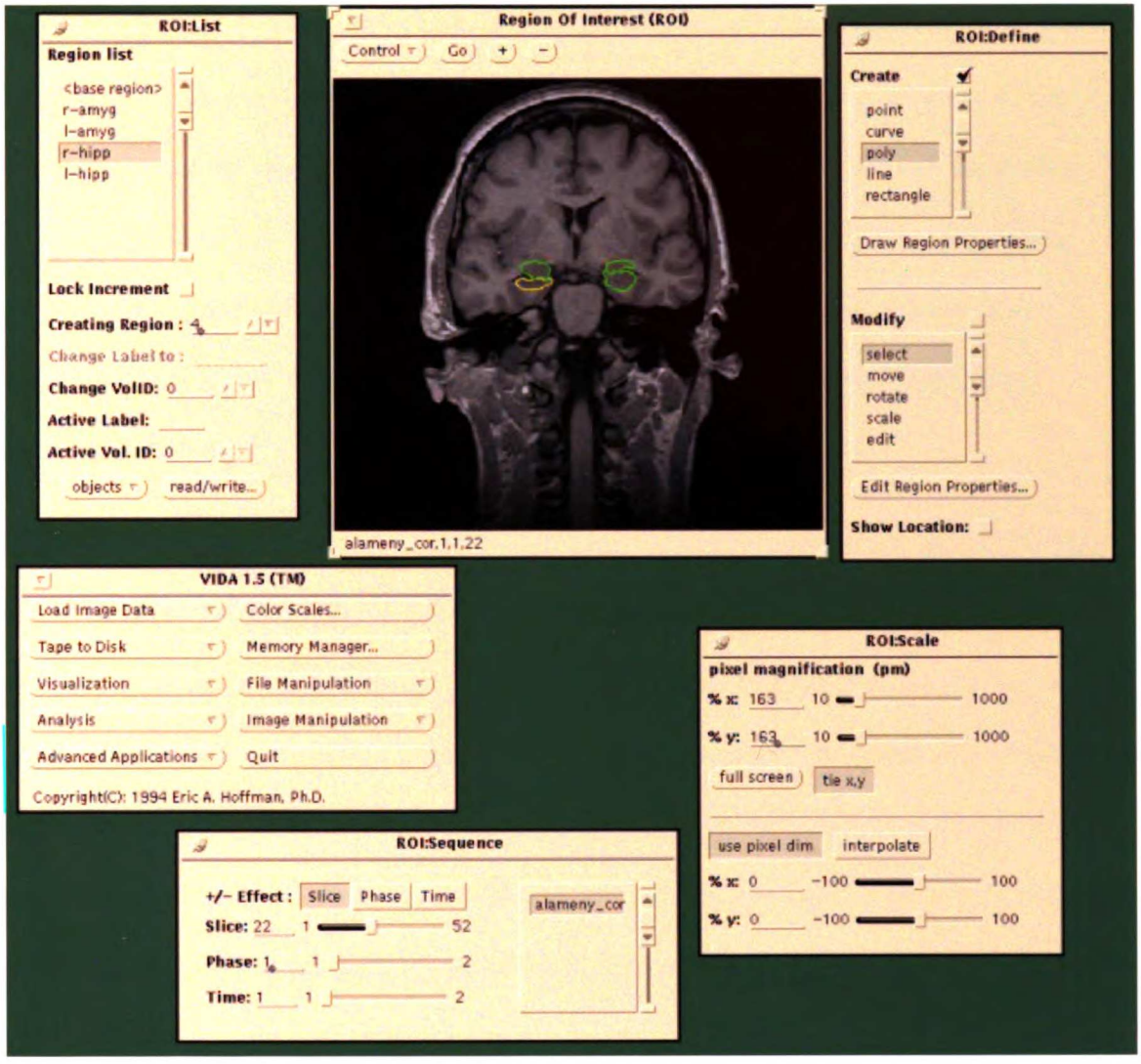

Figure 31. A screenshot taken from the neurodiagnostic workstation showing the interactive segmentation of temporal lobe structures from MR images using VIDA. The ROIs have been outlined in green, and the yellow outline corresponds to the active region under analysis. The regions extracted here are the amygdala and hippocampus.

Exploiting MRI's excellent anatomic detail, the hippocampus and amygdala are interactively segmented using the ROI (region of interests) utilities of the neuroimaging data warehouse system (Figure 31). The resulting segmentation parameters are combined with the transformation matrix and PET sinogram files to yield glucose counts for these mesial temporal structures (see Figure 27). Such quantitative data, volumes and glucose counts, cannot be obtained by conventional workups and are important in determining the suitability of patients for

surgical treatment. MRSI registration is done prospectively before each data acquisition. A coordinate transformation from the MEG space to the MRI space allows the projection of all or parts of the reconstructed dipole pathway into a multislice or 3-D MR image of the patient. With the temporal lobe structures of the amygdala and hippocampus now segmented and analyzed for volume, metabolic rate, electrical activity, and metabolite concentration, the epileptogenic zone can be lateralized and localized if there is sufficient concordance of pathological findings.

After the workup, the clinician saves all the analyzed results into the epilepsy data warehouse for future reference and research. This includes not only the final numerical values of volume, glucose counts, electrical spike magnitude and location, and metabolite concentration, but also the scalp-less MRI, segmentation parameters, and transformation matrix that were generated at the workstation. The data can then be accessed again at a future date for analysis and reference purposes, allowing the assessment of the accuracy of segmentation and findings and comparison to new cases. The database can manage and store the analysis work of multiple clinicians on multiple patients.

The power of organizing the analyzed data in the data warehouse is the ability to do on-line analytical processing of the collected data. The database can be queried on any number of keys ranging from patient name to image features to report keywords. Complex queries can be executed such as "Find female patients age over 21 years with right hippocampal atrophy > 10% and corresponding depletion of N-acetyl-aspartate > 15%." Matching patients are returned to the workstation, and clicking on the thumbnail images can retrieve full image datasets. The textual information is displayed in a variety of lists, entry fields, and textboxes. Thus, not only is

it possible to index into the textual data, but also into the images themselves and the quantitative data they contain.

6.6 Diagnostic example using neurodiagnostic workstation

The workstation has been utilized to analyze brain images of 40 patient cases. In cases where there were no hippocampal abnormalities on MRI, the co-registered MRI was used to increase the ability to interpret subtle lateralized abnormalities on PET. In all 7 cases lateralized relative hypometabolism was identified concordant with ictal EEG findings. In preliminary results, missed abnormalities and false interpretations of independently interpreted high resolution FDG-PET were correctly identified with co-registration to MRI, allowing both an increase in sensitivity and specificity in the detection of hypometabolism in patients with partial epilepsy of mesial and neocortical temporal origin.

The following example demonstrates the identification and correct interpretation of focal hypometabolism only after co-registration on the workstation. Figure 32 shows an FDG-PET scan from a patient with right neocortical temporal lobe epilepsy. The scan was originally interpreted as "probably normal". Although intracranial ictal EEG recordings were non-localizing, interictal data from MEG spike source localization an intracranial EEG suggested that the epileptogenic zone was located in the right lateral temporal region. MRI in this region as well as mesial temporal structures was normal. After co-registration of MRI, interpretation of focal hypometabolism on PET in the posterior superior lateral temporal region became unequivocal. Confidence from co-localization of the local PET abnormality and focal neurophysiologic disturbance directed surgery leading to a seizure free outcome for the patient.

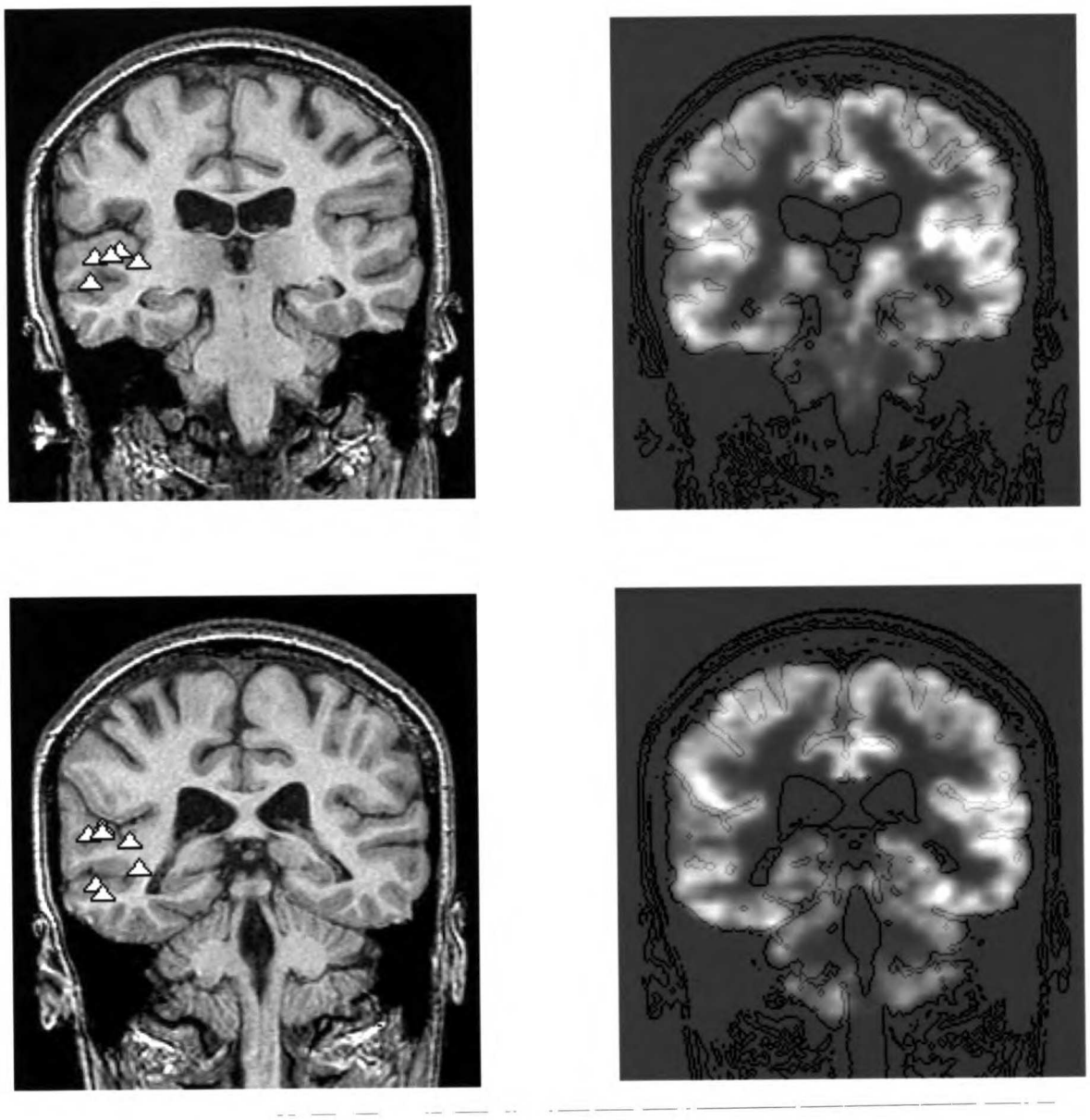

Figure 32 MRI-PET-MEG co-registration to detect a focal electrophysiologic and metabolic interictal disturbance. Left--MEG spike dipole source localization (white triangles) overlaid on selected co-registered coronal MRI slices from the temporal lobes--dipole sources correspond to an active disturbance of epileptiform activity recorded bipolarly over the right temporal lobe with scalp-sphenoidal EEG (sharp waves maximum at T4); the MRI is normal. Right--corresponding FDG-PET slices with overlayed contours from MRI anatomy--focal hypometabolism is present in the right superior temporal gyrus, remarkably colocalized with MEG spike sources. Pathologic examination cortical resection confined to the superior temporal gyrus and superior bank of the posterior middle temporal gyrus revealed hamartomatous dysplasia. Co-registration was performed with AIR©.

Direct comparison of quantitative data between different metabolic imaging volumes of interests can be done on the workstation. In Figure 33 two types of metabolic data--the concentration of

NAA (a marker for neuronal cell density) and glucose uptake (a measure of synaptic activity)--are calculated for the same volume, in this case a single voxel within the hippocampus. Further application afforded by co-registered MRI anatomy is the ability segment the MRSI voxel such that only the contribution from hippocampal or parahippocampal gray matter is sampled in the metabolite signal analysis.

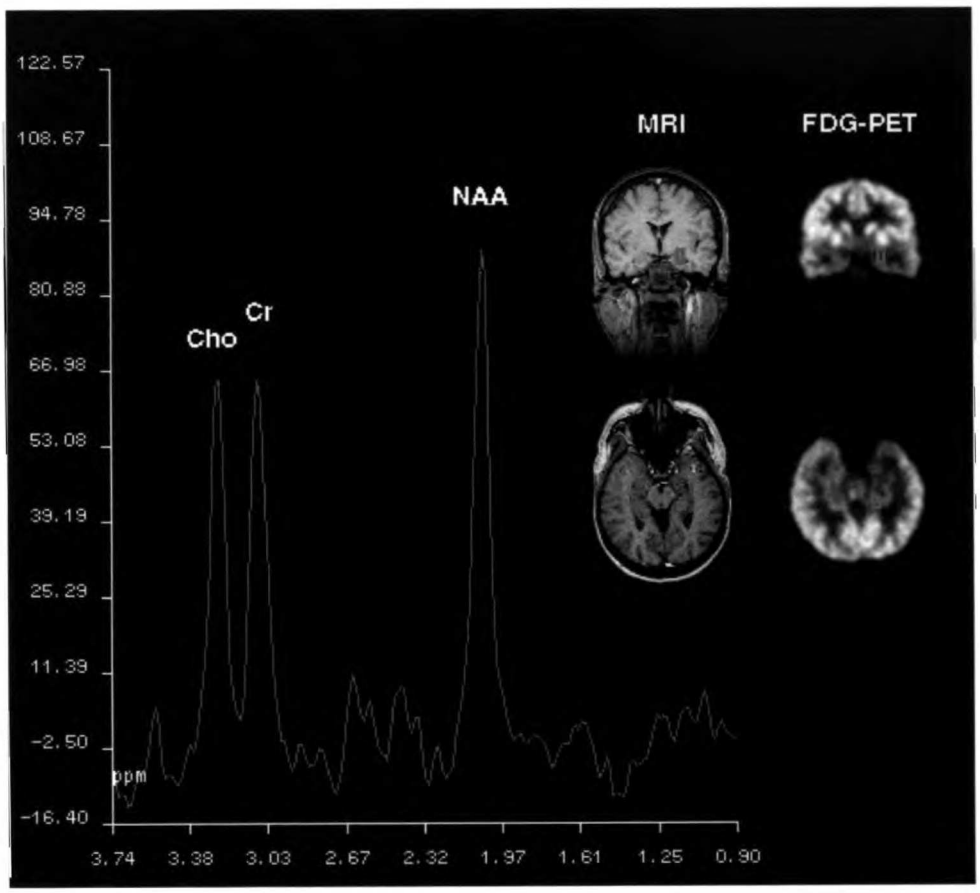

Figure 33 MRI-MRSI-PET co-registration for direct comparison of [NAA] and specific activity of glucose uptake. ^{1}H-MRS spectra from voxel in left hippocampus on MRI (left inset). Same voxel is placed on coregistered FDG-PET (right inset). The normalized [NAA] (using water as an internal standard reference) for this region of the hippocampus can be directly compared to the normalized specific activity of glucose uptake (or actual metabolic rate of glucose metabolism if arterial blood flow curve of FDG is available) of this same region. Co-registration was performed with AIR©. Spectroscopy courtesy of Gabriele Ende (Central Institute of Mental Health, Mannheim, Germany, 1995).

Results of the preliminary image data analysis indicate that dipole sources of interictal spikes could be estimated in 19 of 40 patients. Twelve of the patients have had their outcomes assessed

while the remaining patients will be reported in the future. All twelve patients had a MEG study, and eleven had a PET study. The imaging results and outcomes of these twelve epilepsy patients are given in Table 5. Seven of the twelve patients had localizing MEG studies, and 6 of eleven patients displayed hypometabolic activity lateralized to a specific lobar region. The six patients who had both localizing MSI and PET all localized to the same lobar region; four were in the medial temporal lobe and 2 in the lateral temporal lobe. Five of the six patients had sublobar region of seizure onset agreement. Case C0028 is exceptional because both ictal EEG and MRI provided no localization information. Blinded nuclear medicine specialists originally interpreted the PET scan as normal. Only with co-registration to the MEG spike sources were clear focal hypometabolism in the corresponding region revealed. In the group as a whole correlation of MSI with final localization of the epileptogenic zone was higher than video EEG, MRI, or high resolution PET. MSI and PET provided the highest correlation of any combination of non-invasive modalities.

Case no.	Ictal EEG	MRI	PET	EEG/MEG	Surgery	Outcome (months)
C0003	LT	L hipp atrophy	NL	not done/neg.	LTL	Sz. free (5)
C0015	LT	L hipp atrophy & focal increase T2	-	FP1,F7,F3,SP1/LMT	LTL	Engel II (15)
C0026	LT	Normal	LMT	F7,T3/LMT	LTL	Engel II (15)
C0029	LT	L hipp atrophy	LT	neg/neg	LTL	Sz free (15)
C0039	LT	Normal	LMT	SP1/LMT	LTL	Sz free (5)
C0075	RT	Normal	NL	neg/neg	RTL	Sz free (8)
C0081	RT	R hipp atrophy & increased T2	RMT	neg/neg	RTL	Sz free (8)
C0088	RT	R hipp atrophy & focal increase T2	RT	F8,T4/RLT	RTL	Sz free (9)
C0091	RT	Rt. hipp atrophy	RT	neg/neg	RTL	Sz free (7)
C0096	LT	L hipp atrophy & focal increase T2	LMT	SP1/LMT	LTL	Sz free (5)
C0028	NL (SDE)	Normal	RLT (focal)	T4/RLT	RSTG/MTG topectomy	Sz free except some SPS (10)
C0055	NL (SDE)	L lateral temporal focal increase T2	LLT (focal)	T3/LLT	LLT lesionectomy and additional AILT resection	Sz free (4)

Table legend:

Ictal EEG
LT = Left Temporal
RT = Right Temporal
NL = Non-Localizing
SDE = Subdural Electrodes

PET
LMT = Left Medial Temporal
NL = Non-Lateralized
RLT = Right Lateral Temporal
- = study not done

EEG/MEG
LLT = Left Lateral Temporal
LMT = Left Medial Temporal
RLT = Right Lateral Temporal

Surgery
AILT = Anterior Inferior Lateral Temporal
LLT = Left Lateral Temporal
LTL = Left Anterior Temporal Lobectomy
MTG = Medial Temporal Gyrus
RSTG = Right Superior Temporal Gyrus
RTL = Right Anterior Temporal Lobectomy

Table 5 Patient clinical features and epilepsy evaluation. These patients have either mesial temporal lobe epilepsy (MTLE) or neocortical epilepsy.

6.7 Neurodiagnostic workstation observations

The multimedia PACS workstation enables clinicians to more effectively evaluate epilepsy patient data from PACS through the use of registration, 3-D rendering and visualization, ROI analysis, and database management. It also enables better understanding of the epileptogenic process itself and promises to facilitate multimodality investigation of brain functions and anatomy in other brain diseases such as multiple sclerosis. The intuitive GUI frees the clinician to concentrate on the clinical aspects of the case, and its integrated software utilities expand the utilization of PACS to clinicians outside the radiology department. By storing the extracted image and text data in the relational data model, the workstation increases the knowledge base of PACS. This knowledge augmentation increases the power of PACS for clinical applications.

6.8 Data analysis on epileptic foci lateralization

Electroencephalography (EEG) is the most common method to localize the epileptogenic zone. Nevertheless, paroxysmal abnormalities occur intermittently and may not be easily captured. Inpatient recording of scalp EEG with video is necessary to capture the seizures. MRI examinations, and sometimes PET scans, are used to provide additional information regarding localization of the epileptogenic zone [54].

The Epilepsy Center currently performs additional non-invasive neuroimaging examinations, i.e., PET, MRS, and MEG on a selected group of epilepsy patients related to clinical research. The multiple image datasets of these patients are processed, organized, and modeled for on line data interpretation and analysis. The use of combined non-invasive tests to eliminate or reduce the frequency of intracranial EEG recordings will help to improve patient care, minimize complications of invasive tests, cut down costs, and save time of hospital stay. In addition,

improved accuracy of epilepsy localization will increase the number of medically refractory epilepsy patients remediable by surgery treatment.

The neuroimaging data warehouse framework has been utilized to analyze brain images of 80 patient cases. In cases where there were no hippocampal abnormalities on MRI, the co-registered MRI was used to increase the ability to interpret subtle lateralized abnormalities on PET. Missed abnormalities and false interpretations of independently interpreted high resolution FDG-PET were correctly identified with co-registration to MRI, allowing both an increase in sensitivity and specificity in the detection of hypometabolism in patients with partial epilepsy of mesial and neocortical temporal origin.

The data analysis module of the image data warehouse is used to investigate the lateralization concordance between various neuroimaging modalities in epilepsy. Such types of queries are valuable for determining the clinical efficacy of the diagnostic procedure. Figure 34 illustrates an example of data analysis. In this application, surgery result is used as the gold standard for reference and MRI and scalp electroencephalography predictions are compared between each other and surgery results in patients who have undergo the surgical treatment from more than a year. The data warehouse allows the users to customize the presentation format beforehand, i.e., personalization of display layout. In this case, the user selects pie charts and bar graphs to illustrate the analyzed results instead of tables or text formats. Further, as shown in Figure 35

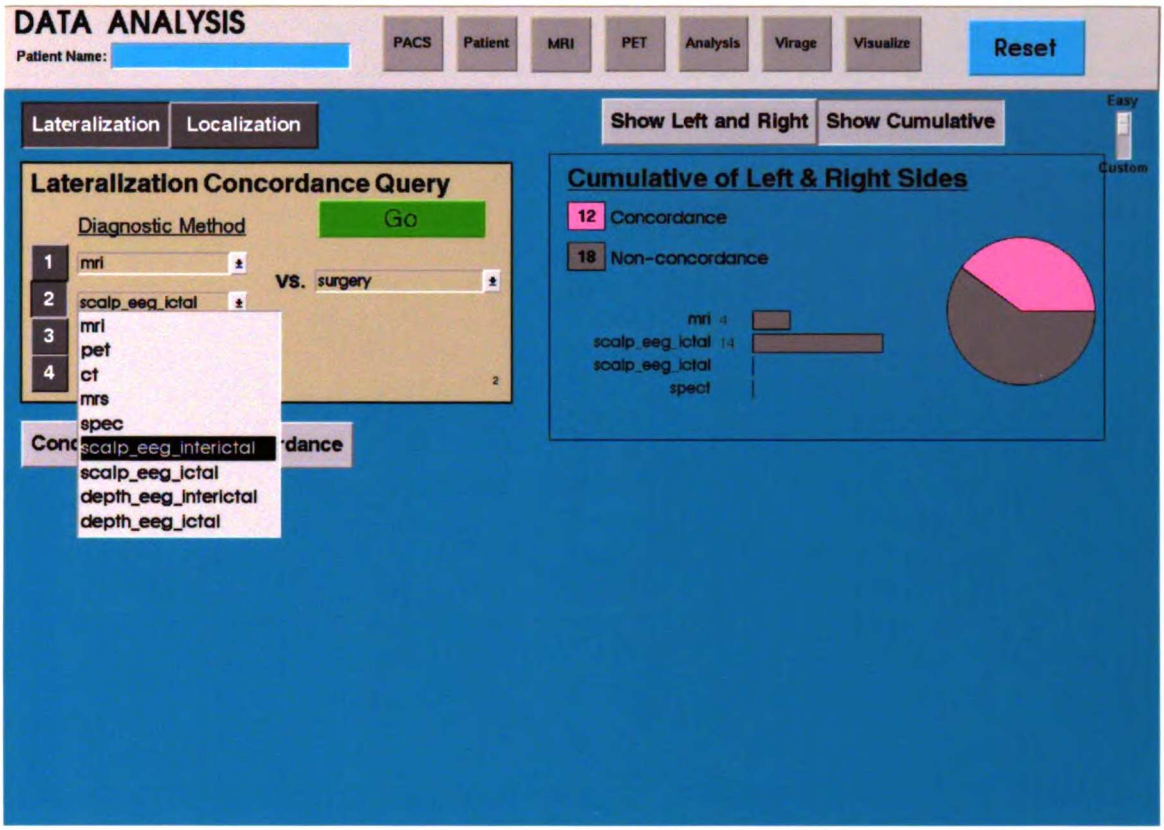

Figure 34 Data analysis GUI illustrates the data analysis functions on lateralization and localization concordance. Bar graphs and pie charts aid in the visualization of the data analysis results. User queries are handled by the middle layer of the data warehouse framework which accesses the underlying database containing the actual lateralization information.

a detailed non-concordance listing in the lower left text field allows the user to select a particular patient case and then retrieve the rest of the epilepsy record for detailed study. The analytical power of such an image data warehouse increases with the increase of the content, i.e., processed patient images and medical cases.

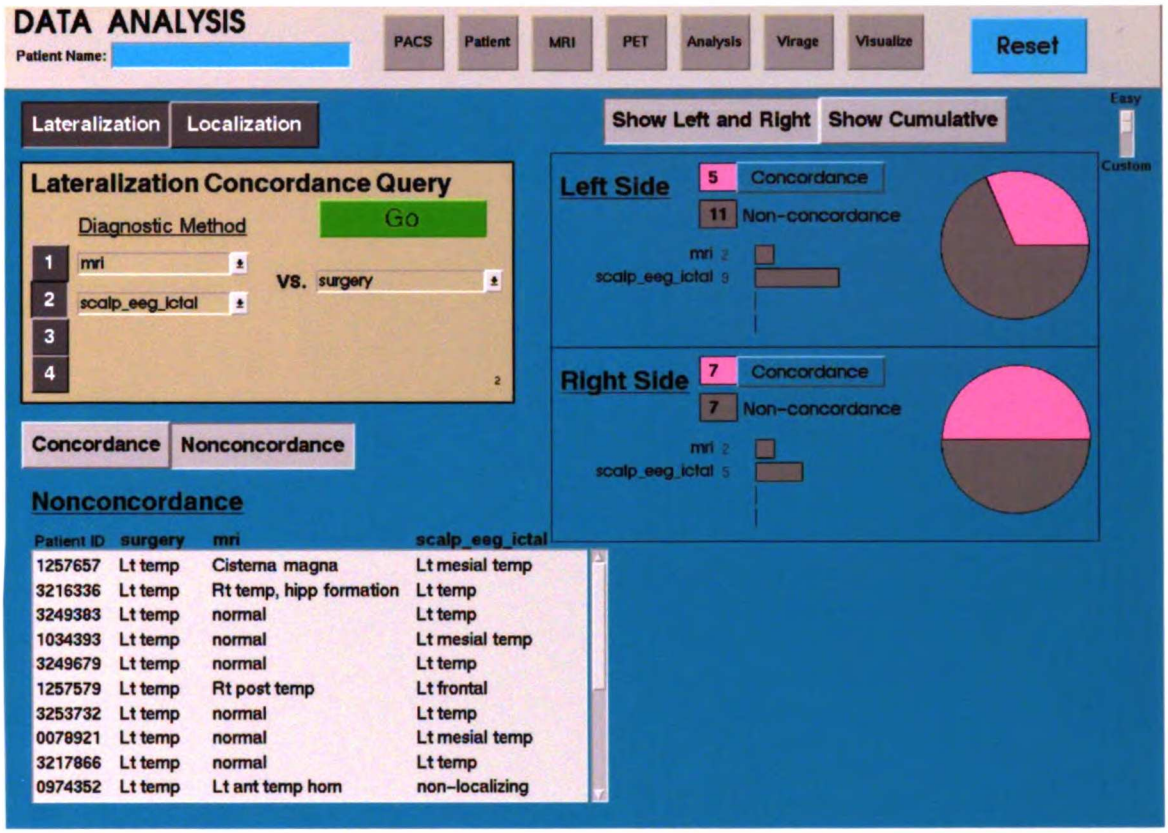

Figure 35 Results from data analysis query in Figure 34

Twenty-three of 24 patients studies with PET had one or more regions with relative hypometabolism confined to a single temporal lobe. MRI revealed easily discernible relative hippocampal atrophy in fifteen patients. T2 hyperintensity was seen only with concurrent hippocampal atrophy. All cases of MRI identified hippocampal atrophy were concordant with ictal EEG. Seventeen of 25 patients were lateralized with HV. Nine of 13 patients were lateralized with T2 relaxometry. ^{1}H-MRS lateralized 15 of 24 patients with once discordant lateralization in one patient. The results of each modality's ability to lateralize the epileptogenic zone are summarized in Table 6:

Modality	Lateralized	n	%	AI
PET	23	24	96%	NA
MRI - hippocampal atrophy	15	25	60%	NA
MRI - T2 increase	9	25	36%	NA
HV	17	25	68%	$\geq$ 8%
T2 relaxometry	9	13	69%	$\geq$ 4%
^{1}H-MRS	15	24	63%	$\geq$ 12%

Table 6 Lateralization of epileptogenic zone by neuroimaging modalities.

FDG-PET was the most sensitive imaging methodology for lateralizing complex partial seizures in the temporal lobe, lateralizing all but one patient with hippocampal atrophy and 75% of patients without atrophy. HV lateralized 68% of patients, and T2 relaxometry did not provide additional lateralizing information beyond that provided by HV.

Comparisons of lateralization can only be done in those patients who completed all exams included in the evaluation. Table 7 lists the lateralization from the 23 patients who completed

Modality	Concordant	Discordant	Non-lateralized
FDG-PET asymm. score > 3	20	0	3
HV AI $\geq$ 8%	15	0	8
^{1}H-MRS [NAA] AI $\geq$ 12	15	1	7

Table 7 Comparison of lateralization (n=23)

FDG-PET, HV, and ^{1}H-MRS studies (from the total of 25 patients, one did not have a PET, and in another the ^{1}H-MRS volume selection was displaced above the plane of the hippocampi). No

discordance was found with FDG-PET or HV. One patient was discordant with ^{1}H-MRS measures.

The surgical planning of medically refractory epilepsy often requires invasive, intracranial EEG recordings to localize the epileptogenic zone for resection. There are, however, definite risks and considerable costs associated with such invasive procedures. Planning for surgery in epilepsy requires analyzing and combining structural and functional data from numerous sources to localize the seizure foci for resection. This reported work shows the results of studying the lateralizing accuracy of multiple neuroimaging modalities, e.g., MRI, PET, and ^{1}H-MRS, used in noninvasive planning of epilepsy surgery. Image analysis including ROI segmentation, ROI quantitation, and image registration was carried out on a CAD workstation. FDG-PET was the most sensitive imaging modality for lateralization in this study. FDG-PET was even able to lateralize the abnormality even in the absence of HV and other MRI evidence for hippocampal sclerosis, including T2 relaxometry, supporting the continued role for FDG-PET in the evaluation of patients with complex partial seizures in the temporal lobe. ^{1}H-MRS was not as sensitive as other MR methods. Future work will focus on optimizing the use of these multiple imaging modalities in concert to plan surgeries in patients with complex partial seizures.

6.9 Decision thresholds for epilepsy imaging diagnosis

The current approach of lateralization of epileptic foci is qualitative and often depends on the experience of individual imaging specialists. Decision thresholds are numerical thresholds for multimodality lateralization and localization of the epileptogenic zone that leads to efficacious resective surgery. These thresholds are determined by analyzing the neuroimages of many patients for volume loss in MRI, hypometabolism in PET, and metabolite loss in MRSI. Many studies have shown a high correlation exists between the degree of MR-defined volume loss in

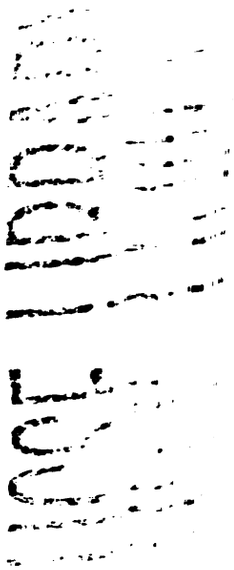

the hippocampus ipsilateral to the seizure focus, and the severity of mesial temporal sclerosis [3]. This threshold is defined in terms of the percentage ratio between the abnormal and normal volumes of identical contralateral brain regions. Interictal ^{FDG}-PET usually reveals a single unilateral region of variably mild to severe hypometabolism that is used to calculate two abnormality thresholds. One is a ratio with the metabolism of the contralateral region and the other is a ratio with the entire contralateral hemisphere tissue. In proton MRSI, the ratio, NAA/(CR+choline), for identical contralateral regions is calculated in both patients and normal control subjects. Epilepsy patients have decreases in the metabolite concentrations on both sides of the brain, albeit the decrease on the side of the epileptogenic focus is more severe than the contralateral side. The image data warehouse provides a platform to investigate the quantitative decision thresholds in epilepsy imaging diagnosis.

6.10 Partial volume correction effect on image interpretation

The appearance of decrease FDG uptake indicated from PET study in the mesial temporal region in temporal lobe epilepsy may simply reflect loss of gray matter due to hippocampal atrophy. Increased partial volume effects due to atrophic hippocampi may further increase appearance of hypometabolism. We used a combination of facilities provided by the image data warehouse, i.e., MRI-PET co-registration, with MRI based gray matter segmentation, and partial volume correction to improve the evaluation of hippocampal specific glucose uptake in FDG-PET. The goal was to determine 1) if relative mesial temporal hypometabolism is an artifact of gray matter (hippocampal) atrophy, 2) whether hippocampal metabolism correlates with atrophy evaluated on MRI, and 3) if MRI-based partial volume correction influences measurement of hippocampal metabolic-volume relationships, including epilepsy lateralization. Using the image data warehouse, the analyzed queried results showed that ipsilateral hippocampi of MTLE are

relatively hypometabolic per unit of gray matter volume, and that hippocampal metabolism directly correlates with hippocampal volume. Specifically, partial volume corrected hippocampal metabolism correlated strongly ($r=0.613$, $P<0.001$) with hippocampal volume. Without partial volume correction a weaker, but still significant, correlation was present ($r=0.482$, $P<0.001$). Degree of asymmetry was consistently greater and provided higher sensitivity of lateralization with partial volume versus non-partial volume corrected metabolic measurements.[27]

6.11 Linkage with focal cortical dysplasia

The neuroimaging data warehouse is used to investigate the possibility that a link may exist between focal cortical dysplasia (FCD) and temporal lobe epilepsy. FCD is characterized by abnormally large and misshaped neurons, and is found in isolated patches throughout the brain (hence, focal). Tissue specimens from the surgery team were obtained. The resected tissue from a single patient could take the form of several "chunks" of tissue. The largest chunks may have been cut into smaller chunks. The chunks are fixed and frozen before being cut on the microtome. The chunks were cut into as many as 30 sections (slices) of 40-micron thickness. For reference, the pathology usually slices as 5-micron thickness, but the FCD is easier to see on thicker sections. We applied a cresylviolet stain to each section after which three neurologists examined the section to determine whether it exhibited FCD. Normally, one section per chunk was selected for imaging with the SPOT II digital camera. The pathological image files of 20 patients are saved as color JPEGs and inserted into the image data warehouse (see Figure 36). The participating neuropathologists then downloaded, viewed, and cross-examined the colored sections together with the MRI or PET images of the same patients, as well as associated neurological records and lab tests. So far, the initial study indicates that there is not enough

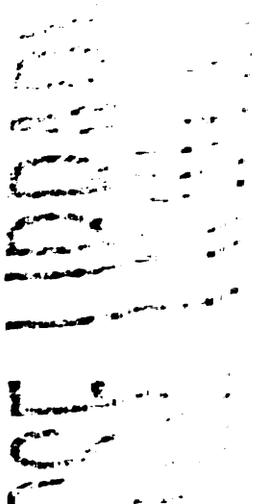

evidence of FCD. We would collect more image data to enrich the statistical power of the data warehouse for more detailed investigation.

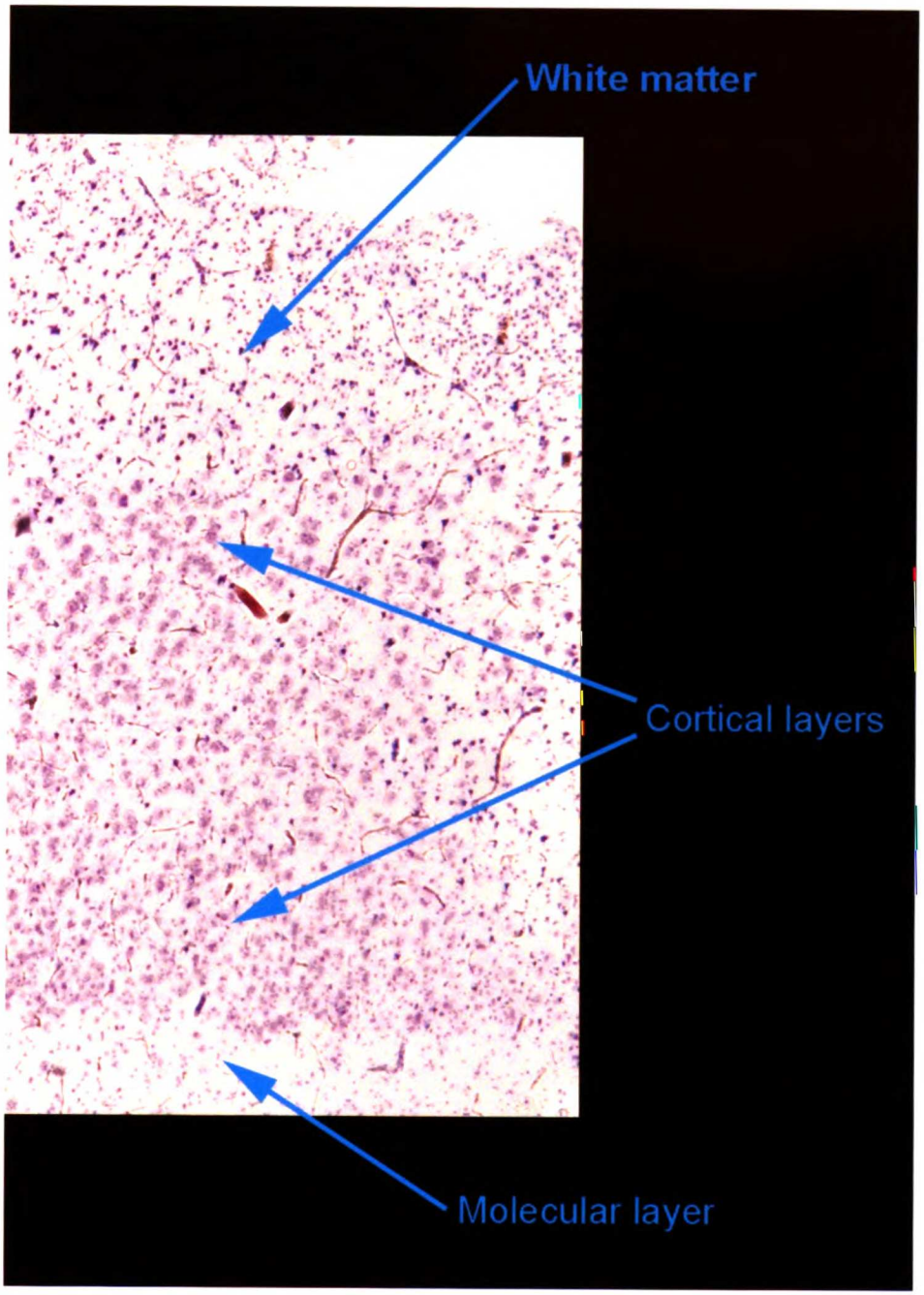

Figure 36 This image was acquired at a magnification of 500x. The images are actually 1300 x 1000 pixels, but we are showing a portion of one such image. This slide exhibits the dislamination of the cortical layer. The neurons should be highly organized into 6 layers. Furthermore, we can see balloon cells, i.e. large and abnormally shaped neurons.

6.12 Conclusion

With the rapid advances and proliferation in medical imaging techniques, today clinicians and biomedical scientists collect complex data in ever-increasing amounts, fostering increased specialization, with resultant challenges to integrate data between and across levels of interaction, control, and function. The sheer quantity and complexity of the image data is such that biomedical research and clinical services would benefit considerably from an information management system approach for its experimental and clinical data. In this paper, I described the design and development of a multi-tier image data warehouse framework in supporting neuroimaging diagnosis and neurological disease management. For the initial implementation, the focus is clinical epilepsy and the informatics applications include: diagnostic workup of seizure disorder, lateralization analysis of surgically operated patients, decision threshold of imaging diagnosis, partial volume correction effect on image interpretation, and focal cortical dysplasia pathological analysis. The collaborating clinicians, neurologists, and neuroimaging specialists are currently evaluating the image data warehouse. I am gathering user feedback to make iterative improvements and to incorporate more data analysis functions for testing and verifying hypotheses.

6.13 Future work

The effort to collect and process more patient cases continues in order to increase the size and statistical power of the image data warehouse. In addition, future work will explore the image data warehouse in three application areas. First, I plan to test the scalability of the seizure data warehouse to include patient undergo gamma knife radiosurgery, in addition to resective surgery. Second, I plan to test the generality of the framework by using it to analyze other neuroimaging related disease progress and treatment methods, such as multiple sclerosis. Third, we plan to

extend the level of data abstractions by including genotype information. Many forms of epilepsy appear to be related to a genetic predisposition. It has been suggested that 15-20% of all patients with epilepsy have one or more gene mutations that contribute significantly to the seizure phenotype. The genometric approach to studying the genetics of epilepsy attempts to identify phenotypic linkage based on genotypic linkage. Large numbers of families in which there are multiple members with epilepsy are sequentially genotyped and relevant data will be modeled in the Epilepsy data warehouse.

On the technological side, the methodologies I have implemented need to be finalized and distilled into a software toolkit that can be readily utilized by other researchers interested in neuroimaging image analysis and management. The data model needs to be refined to allow for more effective modeling on a large scale; for example, to include the seizure data from gamma knife surgery workups as indicated previously. The data warehouse will be iteratively expanded with the addition of smaller data marts where a data mart corresponds to all the data associated with a given treatment protocol. Finally, these technologies could be applied to image-based clinical trials where many clinicians spread out among multiple institutions would need a centralized neuroimaging data warehouse to manage all the multimodality data for analysis, exchange, communication, collaboration, record-keeping, etc. In this case, the data warehouse will have to be expanded into a fourth dimension, time, where it is essential to track the progress of diseases in the patients under study. For example, multiple sclerosis patients undergoing beta interferon treatment need to have their lesion load tracked over time using MRI.

BIBLIOGRAPHY

1. Newell JD, Kelsey CA. *Digital imaging in diagnostic radiology.* New York: Churchill Livingstone, 1990.
2. Krestel E. *Imaging systems for medical diagnosis.* Berlin: Siemens Aktiengesellschaft, 1990.
3. Laxer KD, Rowley HA, Novotny EJ, eds. *Experimental Technologies,* 2nd ed. New York: Raven Press, 1993.
4. Huang HK. *PACS : Picture Archiving and Communication Systems in biomedical imaging.* New York: Vch, 1996.
5. Huang HK. *Elements of digital radiology : a professional handbook and guide.* Englewood Cliffs, NJ: Prentice-Hall, 1987.
6. Wong STC, Zaremba L, Gooden D, *et al.* Radiologic image compression-a review. *Proceedings of the IEEE* 1995;**83**(2):194-219.
7. Zink S, Jaffe CC. Medical imaging databases. A National Institutes of Health workshop. *Investigative Radiology* 1993;**28**(4):366-72.
8. Trevert E. *Something about X rays for everybody.* Lynn, Mass.,: Bubier Publishing Co., 1897.
9. Antonuk LE, Boudry J, Huang W, *et al.* Demonstration of megavoltage and diagnostic x-ray imaging with hydrogenated amorphous silicon arrays [published erratum appears in Med Phys 1993 May-Jun;20(3):825]. *Medical Physics* 1992;**19**(6):1455-66.
10. Kruger RA, Riederer SJ. *Basic concepts of digital subtraction angiography.* Boston: G.K. Hall Medical Publishers, 1984.
11. Ovitt TW, Christenson PC, Fisher HDd, *et al.* Intravenous angiography using digital video subtraction: x-ray imaging system. *American Journal of Roentgenology* 1980;**135**(6):1141-4.
12. Bloch F, Hansen WW, Packard ME. Nuclear induction. *Phys. Review* 1946;**69**(3-4):127.
13. Purcell EM, Torrey HC, Pound RV. Resonance absorption by nuclear magnetic moments in a solid. *Phys. Review* 1946;**69**(1-2):37-38.
14. Crooks LE, Ortendahl DA, Kaufman L, *et al.* Clinical efficiency of nuclear magnetic resonance imaging. *Radiology* 1983;**146**(1):123-8.
15. Runge VM, Brack MA, Garneau RA, *et al. Magnetic resonance imaging of the brain.* Philadelphia: Lippincott, 1994.
16. Hevesy Gv. *Adventures in radioisotope research; the collected papers of George Hevesy.* New York,: Pergamon Press, 1962.
17. Kuhl DE, Edwards RQ. Image separation radioisotope scanning. *Radiology* 1966;**87**:278-284.

18. Brownell GL, Sweet WH. Localization of brain tumors. *Nucleonics* 1953;**11**:40-45.

19. Hounsfield GN. Computed medical imaging. Nobel lecture, December 8, 1979. *Journal of Computer Assisted Tomography* 1980;**4**(5):665-74.

20. Ludwig GD. The velocity of sound through tissues and the acoustic impedance of tissues. *J. Acoust. Soc. Am.* 1950;**22**(862).

21. Goldberg BB, Liu JB, Forsberg F. Ultrasound contrast agents: a review. *Ultrasound in Medicine and Biology* 1994;**20**(4):319-33.

22. Rubin GD, Dake MD, Semba CP. Current status of three-dimensional spiral CT scanning for imaging the vasculature. *Radiologic Clinics of North America* 1995;**33**(1):51-70.

23. Ryhanen T, Seppa H, Ilmoniemi R, *et al.* SQUID magnetometers for low-frequency applications. *Journal of Low Temperature Physics* 1989;**76**(5-6):287-386.

24. Baule G, McFee R. Detection of the magnetic field of the heart. *Am. Heart J.* 1963;**66**:95-96.

25. Zimmerman JE, Thiene P, Harding JT. Design and operation of stable rf-biased superconducting point- contact quantum devices, and a note on the properties of perfectly clean metal contacts. *Journal of Applied Physics* 1970;**41**(4):1572-80.

26. Katila TE. On the current multipole presentation of the primary current distributions. *Nuovo Cimento D* 1983;**2**:660-664.

27. Huang HK, Arenson RL, Lou SL, *et al.* Multimedia in the radiology environment: current concept. *Computerized Medical Imaging and Graphics* 1994;**18**(1):1-10.

28. Kim Y, Park H, Haynor D. Requirements for PACS workstation. *Proc. 2nd Int. Conference on Image Management and Communication in Patient Care.* Kyoto, Japan: IEEE Computer Society Press, 1991:36-41.

29. Institute of Medicine (U.S.). Committee on Improving the Patient Record, Dick RS, Steen EB, *et al. The computer-based patient record : an essential technology for health care,* Rev. ed. Washington, D.C.: National Academy Press, 1997.

30. Wong STC, Abundo M, Huang HK. Authenticity techniques for PACS images and records. In: Jost RG, Dwyer SJ, eds. *Medical Imaging 1995: PACS Design and Evaluation: Engineering and Clinical Issues.* Vol 2435. San Diego: SPIE, 1995:68-79.

31. Huang H, Ratib O, al e. Picture Archiving and Communication System (PACS). *Journal of Digital Imaging* 1992;**5**(1):22-25.

32. Huang HK, Arenson RL. Second generation PACS at UCSF. *Radiology* 1993;**189**:290.

33. Osteaux M. *A Second generation PACS concept : hospital integrated picture archiving and communication systems.* Berlin ; New York: Springer-Verlag, 1992.

34. Seven HL. Health Level Seven (HL7). An Application Protocol For Electronic Data Exchange in Health Care Environments Version 2.1. Ann Arbor, Michigan, 1991.

35. Ratib O, Ligier Y, Bandon D, *et al.* Update on digital image management and PACS. *Abdominal Imaging* 2000;**25**(4):333-40.

36. Irie G. Clinical experience - 16 months of HU-PACS. In: Huang HK, Ratib O, Bakker AR, *et al.*, eds. *Picture Archiving and Communication Systems (PACS).* Vol 74: Springer-Verlag, 1991;213-230.

37. Huang HK, Wong WK, Lou SL, *et al.* Architecture of a comprehensive radiologic imaging network. *IEEE Journal on Selected Areas in Communications* 1992;**10**(7):1188-96.

38. Georinger F. Medical diagnostic imaging support system for military medicine. In Picture Archiving and Communication Systems (PACS). In: Huang HK, Ratib O, Bakker AR, *et al.*, eds. *NATO ASI Series F, PACS in Medicine.* Vol 74. New York: Springer-Verlag, 1991;213-230.

39. Masser H, Mandl A, Urban M, *et al.* The Vienna Project SMZO in Picture Archiving and Communication systems (PACS). In: Huang HK, Ratib O, Bakker A, *et al.*, eds. *NATO ASI Series F, PACS in Medicine.* Vol 74. New York: Springer-Verlag, 1991;247-250.

40. Allen L, Frieder O. Exploiting database technology in the medical arena. *IEEE Engineering in Medicine and Biology Magazine* 1992;**11**(1):42-9.

41. Oliver DE, Altman RB. Extraction of SNOMED concepts from medical record texts. *Proceedings of the Eighteenth Annual Symposium on Computer Applications in Medical Care(SCAMC)* 1994:179-83.

42. Shortliffe EH. *Medical informatics : computer applications in health care and biomedicine,* 2nd ed. New York: Springer, 2001.

43. Larman C. *Applying UML and patterns : an introduction to object-oriented analysis and design.* Upper Saddle River, N.J.: Prentice Hall PTR, 1998.

44. DeMarco T. *Structured analysis and system specification.* Englewood Cliffs, N.J.: Prentice-Hall, 1979.

45. Booch G. *Object-oriented analysis and design with applications,* 2nd ed. Redwood City, Calif.: Benjamin/Cummings Pub. Co., 1994.

46. Cockburn A. *Writing effective use cases.* Boston: Addison-Wesley, 2001.

47. Buckley C, Pulsipher D. Destroying the Tower of Babel. *Rose Architect* Winter, 1999:60-65.

48. Gamma E. *Design patterns : elements of reusable object-oriented software.* Reading, Mass.: Addison-Wesley, 1995.

49. Dreifuss FE. Establishment of what constitutes medical failure. In: Engel J, ed. *Surgical treatment of the epilepsies,* 2nd ed. New York: Raven Press, 1993;133-136.

50. National Institutes of Health Consensus Conference. Surgery for epilepsy. *Jama* 1990;**264**(6):729-33.

51. Spencer SS. The relative contributions of MRI, SPECT, and PET imaging in epilepsy. *Epilepsia* 1994;**35 Suppl 6**(11):S72-89.

52. Engel J, Jr., Henry TR, Risinger MW, *et al.* Presurgical evaluation for partial epilepsy: relative contributions of chronic depth-electrode recordings versus FDG-PET and scalp-sphenoidal ictal EEG. *Neurology* 1990;**40**(11):1670-7.

53. Cendes F, Andermann F, Dubeau F, *et al.* Proton magnetic resonance spectroscopic images and MRI volumetric studies for lateralization of temporal lobe epilepsy. *Magnetic Resonance Imaging* 1995;**13**(8):1187-91.

54. Engel J. *Surgical treatment of the epilepsies,* 2nd ed. New York: Raven Press, 1993.

55. Sadler M, Desbiens R. Scalp EEG in temporal lobe epilepsy surgery. *Can J Neurol Sci* 2000;**27 Suppl 1**:S22-8; discussion S50-2.

56. Velioglu SK, Ozmenoglu M, Komsuoglu SS. EEG investigation of temporal lobe epilepsy. *Clin Electroencephalogr* 1997;**28**(2):121-6.

57. Lehericy S, Semah F, Hasboun D, *et al.* Temporal lobe epilepsy with varying severity: MRI study of 222 patients. *Neuroradiology* 1997;**39**(11):788-96.

58. Grunewald RA, Jackson GD, Connelly A, *et al.* MR detection of hippocampal disease in epilepsy: factors influencing T2 relaxation time. *AJNR Am J Neuroradiol* 1994;**15**(6):1149-56.

59. Jackson GD, Connelly A, Duncan JS, *et al.* Detection of hippocampal pathology in intractable partial epilepsy: increased sensitivity with quantitative magnetic resonance T2 relaxometry. *Neurology* 1993;**43**(9):1793-9.

60. Ende G, Laxer KD, Knowlton RC, *et al.* Quantitative ^{1}H SI shows bilateral metabolite changes in unilateral TLE patients with and without hippocampal atrophy. *Proc. SMR Third Meeting,* 1995:144.

61. Udupa JK, Herman GT. *3D imaging in medicine,* 2nd ed. Boca Raton: CRC Press, 2000.

62. Hoffman EA, Gnanaprakasam D, Gupta KB, *et al.* VIDA: an environment for multidimensional image display and analysis. In: Acharya RS, Cogswell CJ, Goldgof DB, *et al.*, eds. *Biomedical image processing and three-dimensional microscopy : 10-13 February 1992, San Jose, California.* Vol 1660. Bellingham, Wash.: SPIE, 1992;694-711 2 v. (xiv, 835).

63. Woods RP, Mazziotta JC, Cherry SR. MRI-PET registration with automated algorithm. *Journal of Computer Assisted Tomography* 1993;**17**(4):536-46.

64. Klein GJ, Reutter BW, Huesman RH, *et al.* Volume-of-interest specification on arbitrarily resliced volume datasets. In: Hoffman EA, ed. *Medical Imaging 1995: Physiology and Function from Multidimensional Images.* Vol 2433. Newport Beach, CA: SPIE-Int. Soc. Opt. Eng, 1995:214-223.

65. Gudivada VN, Raghavan VV. Content based image retrieval systems. *Computer* 1995;**28**(9):18-22.

66. Flickner M, Sawhney H, Niblack W, *et al.* Query by image and video content: the QBIC system. *Computer* 1995;**28**(9):23-32.

67. Kiebel SJ, Ashburner J, Poline JB, *et al.* MRI and PET coregistration--a cross validation of statistical parametric mapping and automated image registration. *Neuroimage* 1997;**5**(4 Pt 1):271-9.

68. Wong STC, Knowlton RC, Kent Soo Hoo J, *et al.* Use of multidimensional, multimodal imaging and PACS to support neurological diagnosis. In: Hoffman EA, ed. *Medical Imaging 1995: Physiology and Function from Multidimensional Images.* Vol 2433. Newport Beach, CA: SPIE-Int. Soc. Opt. Eng, 1995:236-247.

69. Strother SC, Anderson JR, Xu XL, *et al.* Quantitative comparisons of image registration techniques based on high-resolution MRI of the brain. *Journal of Computer Assisted Tomography* 1994;**18**(6):954-62.

70. Pierre DA. *Optimization theory with applications.* New York: Dover Publications, 1986.

71. Laboratory SPN. BrainImage Software. 2001.

72. Wong STC. *Medical image databases.* Boston: Kluwer Academic, 1998.